Supporting Information.

- General experimental methods and instrumentation
- Peptoid synthesis
- Determination of $K_{cis/trans}$ values for peptoid main chain amides
  - ^{1}H NMR and NOESY 1D methods and spectra for peptoids **2** and **2'**
  - ^{1}H-^{13}C HSQC methods and spectra for peptoids **3**–**8**
- NMR structural studies
  - 2D NMR methods and spectra for peptoids **4a** and **4b**
  - 2D NMR methods and spectra for peptoid ***6i***
  - Structure determination for peptoid ***6i***
- Supplemental X-ray crystallographic data and crystal packing diagrams for **Br-Nph-Ns1npe-dma**, **3**, and **4a**
- Main chain dihedral angles for **Br-Nph-Ns1npe-dma**, **3**, **4a**, and ***6i*** as determined by X-ray crystallography or NMR
- Supplemental CD data
  - Variable concentration spectra for **8** (CH_3CN, 20 °C)
  - Variable temperature spectra for **8** (30 μM: CH_3CN, CH_3CN:H_2O, and MeOH)
- Characterization data for all peptoid synthesis intermediates
- Characterization data for target peptoids **2**, **2'**, and **3**–**8**.
- References (including full citations for references [2] and [13] in text)

General experimental methods and instrumentation.

All reagents were purchased from commercial sources [Aldrich, Alfa Aesar ((*S*)-(-)-1-(1-naphthyl)-ethylamine), and Cambridge Isotopes (^{13}C-2 bromoacetic acid)] and used without further purification. Solvents were purchased from commercial sources (Aldrich and Fisher) and used as is, with the exception of hexane, which was distilled immediately prior to use. Thin layer chromatography (TLC) was performed on silica gel 60 F_{254} plates (E-5715-7, EMD). SiliaFlash P60 silica gel (40–63 μm, Silicycle) was used for manual flash column chromatography.[1]

Details of instrumentation and analytical methods are outlined below:

- Reversed-phase high performance liquid chromatography (RP-HPLC) was performed using a Shimadzu system equipped with an SCL-10Avp controller, an LC-10AT pump, an FCV-10ALvp solvent mixer, and an SPD-10MAvp UV/vis diode array detector. All analytical RP-HPLC work was performed using a Shimadzu Premier C18 column (5 μm, 4.6 mm x 250 mm). Standard RP-HPLC conditions were as follows: flow rate = 1.0 mL/min; mobile phase A = 0.1% trifluoroacetic acid (TFA) in water; mobile phase B = 0.1% TFA in acetonitrile. Purities were determined by integration of peaks with UV detection at 220 nm.

- High resolution mass spectrometry (MS) data were obtained with a Waters (Micromass) LCT™ instrument equipped with a time-of-flight analyzer (electrospray ionization, ESI).

- Attenuated total reflectance (ATR)-IR spectra were recorded with a Bruker Tensor 27 spectrometer outfitted with a single reflection MIRacle Horizontal ATR containing a Ge crystal with a refractive index of 4.0 at 1000 cm^{-1} and a long wave cutoff of 575 cm^{-1}.

- ^{1}H NMR (300 MHz, 500 MHz, 600 MHz, 700 MHz) and ^{13}C NMR (75 MHz) spectra were recorded on either a Bruker AC-300, Varian MercuryPlus 300, Varian Inova 500, Varian Inova 600, or a Bruker Avance-700 spectrometer in deuterated solvents. Chemical shifts are reported in parts per million (ppm, δ) and referenced to solvent or tetramethyl silane (TMS, 0.0 ppm). One dimensional NOESY experiments were conducted on a Varian Inova 500 MHz spectrometer equipped with a 5 mm broadband probe with axis gradients, using a standard Varian Chempack pulse sequence. Heteronuclear single-quantum correlation (HSQC)[2-4] experiments were conducted on a Bruker Avance-700 MHz spectrometer equipped with a 5 mm cryogenic probe. Gradient homonuclear correlation spectroscopy (gCOSY), gradient heteronuclear multiple bond correlation adiabatic (gHMBCAD), two dimensional nuclear Overhausser effect spectroscopy (NOESY), and rotating frame Overhausser spectroscopy (ROESY) NMR experiments were performed on a Varian Inova 600 MHz spectrometer equipped with a 5 mm inverse triple resonance probe, using the standard Varian Chempack pulse sequences. The 2D NMR data were processed using TopSpin 3.0 (Bruker) software or the Varian VNMR software package (v. 6.1C) and visualized using TopSpin or SPARKY (v. 3.114) software.[5] Molecular dynamics calculations for the NMR refined structure determination of ***6i*** were performed on a computer with a Supermicro 4 X Quad-Core and AMD Opteron(tm) 8350 Processors running CentOS Linux using the AMBER11 software program.

- Circular dichroism (CD) spectra were obtained on an Aviv Biomedical Inc. 420 spectrophotometer using Aviv CDS software.

- X-ray diffraction data for peptoids **Br-*N*ph-*N*s1npe-dma**, **3**, and **4a** were collected on a Bruker SMART APEXII diffractometer.

Peptoid synthesis.

All peptoids were synthesized in solution in an iterative fashion according to Scheme S-1, except for the synthetic step used to incorporate the ^{13}C-labeled acetamide within **6*i***. Bromoacetamides were generated from reaction of amines with bromoacetyl bromide using a modified version of previously reported methods.[10,11] Nucleophilic substitution with either (*S*)-(-)-1-(1-naphthyl)-ethylamine or aniline derivatives yielded alkylated secondary amines. To generate the target peptoids, the *N*-termini were acetylated using acetic anhydride. Every peptoid intermediate and target compound was purified by manual flash silica gel chromatography. Flash chromatography conditions are provided for all compounds in the compound characterization section (elution solvents and R_f values; pages S-46–S-85). General synthetic procedures are outlined below.

****Note – Characterization data for all peptoid intermediates and final targets are placed at the end of this document for ease of use*.

Scheme S-1. General synthetic route utilized to obtain peptoids **2**–**8**.[a]

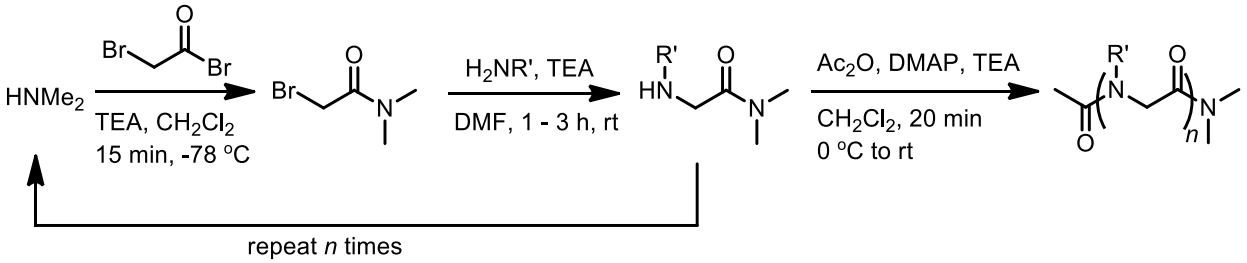

[a] Abbreviations: TEA = triethylamine, DMF = dimethylformamide, Ac_2O = acetic anhydride, DMAP = *N*,*N*-dimethyl-4-aminopyridine

Representative bromoacetylation procedure. (*Synthesis of BrAc-dma, Scheme S-1*)
Bromoacetyl bromide (4.0 mL, 46.1 mmol) was added to CH_2Cl_2 (30 mL) in a flame-dried, three-necked flask equipped with an addition funnel and a magnetic stir bar. Dimethylamine • HCl (2.5 g, 30.7 mmol) was added, and the solution was stirred. The flask was purged with N_2 for 5 min, and cooled to -78 °C in a dry ice/acetone bath. TEA (11.0 mL, 78.9 mmol) in CH_2Cl_2 (40 mL) was added drop-wise *via* the addition funnel to the stirring solution under a gentle stream of N_2. After the addition was complete, the reaction mixture was stirred at -78 °C for 15 min, then removed from the bath and stirred for 15 min at room temperature (rt). Thereafter, the reaction mixture was transferred to a separatory funnel, washed with 10% w/v aq. citric acid

(1x), sat. aq. $NaHCO_3$ (1x), and dried over anhydrous $MgSO_4$. The organic solvent was removed *in vacuo*, and the crude product was purified to homogeneity by flash silica gel chromatography (*note:* subsequent acylations required the slow addition of polypeptoids bearing free secondary amines dissolved in CH_2Cl_2 to bromoacetyl bromide in CH_2Cl_2 at -78 °C under a stream of N_2, followed by the addition of TEA/CH_2Cl_2).

Representative alkylation procedure. (*Synthesis of H-Ns1npe-dma, Scheme S-1*)
(*S*)-(-)-1-(1-Naphthyl)-ethylamine (3.56 mL, 22.2 mmol) was added to dry DMF (10 mL) in a flame-dried flask equipped with an addition funnel and a magnetic stir bar. Br-dma (*see above*; 1.84 g, 11.08 mmol) in dry DMF (15 mL) was added drop-wise *via* the addition funnel to the stirring solution. TEA (1.93 mL, 11.08 mmol) in dry DMF (5 mL) was then added drop-wise. After the addition was complete, the reaction mixture was stirred for 1 h at rt (*note:* alkylations of pyridine derivatives were allowed to stir for 3 h at rt). The reaction mixture was transferred to a separatory funnel, and EtOAc (120 mL) was added. The organic layer was washed with sat. aq. $NaHCO_3$ (3x) and dried over anhydrous $MgSO_4$. The solvent was removed *in vacuo*, and the crude product was purified by flash silica gel chromatography (*note*: the intermediates H-*N*s1npe-dma and H-*N*2,6mph-Ac*^{13}C-*N*s1npe-*N*4fph-*N*s1npe-dma required at least two columns; other alkylations only required one flash column purification).

Procedure for coupling ^{13}C-labeled bromoacetic acid to H-*N*s1npe-*N*4fph-*N*s1npe-dma.
Bromoacetic acid ^{13}C-2 (330 mg, 2.36 mmol) was added to dry DMF (4 mL) in a flame-dried flask equipped with an addition funnel and a magnetic stir bar. Diisopropylcarbodiimide (365 μL, 2.35 mmol) was added, and the solution was stirred for 15 min at rt. H-*N*s1npe-*N*4fph-*N*s1npe-dma (720 mg, 1.164 mmol) in dry DMF (20 mL) was added drop-wise *via* the addition funnel to the stirring solution. Pelleted DMAP (40 mg) was added, and the mixture was stirred for 30 min at rt. Thereafter, EtOAc (100 mL) was added to the reaction mixture, which was transferred to a separatory funnel, washed with 10 % w/v aq. citric acid (1x), sat. aq. $NaHCO_3$ (1x), and dried over anhydrous $MgSO_4$. The organic solvent was removed *in vacuo*, and the crude product was purified to homogeneity by flash silica gel chromatography.

Representative acetylation procedure. (*Synthesis of peptoid **2**, Scheme S-1*)
Acetic anhydride (200 μL, 2.11 mmol) was added to CH_2Cl_2 (10 mL) in a flamed-dried flask equipped with an addition funnel and a magnetic stir bar, and cooled to 0 °C in an ice bath. H-*N*ph-*N*s1npe-dma (137 mg, 0.352 mmol), TEA (294 μL, 2.11 mmol), and DMAP (5 mg) were dissolved in CH_2Cl_2 (12 mL) and added to the solution of Ac_2O drop-wise. After addition, the solution was stirred at rt for 2 h. Thereafter, the reaction mixture was transferred to a separatory funnel, washed with 10 % w/v aq. citric acid (1x), sat. aq. $NaHCO_3$ (1x), and dried over anhydrous $MgSO_4$. The solvent was removed *in vacuo*, and the peptoid product was purified to homogeneity by flash silica gel chromatography. All isolated yields from these capping acetylation reactions were between 63–88%.

Determination of $K_{cis/trans}$ values of peptoid main chain amides.

*^{1}H NMR and NOESY 1D methods and spectra for peptoids **2** and **2'***

Purified, lyophilized compounds were dissolved in deuterated solvents to give 10 mM solutions. ^{1}H NMR spectra (500 MHz) were acquired at 24 °C using 16 scans and a relaxation delay of 15 s. Multiple NOESY 1D spectra of **2** and **2′** were acquired at 24 °C in both $CDCl_3$ and 1:1 CD_3CN:D_2O to distinguish between the *cis*- and *trans*-amide rotamer-related peaks, in the same manner as previously reported in studies of peptoids.[6,7] The spectral parameters for all NOESY 1D experiments for **2** and **2′** in $CDCl_3$ were as follows: spectral widths (sw) = 8000 Hz; relaxation delays (d1) = 12 s; mixing times = 0.6 s; number of transients (nt) = 64. The spectral parameters for all NOESY 1D experiments for **2** and **2′** in 1:1 CD_3CN:D_2O were as follows: spectral widths = 4529 Hz; relaxation delays (d1) = 12 s; mixing times = 1.2 s; number of transients (nt) = 64.

Both **2** and **2′** contain two unsymmetrical amides; therefore, each dimer could exist as four possible conformers. However, only one set of major conformational peaks were observed by ^{1}H NMR spectroscopy for each peptoid in $CDCl_3$ and CD_3CN:D_2O. One-dimensional NOESY experiments in these solvents ($CDCl_3$, Figures S-1 and S-2; CD_3CN:D_2O, Figures S-4 and S-5) were conducted to determine the geometry of the amide bonds of both residues in **2** and **2′**. These NOESY experiments also permitted the assignments of the minor conformational peaks (assignments in $CDCl_3$ are shown in Figure S-3). We note that the major conformational peaks of the *N*s1npe methine proton observed in all ^{1}H spectra were shifted downfield relative to the minor conformational peaks. The ^{1}H resonance of the *s1npe* methine proton of the *cis*-rotamer was expected to be downfield compared to the *trans* rotamer-related peak, due to magnetic anisotropy effects of the amide carbonyl in the *cis* geometry.

$K_{cis/trans}$ values for each residue of **2** and **2′** in six different solvents were calculated by integration of the major and minor rotamer-related peaks in the ^{1}H spectra and are listed in Table S-1. As expected, the *N*ph amides were found to largely favor *trans* isomers in all solvents. A solvent effect was noted for the $K_{cis/trans}$ values of the *N*s1npe amides. The preference for the *cis*-amide rotamer increased in increasingly polar organic aprotic solvents. This trend is in agreement with data from our previous studies of solvent effects on the conformation of an *N*s1npe monomer.[12] We have previously suggested that there is a favorable stereoelectronic interaction in the *cis*-amide orientation for the *s1npe* side chain in solution, specifically an $n \rightarrow \pi^*_{aromatic}$ interaction between the main chain carbonyl oxygen and the side chain naphthalene π system of this residue. This interaction may be stabilized in solvents with a higher dielectric constant. The diminished $K_{cis/trans}$ values for the *N*1snpe amide of **2** and **2′** in methanol-d_4 and the CD_3CN:D_2O mixture supports this hypothesis, as hydrogen bonding between the main chain carbonyl oxygens and protic solvent molecules would compete with the proposed $n \rightarrow \pi^*_{aromatic}$ interaction.

Peptoid **2**: Ac-*N*ph-*N*s1npe-dma

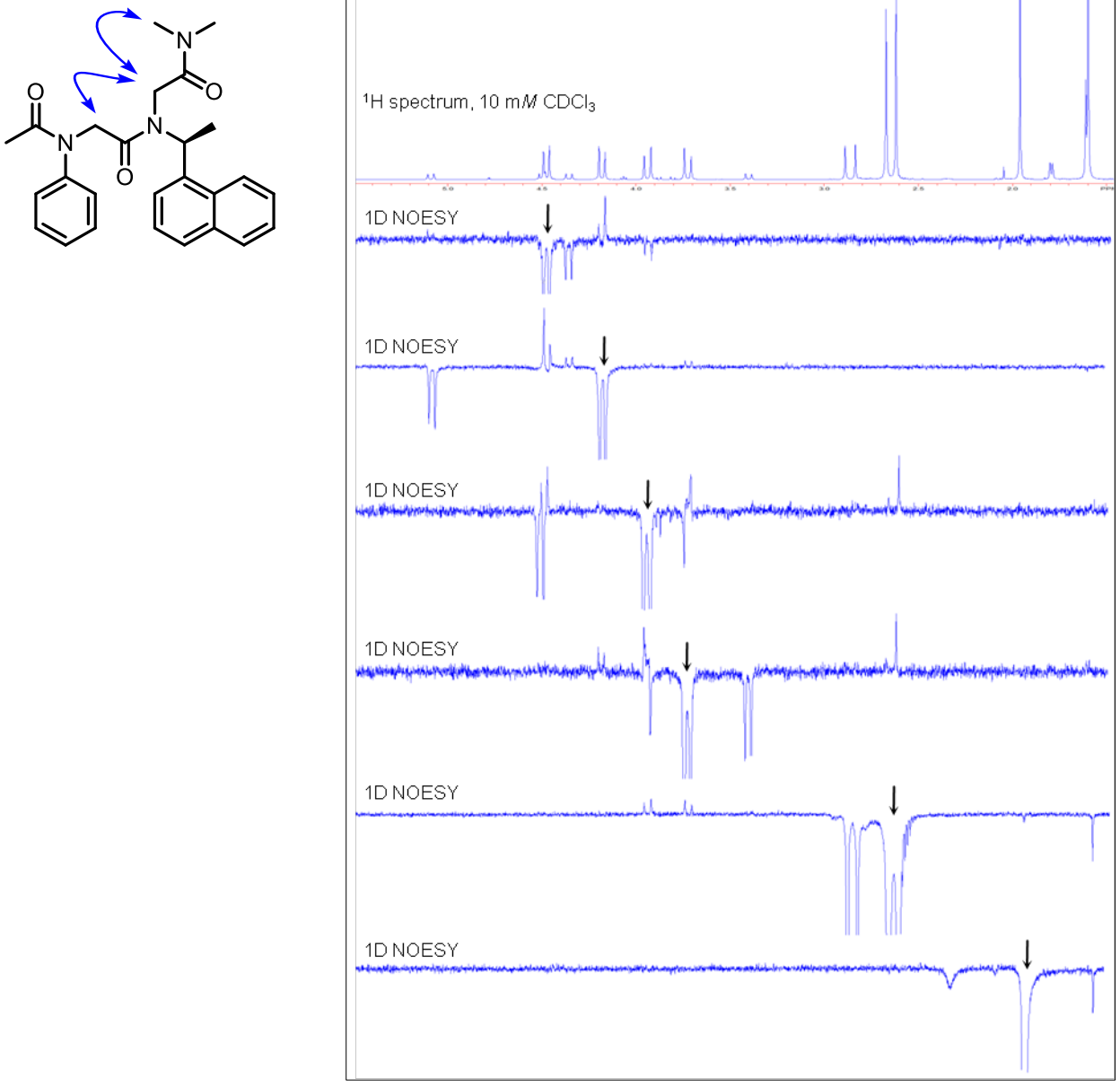

Figure S-1. Chemical structure, partial ^{1}H NMR spectrum, and NOESY 1D spectra of peptoid **2** in $CDCl_3$ (500 MHz, 10 mM, 24 °C). NOESY parameters: d1 = 12 s, mix time = 0.7 s, nt = 32. Curved blue arrows indicate NOE correlations. Black straight arrows indicate the peak that was irradiated in each one dimensional NOESY experiment.

Peptoid **2'**: Ac-*N*s1npe-*N*ph-dma

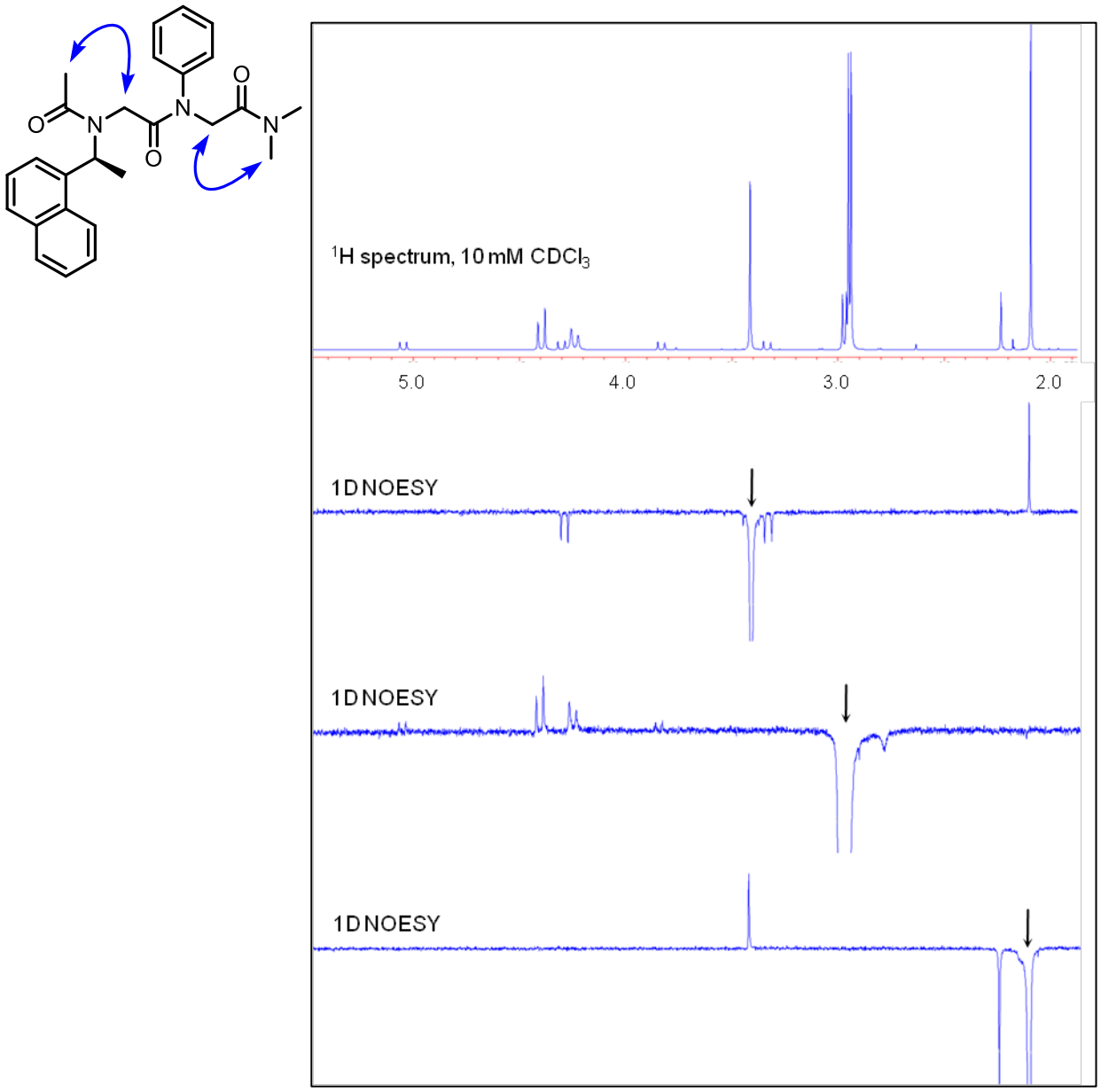

Figure S-2. Chemical structure, partial ^{1}H NMR spectrum, and NOESY 1D spectra of peptoid **2′** in $CDCl_3$ (500 MHz, 10 mM, 24 °C). NOESY parameters: d1 = 12 s, mix time = 0.7 s, nt = 32. Curved blue arrows indicate NOE correlations. Black straight arrows indicate the peak that was irradiated in each one dimensional NOESY experiment.

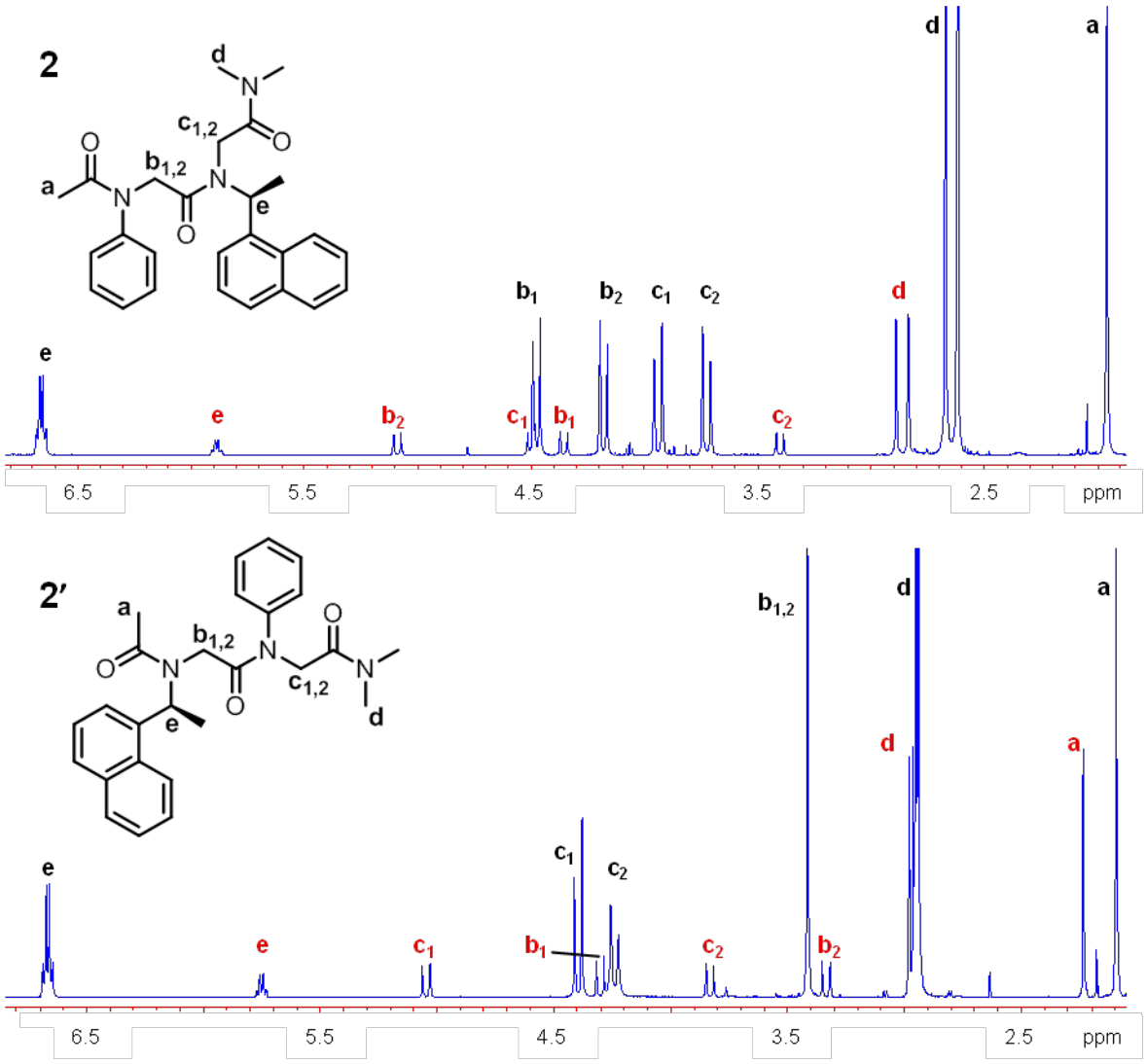

Figure S-3. Assignments of the major (labeled black) and minor (labeled red) conformational peaks in the partial ^{1}H spectra of peptoids **2** and **2′** in $CDCl_3$ (500 MHz, 10 mM). The protons of interest are labeled "**a**–**e**" on each structure.

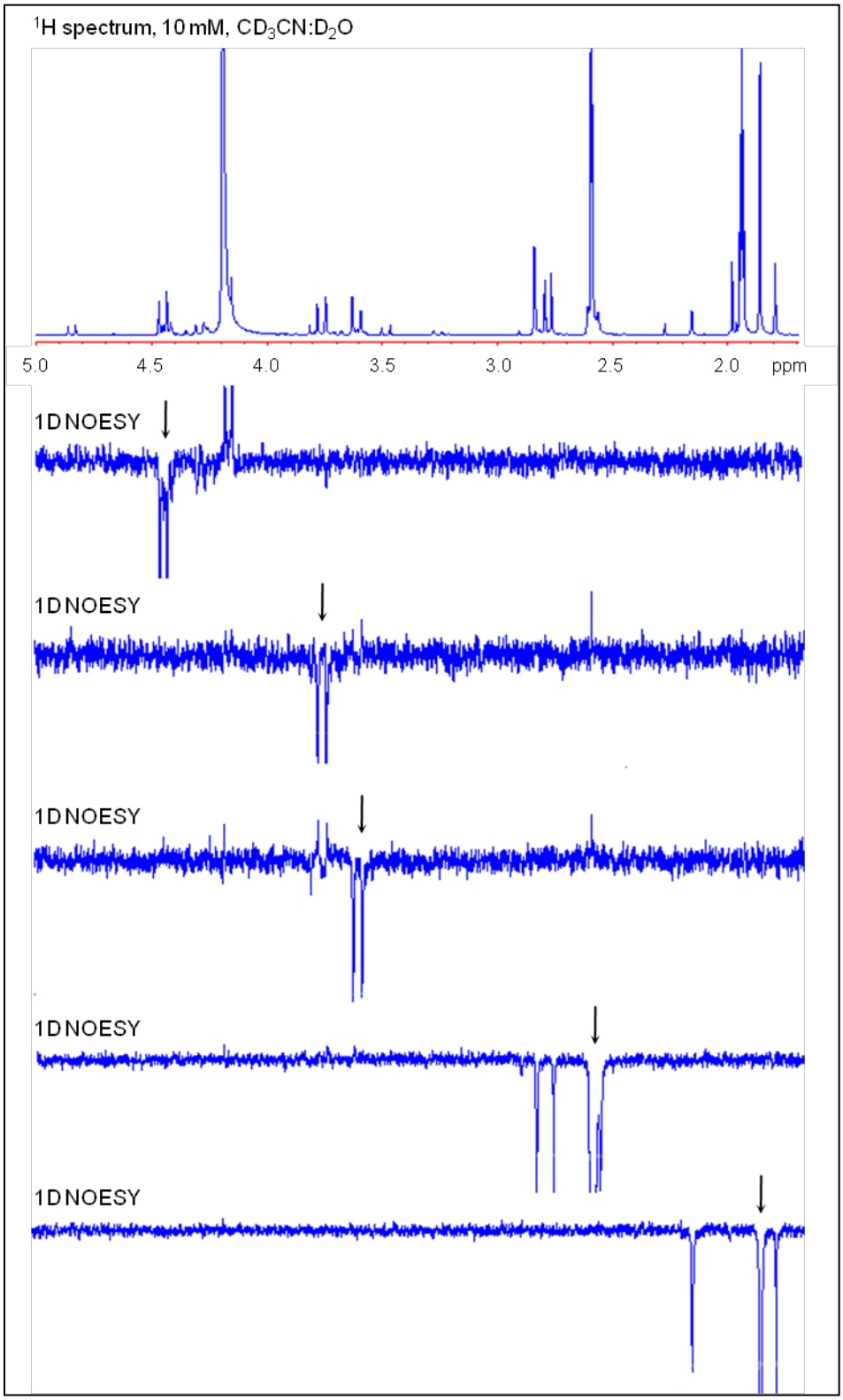

Figure S-4. Partial ^{1}H NMR spectrum and NOESY 1D spectra of **2** in 1:1 $CD_3CN:D_2O$ (500 MHz, 10 mM, 24 °C). NOESY parameters: d1 = 12 s, mix time = 1.2 s, nt = 64. Black straight arrows indicate the peak that was irradiated in each one dimensional NOESY experiment.

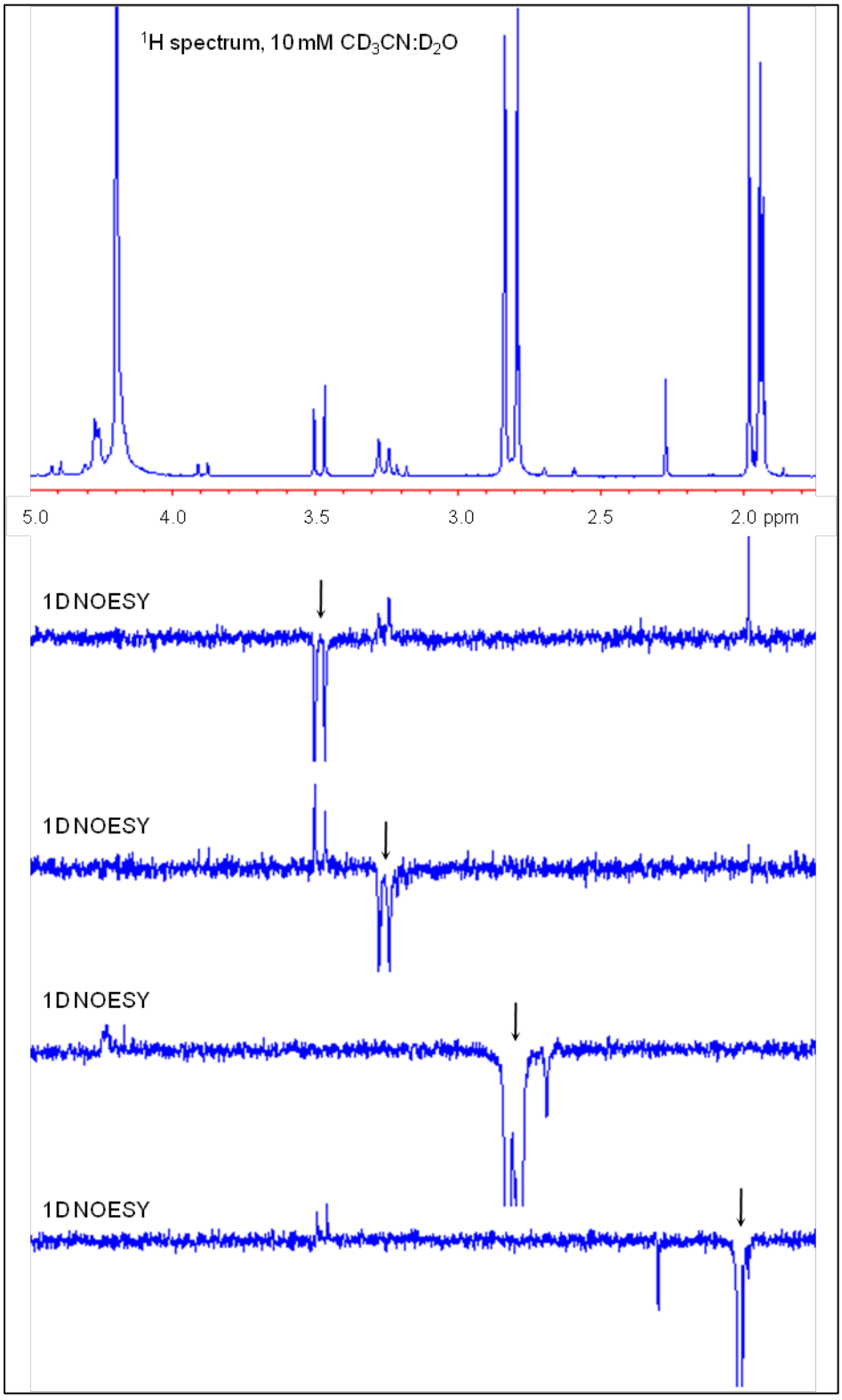

Figure S-5. Partial ^{1}H NMR spectrum and NOESY 1D spectra of peptoid **2′** in 1:1 $CD_3CN:D_2O$ (500 MHz, 10 mM, 24 °C). NOESY parameters: d1 = 12 s, mix time = 1.2 s, nt = 64. Black straight arrows indicate the resonance that was irradiated in each one dimensional NOESY experiment.

Table S-1. $K_{cis/trans}$ values for each residue of peptoids **2** and **2′** in various solvents at 24 °C.

	$K_{cis/trans}$					
residue	C_6D_6	$CDCl_3$	CD_3CN	CD_3OD	$(CD_3)_2SO$	$CD_3CN : D_2O$
peptoid **2**						
*N*ph	< 0.05	< 0.05	0.1	0.1	0.1	0.3
*N*s1npe	4.6	4.9	8.7	5.9	9.8	3.7
peptoid **2′**						
*N*s1npe	--[a]	4.9	10.2	7.5	14.9	4.8
*N*ph	--[a]	< 0.05	< 0.05	< 0.05	0.1	0.1

[a] Not calculated due to poor dispersion of proton signals in the ^{1}H NMR spectrum.

*^{1}H-^{13}C HSQC methods and spectra for peptoids **3–8***

Purified, lyophilized compounds were dissolved in $CDCl_3$ to give between 4–10 mM solutions. ^{1}H-^{13}C HSQC NMR experiments (700 MHz) were performed at 24 °C for peptoids **3**, **4a**, **4b**, **5**, **6**, **6*i***, **7**, and **8** using the following parameter values: sw in the f2 dimension were between 5200 and 5900 Hz; relaxation delays (d1) = 3.4 s; number of increments (ni) = 200; number of transients (nt) = 6. The number of points collected was 2048. The spectra were then zero-filled to generate f1 x f2 matrices of 2048 x 4096 points, respectively. Variable temperature ^{1}H-^{13}C HSQC studies of peptoid **8** in $CDCl_3$ (10 mM; 4, 14, 24, and 44 °C) and methanol-d_4 (10 mM; 4, 24, 44, and 54 °C) were performed using the same parameters as listed above.

Partial ^{1}H-^{13}C HSQC spectra for peptoids **3–8** are shown below. The partial ^{1}H spectra corresponding to the f2 dimension are also shown along the top of each 2D plot. Only the *s1npe* side chain methine regions of each spectrum are displayed, and boxes are drawn and labeled around the peaks associated with either *cis*- or *trans*-amide conformers. These regions were assigned based on previous NMR analyses of similar peptoids containing these side chains.[9,12] The region of these HSQC spectra corresponding to the *s1npe* side chain methine group was analyzed in order to determine the overall $K_{cis/trans}$ values for these residues in each oligomer (listed in Table S-2).

3: Ac-*N*s1npe-*N*ph-*N*s1npe-dma

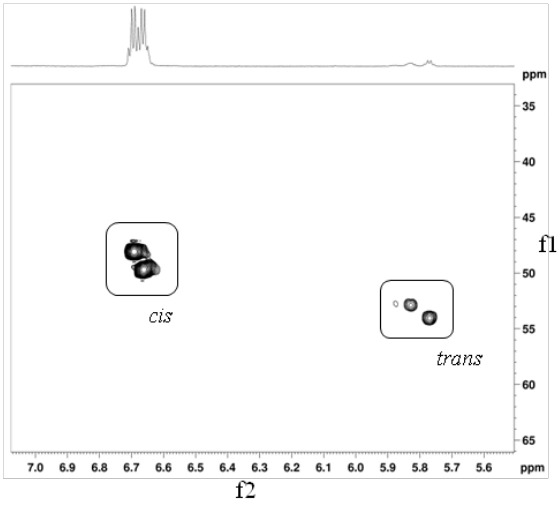

4a: Ac-*N*2,6mph-*N*s1npe-*N*ph-*N*s1npe-dma

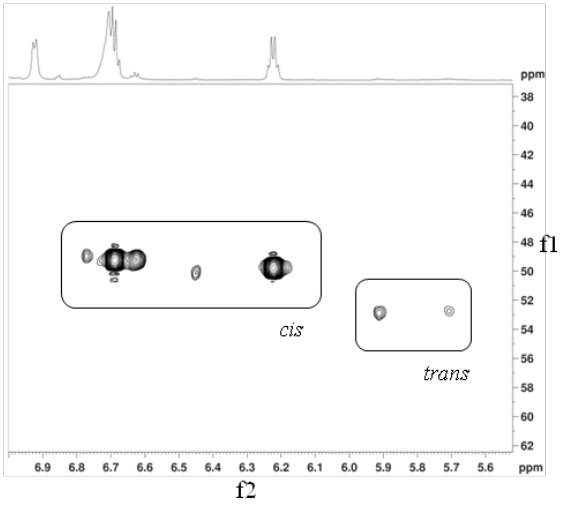

4b: Ac-*N*3,5mph-*N*s1npe-*N*ph-*N*s1npe-dma

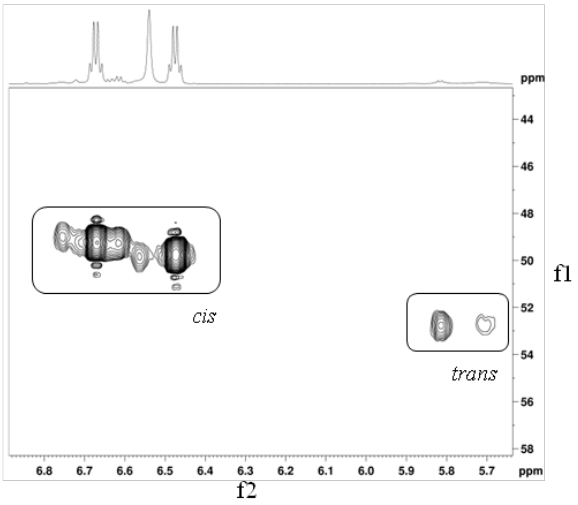

5: Ac-*N*s1npe-(*N*ph-*N*s1npe)$_2$-dma

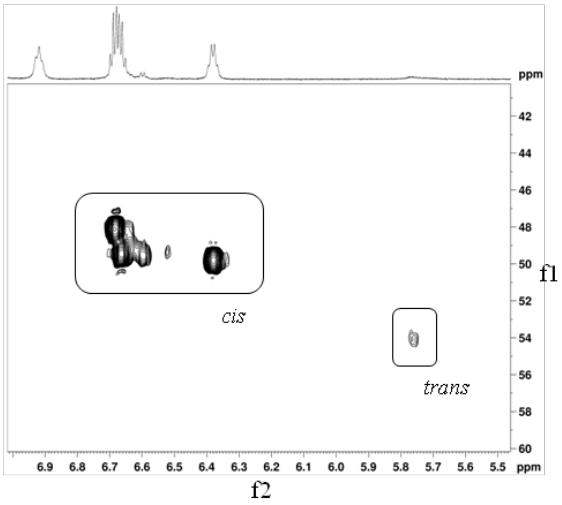

6: Ac-(*N*ph-*N*s1npe)$_3$-dma

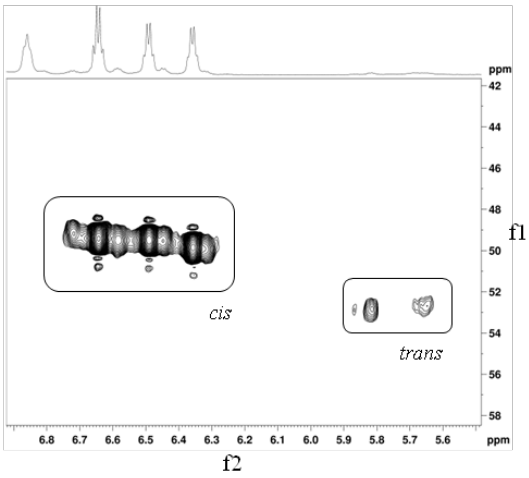

6*i*: Ac-*N*3,5mph-*N*s1npe-*N*2,6mph-ac^{13}C-*N*s1npe-*N*4fph-*N*s1npe-dma

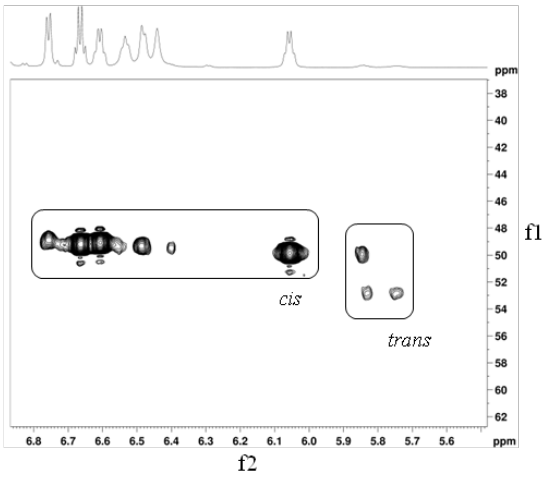

7: Ac-*N*s1npe-(*N*ph-*N*s1npe)$_3$-dma

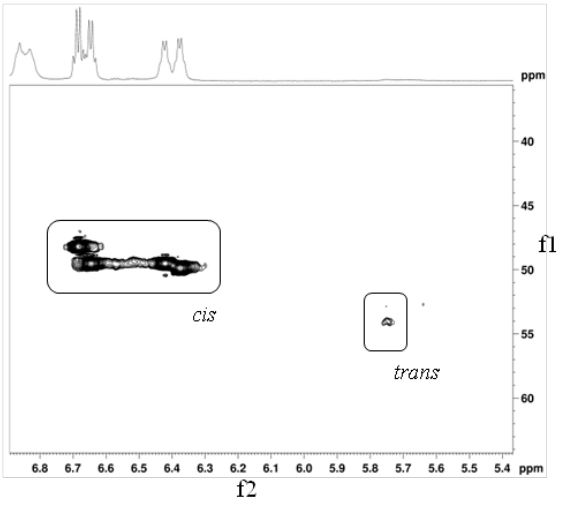

8: Ac-(*N*ph-*N*s1npe)$_4$-dma — $CDCl_3$

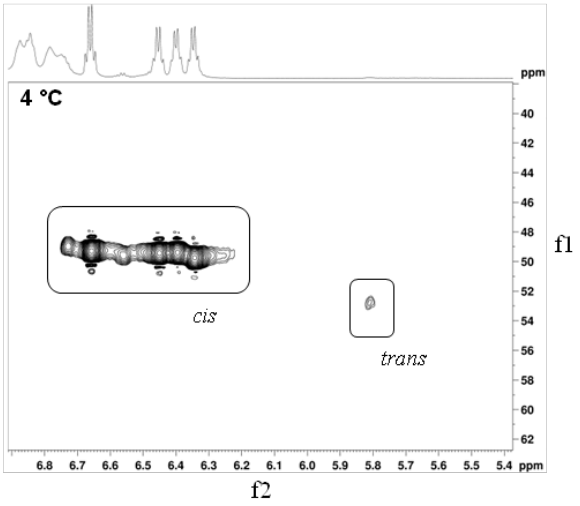

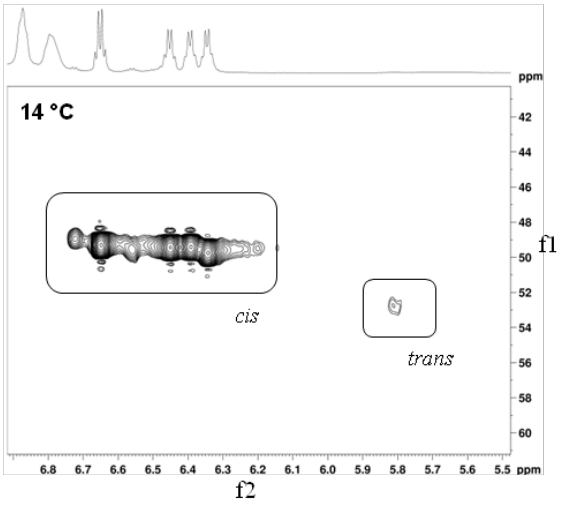

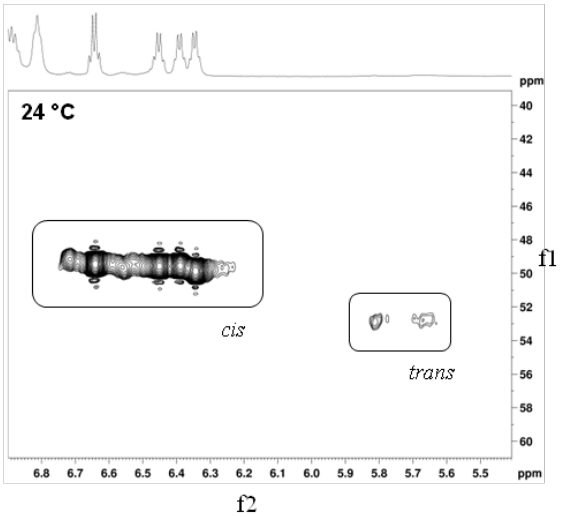

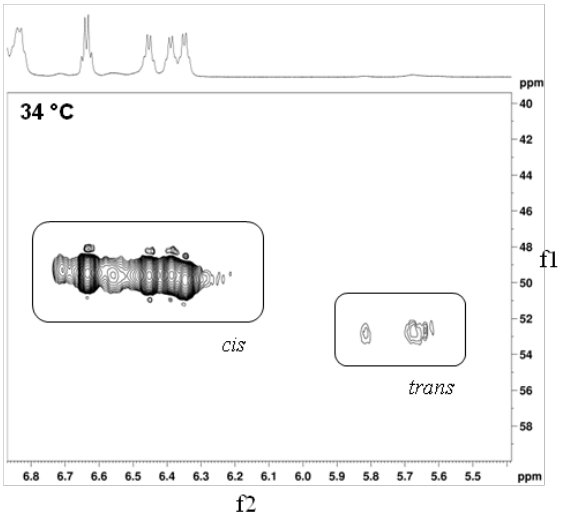

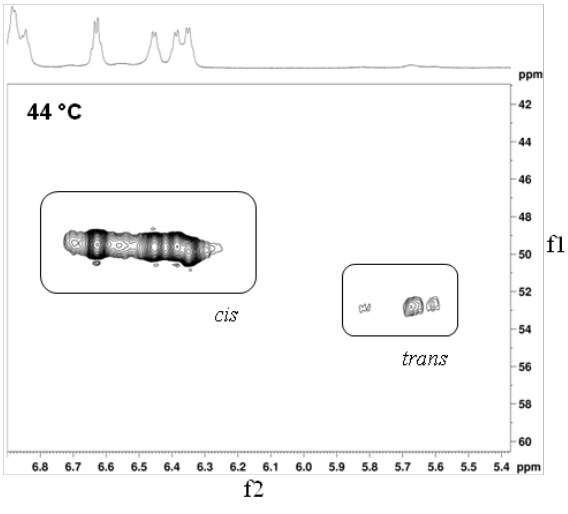

8: Ac-(*N*ph-*N*s1npe)$_4$-dma — CD_3OD

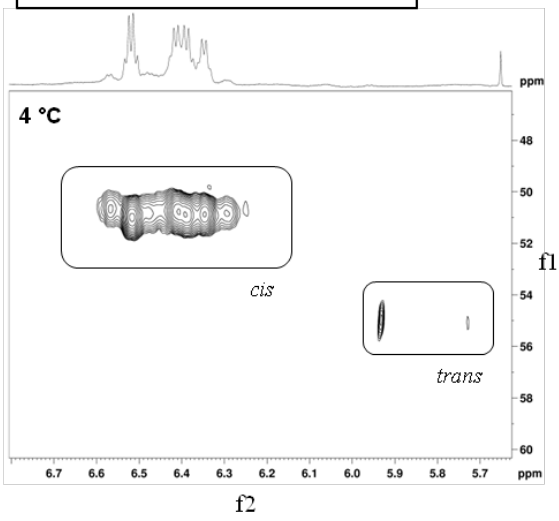

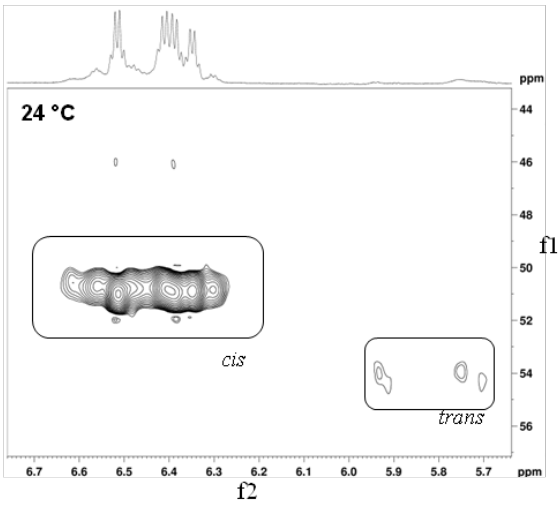

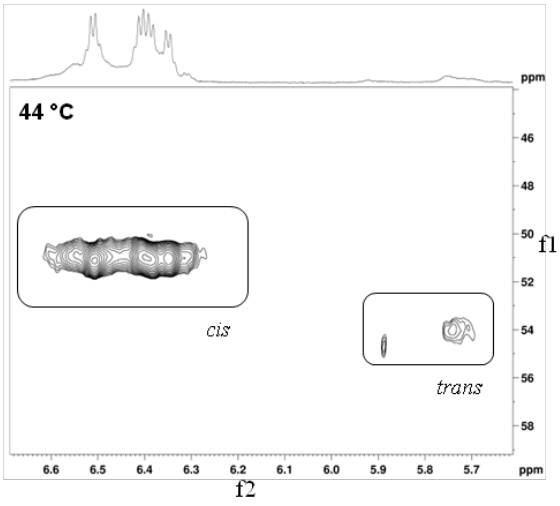

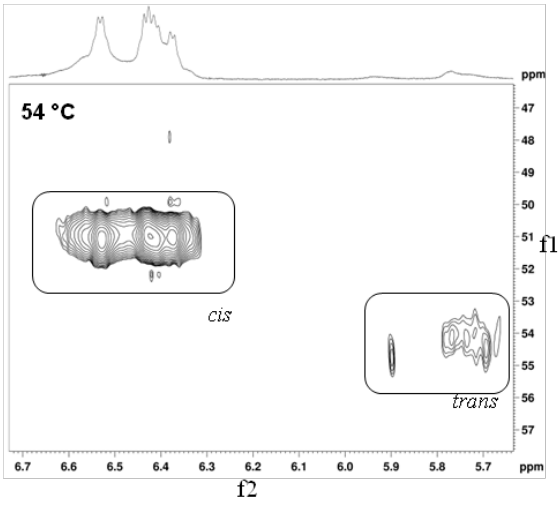

Table S-2. Overall $K_{cis/trans}$ values of the *N*s1npe residues in peptoids **3**–**8.**

Peptoid	Solvent	Temperature (°C)	# of *N*s1npe residues	Overall $K_{cis/trans}$ values for *N*s1npe residues [a]
3	$CDCl_3$	24	2	10
4a	$CDCl_3$	24	2	25
4b	$CDCl_3$	24	2	19
5	$CDCl_3$	24	3	47
6	$CDCl_3$	24	3	30
6*i*	$CDCl_3$	24	3	28
7	$CDCl_3$	24	4	48
8	$CDCl_3$	4	4	144
8	$CDCl_3$	14	4	88
8	$CDCl_3$	24	4	53
8	$CDCl_3$	34	4	37
8	$CDCl_3$	44	4	29
8	CD_3OD	4	4	39
8	CD_3OD	24	4	35
8	CD_3OD	44	4	18
8	CD_3OD	54	4	9

[a] Determined by integrating rotamer-related peaks of the *N*s1npe methine protons in ^1H-^{13}C HSQC spectra (700 MHz, peptoids between 4–10 mM).

NMR structural studies.

*2D NMR methods and spectra for peptoids **4a** and **4b***

Peptoids **4a** and **4b** were further analyzed by NOESY and gCOSY NMR experiments in $CDCl_3$ (10 mM) at 24 °C. NOESY experiments on **4a** and **4b** were performed using the following parameter values: sw = 5178 and 5236 Hz, respectively; d1 = 6.0 s; mixing time = 0.7 s; ni = 431 and 436, respectively; nt = 16. The number of points for both spectra was 2048. The spectra were zero-filled to generate matrices of 4096 x 4096 points. gCOSY experiments on **4a** and **4b** were performed using the following parameter values: sw = 5113 and 5273 Hz, respectively; d1 = 6.0 s; ni = 426 and 440, respectively; nt = 8. The number of points was 2048.

Peptoid **4a** (600 MHz, $CDCl_3$, 10 mM, 24 °C)

4a — NOESY

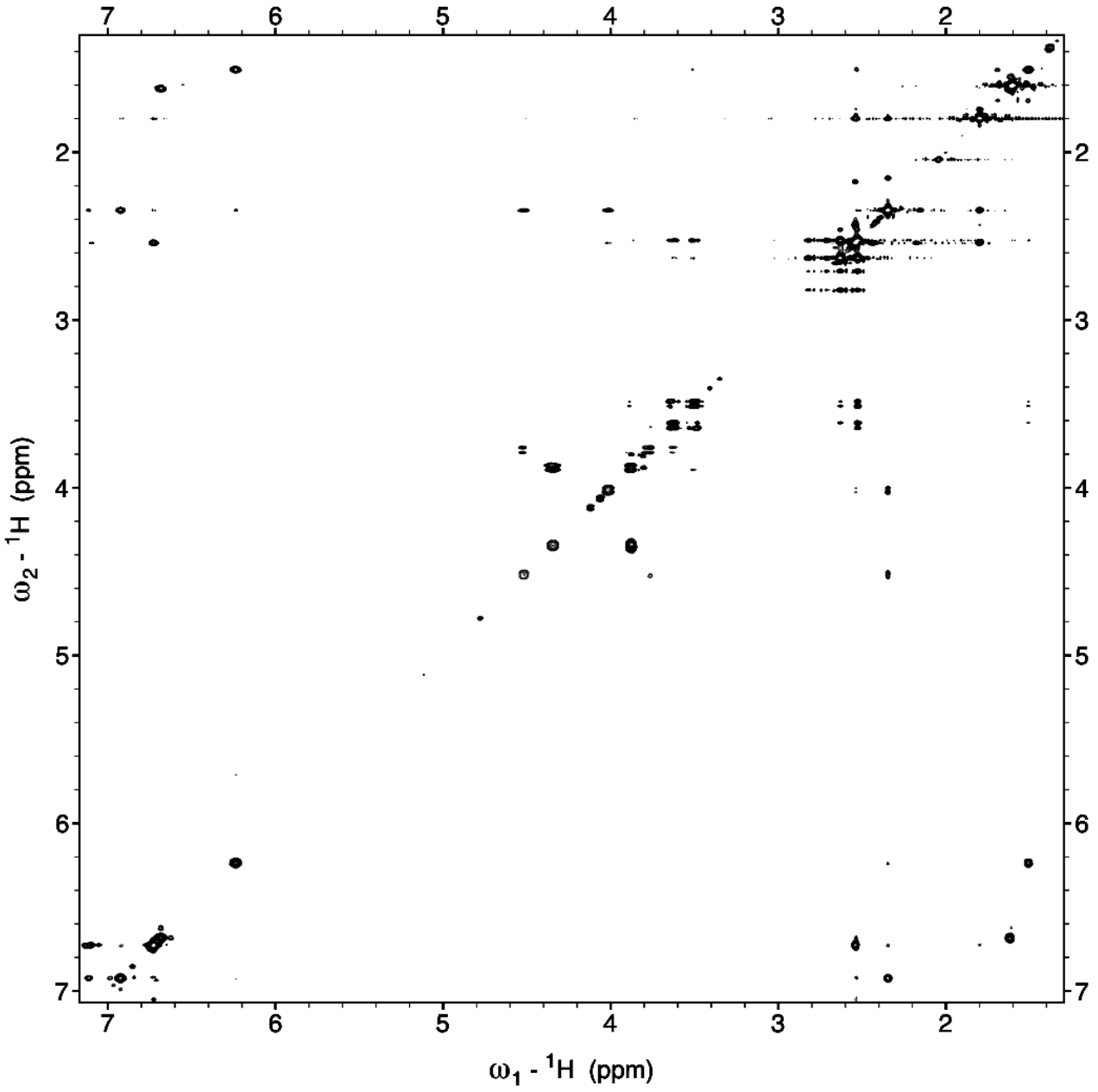

4a — gCOSY

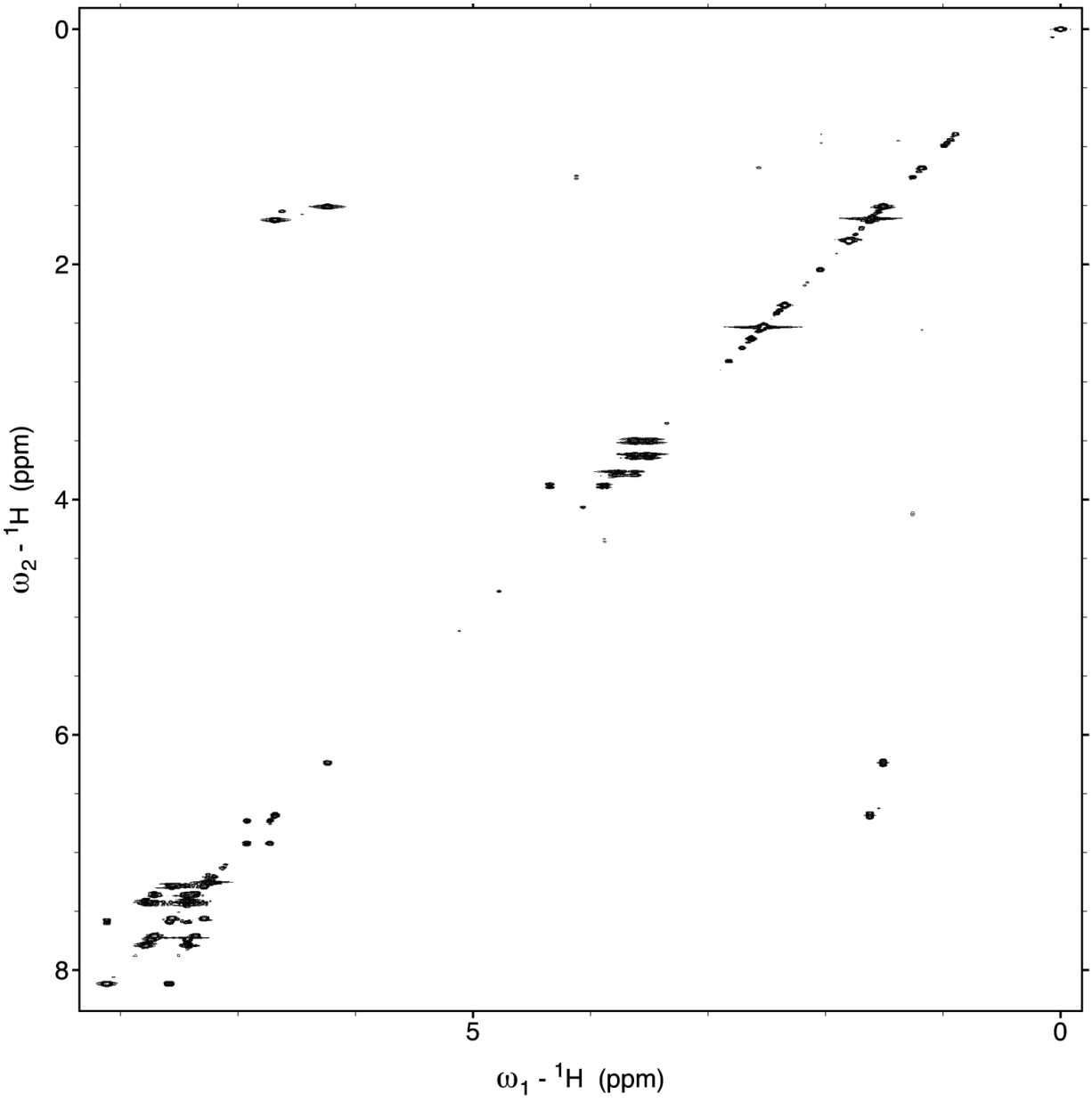

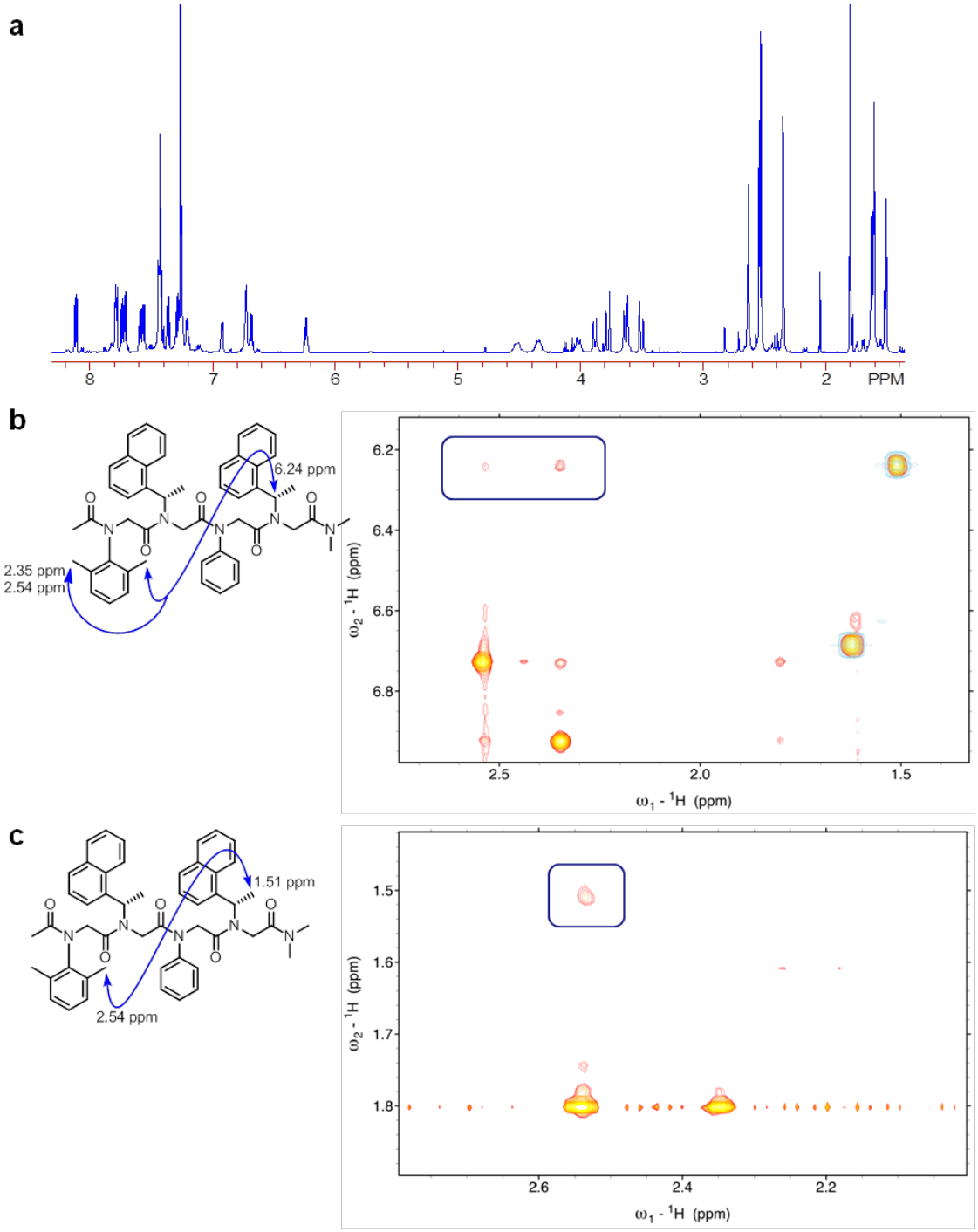

Figure S-6. Side chain to side chain, long-range NOEs observed for peptoid **4a**. Assignments were aided by using NOE correlations to the N- and C-terminal methyl groups. (a) ^{1}H NMR spectrum (600 MHz, $CDCl_3$, 10 mM, 24 °C). (b) NOESY (red-yellow) and gCOSY (light blue) overlaid spectra indicating the NOEs (dark blue box) observed between both methyl groups on the *i* residue and the methine proton of the *i*+3 side chain. (c) NOESY (red-yellow) and gCOSY (light blue – no peaks are present in the region shown) overlaid spectra indicating the NOEs (dark blue box) observed between a methyl group on the *i* residue and the methyl group of the *i*+3 residue.

Peptoid **4b** (600 MHz, $CDCl_3$, 10 mM, 24 °C)

4b — NOESY

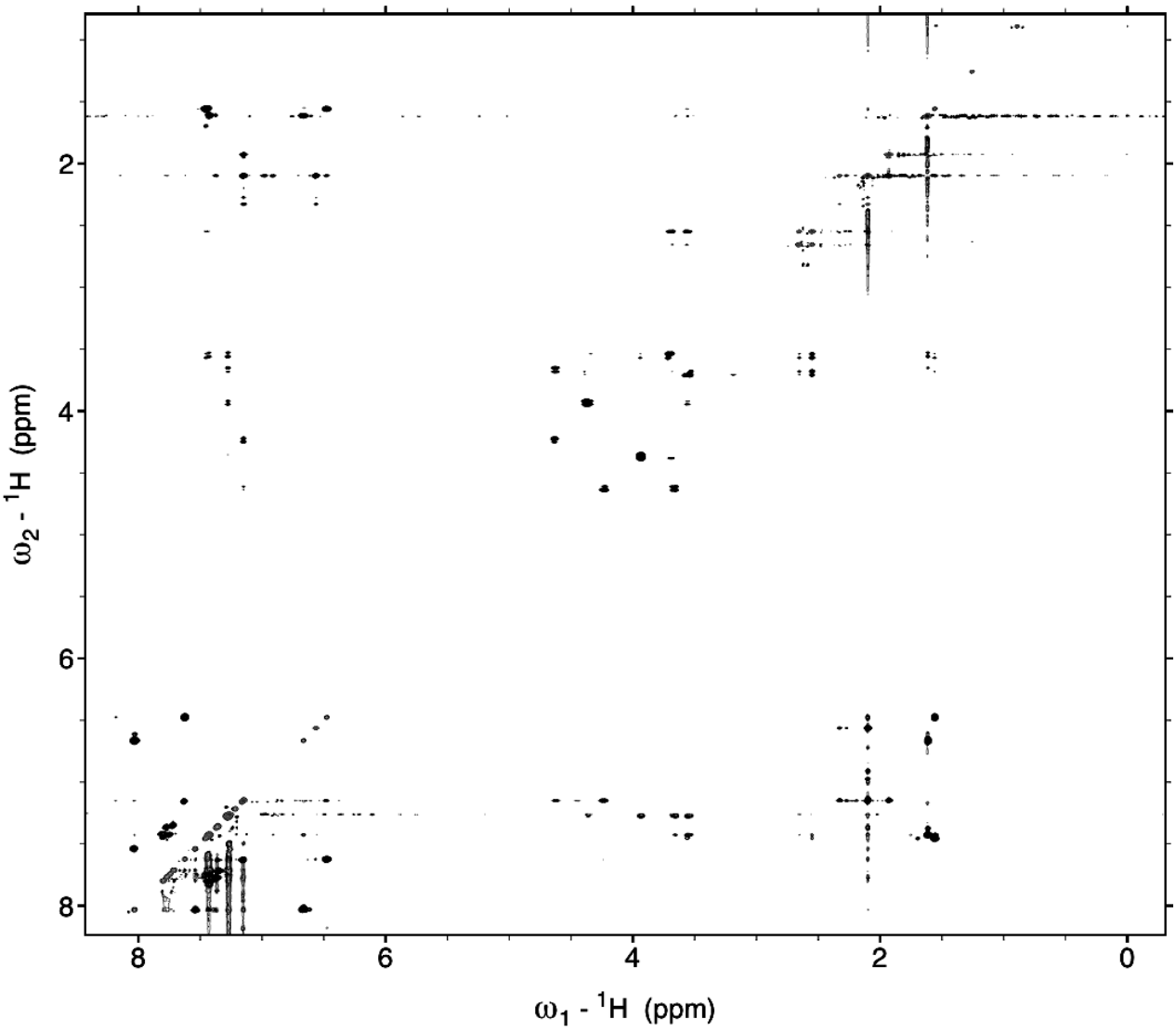

4b—gCOSY

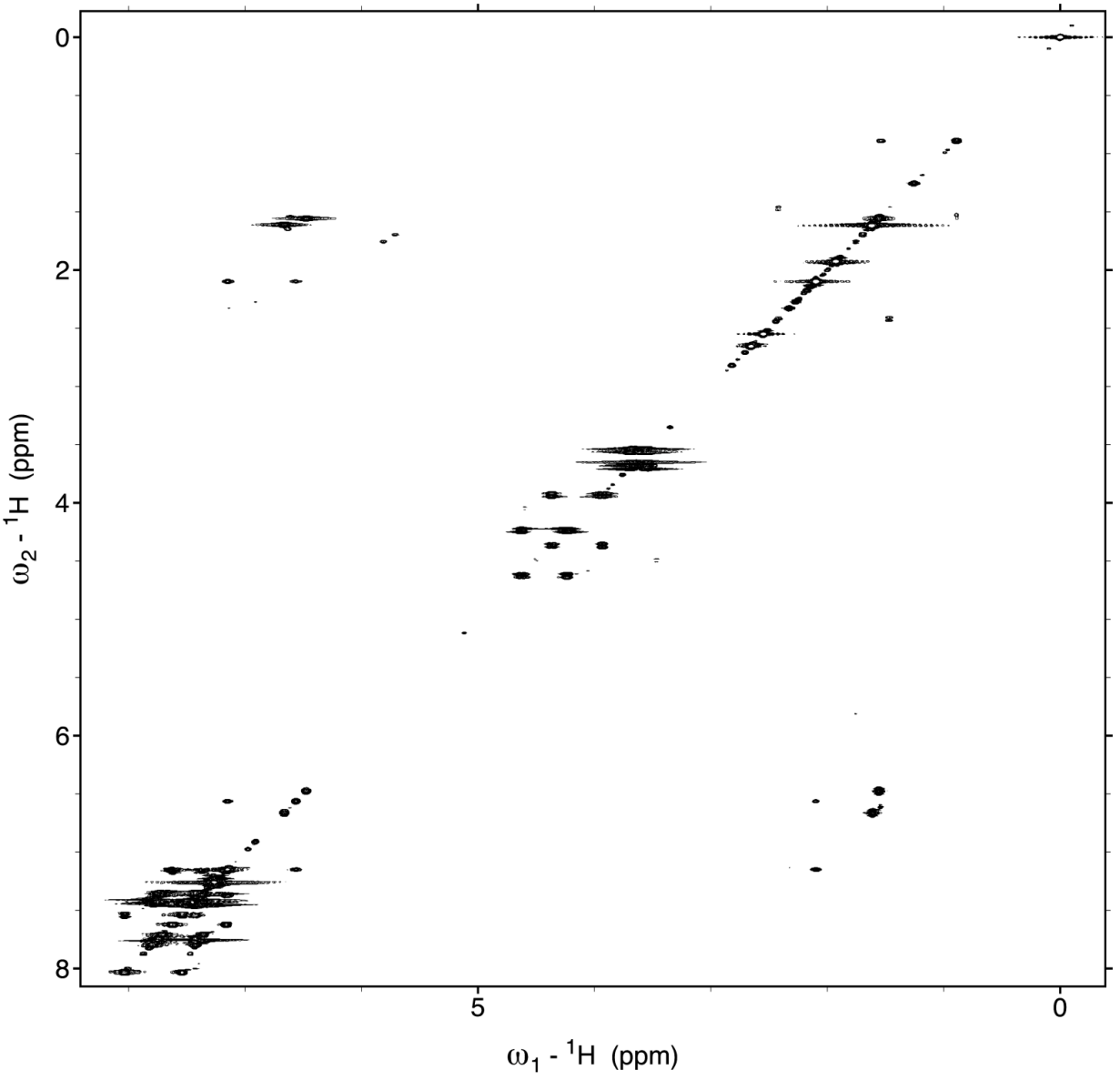

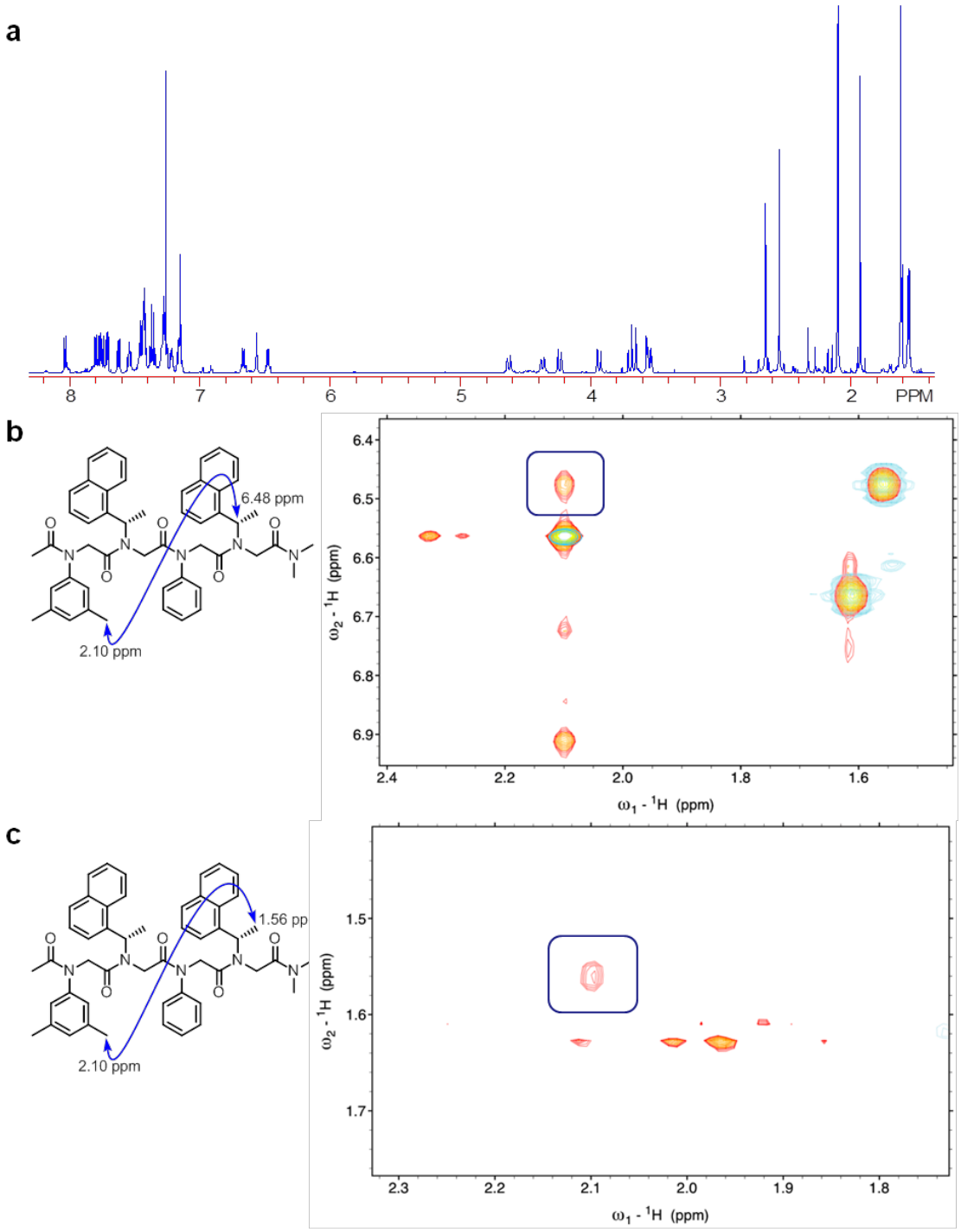

Figure S-7. Side chain to side chain, long-range NOEs observed for peptoid **4b**. Assignments were aided by using NOE correlations to N- and C-terminal methyl groups. (a) ^{1}H NMR spectrum (600 MHz, $CDCl_3$, 10 mM, 24 °C). (b) NOESY (red-yellow) and gCOSY (light blue) overlaid spectra indicating the NOEs (dark blue box) observed between the methyl groups of the *i* residue and the methine proton of the *i*+3 side chain. (c) NOESY (red-yellow) and gCOSY (light blue – no peaks are present in the region shown) overlaid spectra indicating the NOEs (dark blue box) observed between a methyl group on the *i* residue and the methyl group of the *i*+3 side chain.

*2D NMR methods and spectra for peptoid **6i***

Peptoid **6*i*** was further analyzed by ^{1}H-^{13}C gHMBCAD, ^{1}H-^{13}C HSQCAD, gCOSY, and ROESY experiments in $CDCl_3$ (10 mM) at 15 °C for structure determination. Spectral parameters for the ^{1}H-^{13}C gHMBCAD experiment were: sw = 5660 Hz; d1 = 9.0 s; ni = 250; nt = 8; a delay for $^{3}J_{CH}$ scalar couplings of 6–9 Hz = 9 s; number of points = 2048. Spectral parameters for the ^{1}H-^{13}C HSQCAD experiment are provided above (see page S-11). Spectral parameters for the gCOSY experiment were: sw = 5660 Hz; d1 = 9.0 s; ni = 450; nt = 4; number of points = 2048. Spectral parameters for the ROESY experiment were: sw = 5660 Hz; d1 = 10.0 s; mixing time = 1.5 s; ni = 400; nt = 8; number of points = 2048.

Peptoid **6*i*** (600 MHz, $CDCl_3$, 10 mM, 15 °C)

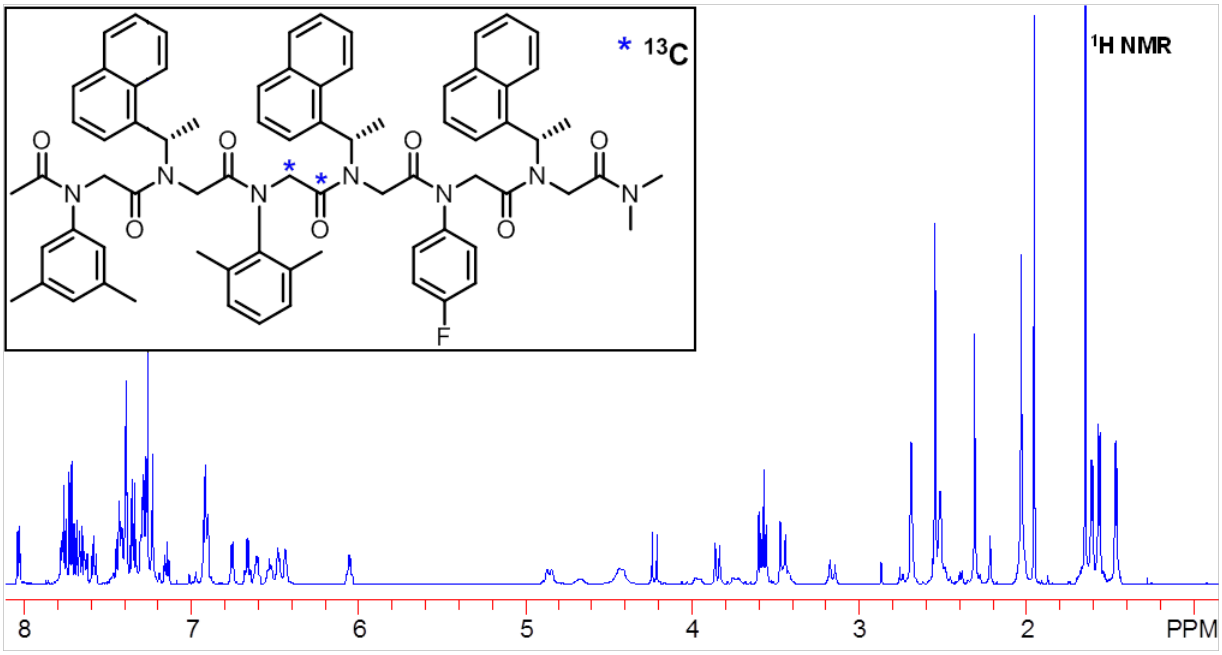

6*i* — ^{1}H-^{13}C gHMBCAD

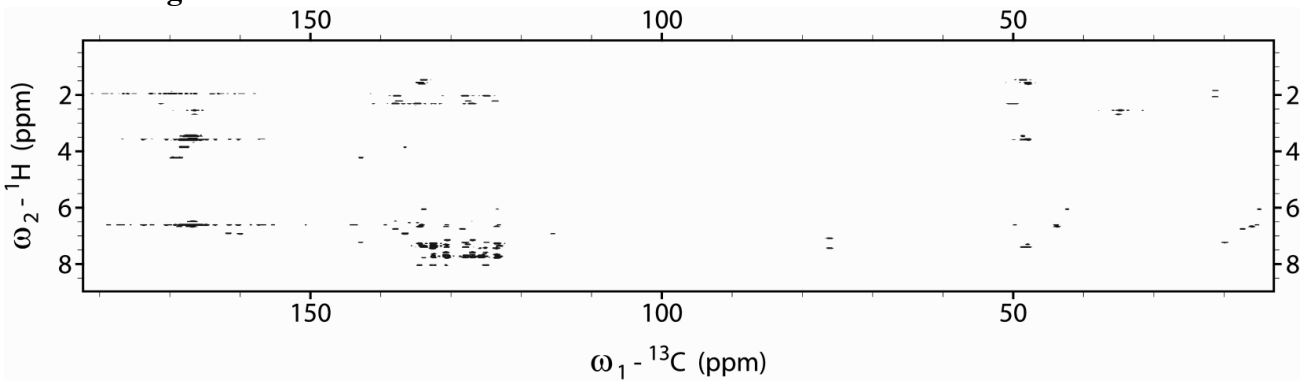

6*i* — ^{1}H-^{13}C HSQCAD

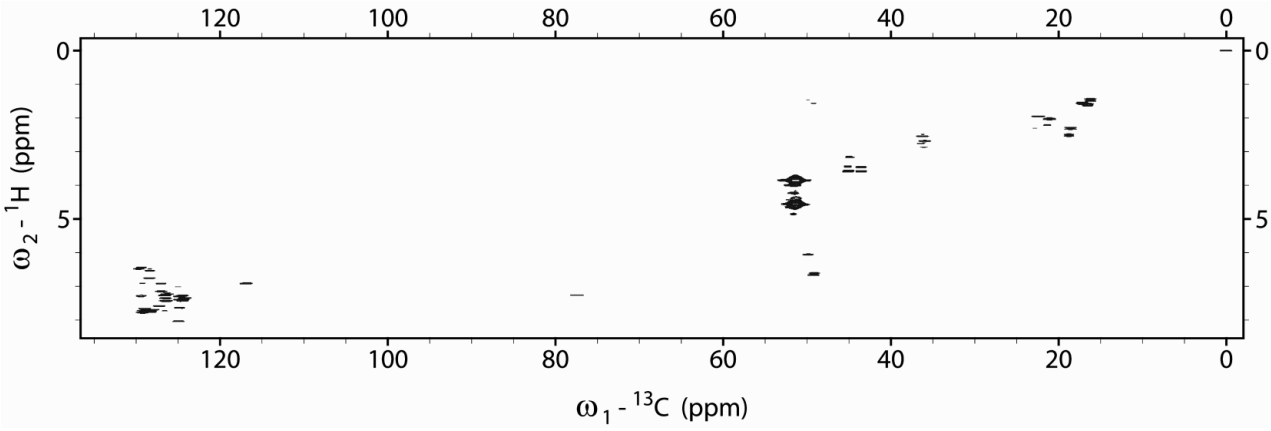

6*i* — gCOSY

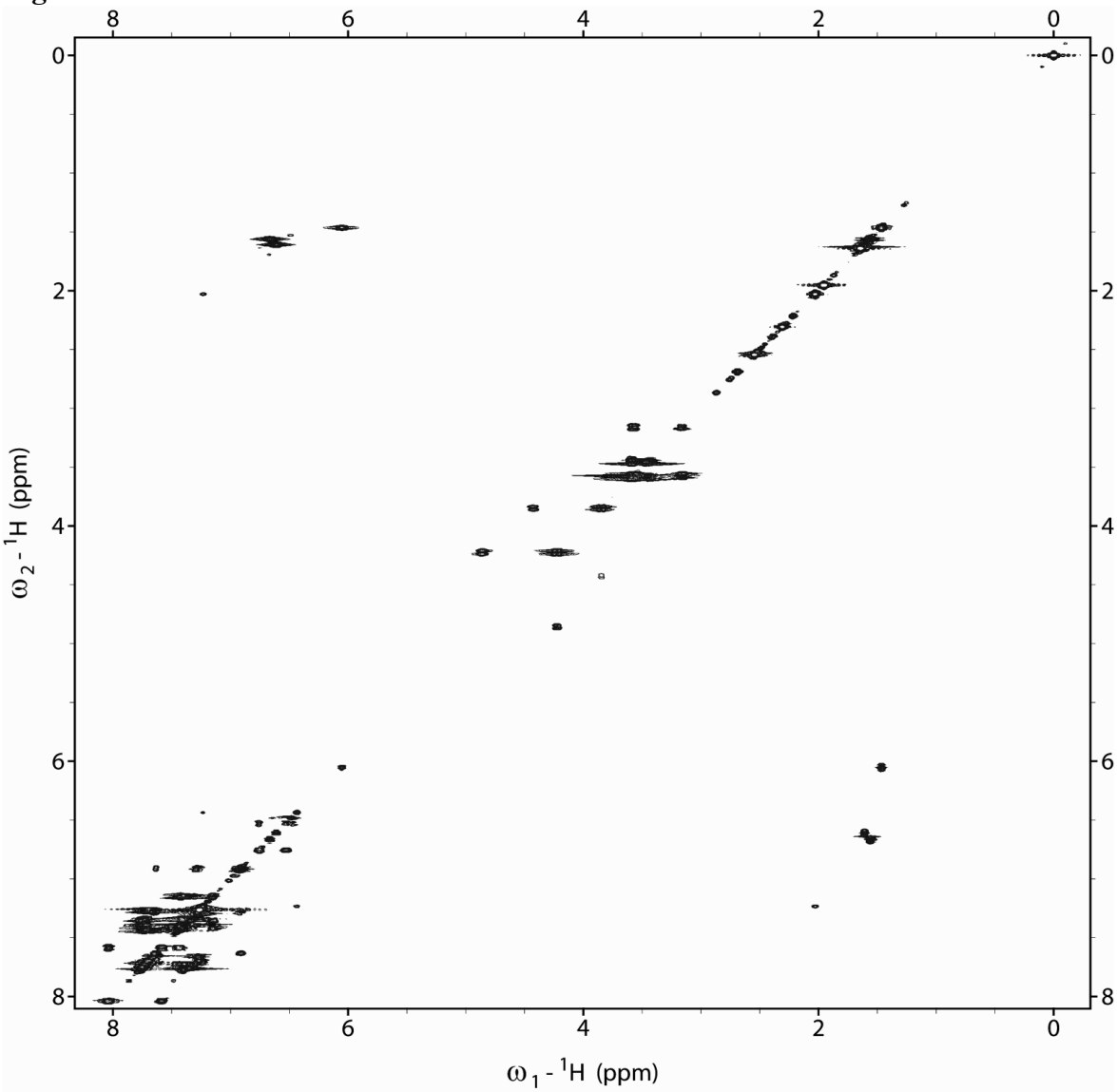

6*i* — ROESY

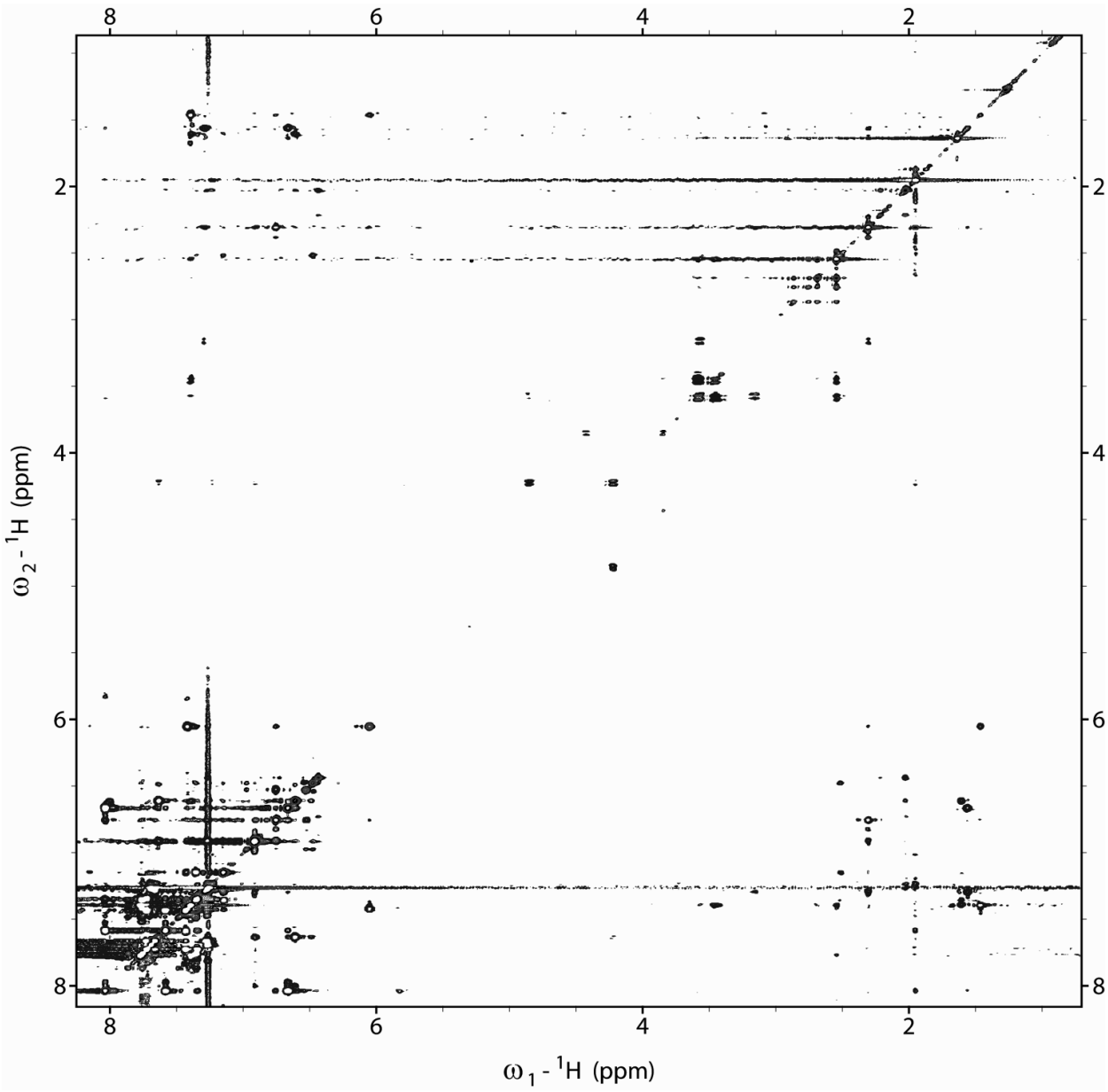

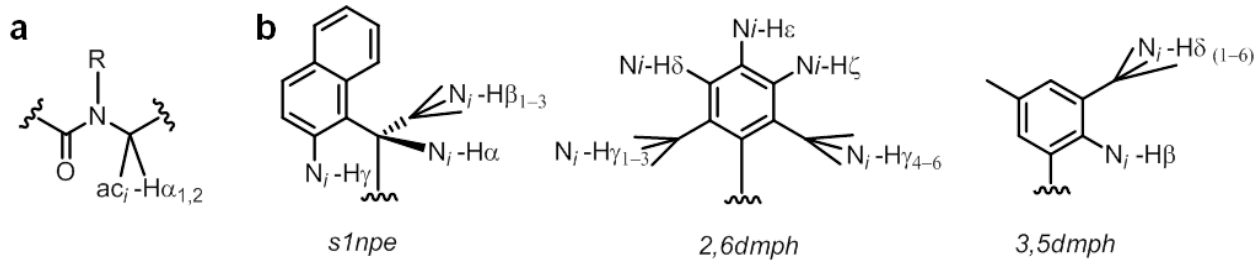

Figure S-8. General atomic nomenclature used for the peptoid main chain (a) and side chain (b) protons that were relevant for NMR assignments.

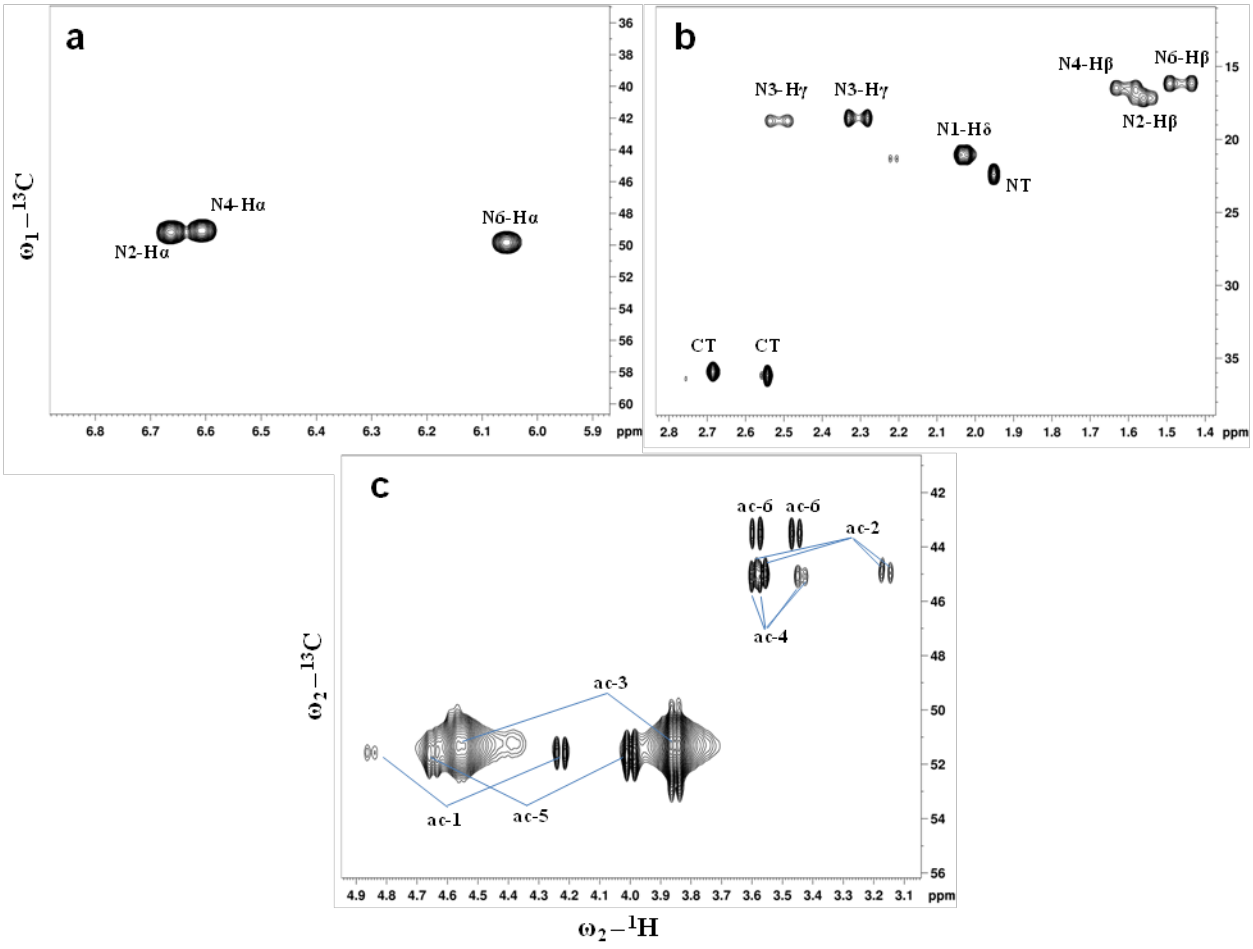

Figure S-9. Assignments of the side chain *s1npe* methine resonances (a), all methyl groups (including N- and C-terminal methyl groups) (b), and the main chain methylene (c) resonances in partial ^{1}H-^{13}C HSQC spectra of peptoid **6*i***.

*Structure determination for peptoid **6i**.*

One major conformer of **6*i*** was observed by NMR in all experiments that were conducted. Assignments of peptoid resonances were made through a combination of examining chemical shifts and integrations and using the correlations from the two dimensional experiments described above, according to standard methods used in previous studies of peptoids.[6-8] Nine unambiguous inter-residue ROEs between side chain proton resonances were used as distance restraints for structure calculations (see Table S-3 below). Rather than bin ROEs into strong, medium, weak, and so forth, we took a more conservative approach, and set all distance restraints to be < 5 or 6 Å. ROESY cross peaks involving the main chain methylene groups were extremely weak and prevented the incorporation of distance restraints involving the peptoid backbone in our calculations. However, the ω main chain torsion angles of the three *N*s1npe residues in this peptoid were restrained to 0° ± 25° based on the chemical shifts of side chain methine resonances (indicating *cis* ω bonds at these residues). Analysis of the X-ray crystal structures presented in this study, and in a previous report from our laboratory,[9] revealed that the main chain amide conformations of *N*s1npe peptoids can significantly deviate from 0°.

NMR-restrained, molecular dynamic simulated annealing calculations of **6*i*** were carried out using the AMBER11 software program. The input coordinate file of an extended structure was generated from a Gaussian Output pdb file by using a combination of the Antechamber tool in AMBER and a natural bond order (NBO) analysis of **6*i*** (to provide partial atomic charges). A molecular parameter/topology file was then generated using the LEaP command. Structure refinement was accomplished by running 150 independent simulated annealing calculations incorporating the NMR restraints discussed above, using the Sander command tool. The annealing protocol is provided below. A pseudo-random number was used as the seed for each starting velocity during individual runs, and the final force constants for the distance and torsion angle restraints were set to 32 kcal mol^{-1} $Å^{-1}$ and 32 kcal mol^{-1} rad^{-1}, respectively. The total energies of the final structures generated from each calculation were compared, and the 10 lowest energy structures were chosen for comparison and structural analysis.

Table S-3. Assignments of ^{1}H peaks and select ROEs that were used as restraints in the calculated structure of peptoid ***6i***.

δ (ppm)	multiplicity	relative integration	assignment	ROE
1.46	d	3	N_6–H$\beta_{1\text{-}3}$	N_6–Hγ
1.56	d	3	N_2–H$\beta_{1\text{-}3}$	N_3–H$\gamma_{1\text{-}3}$
1.60	d	3	N_4–H$\beta_{1\text{-}3}$	
1.95	s	3	*NT–$H_{1\text{-}3}$	
2.03	s	6	N_1–H$\delta_{1\text{-}6}$	N_4–Hα
2.30	s	3	N_3–H$\gamma_{1\text{-}3}$	N_6–Hα
2.52	s	3	N_3–H$\gamma_{4\text{-}6}$	
2.55	s	3	*CT–$H_{1\text{-}3}$	N_6–Hγ
2.69	s	3	*CT–$H_{4\text{-}6}$	
3.16	d	1	ac_2–Hα_1	N_3–H$\gamma_{1\text{-}3}$
3.43	d	1	ac_4–Hα_1	
3.46	d	1	ac_6–Hα_1	*CT–$H_{1\text{-}3}$
3.56	d	1	ac_2–Hα_2	
3.59	d	1	ac_6–Hα_2	*CT–$H_{1\text{-}3}$
3.73	brd d	1	ac_4–Hα_2	
3.85	d	1	ac_3–Hα_1	
3.96	brd d	1	ac_5–Hα_1	
4.23	d	1	ac_1–Hα_1	
4.43	brd d	1	ac_3–Hα_2	
4.66	brd d	1	ac_5–Hα_2	
4.86	brd d	1	ac_1–Hα_2	$^{**}ac_2$–Hα_2
6.05	q	1	N_6–Hα	
6.47	m	1	N_3–Hζ	
6.53	m	1	N_3–Hε	
6.61	q	1	N_4–Hα	
6.67	q	1	N_2–Hα	
6.76	m	1	N_3–Hδ	N_6–Hα
7.23	brd s	2	N_1–H$\beta_{1\text{and}2}$	
7.40	s	1	N_6–Hγ	ac_6–Hα_1

* NT = N-terminal, CT = C-terminal; brd = broad. ** Very weak and not used as a distance restraint

Restraint file for AMBER simulated annealing calculations:

```
# Torsion restraints for Peptoid 6i from NMR data
#
# 2  Ns1npe:  (C59)-(C67)-(N)-(C69)   -25.0 25.0
 &rst     iat =    67,    75,    1,    77,
         r1 = -26.0, r2 = -25.0, r3 = 25.0, r4 = 26.0,
         rk2 =  32.0, rk3 =  32.0,                      &end
# 4  Ns1npe:  (C71)-(C72)-(N3)-(C73)   -25.0 25.0
 &rst     iat =   79,   80,   4,   81,
         r1 = -26.0, r2 = -25.0, r3 = 25.0, r4 = 26.0,  &end
# 6  Ns1npe:  (C1)-(C2)-(N5)-(C10)   -25.0 25.0
 &rst     iat =   9,   10,   6,   18,
         r1 =  -26.0, r2 = -25.0, r3 = 25.0, r4 = 26.0, &end
#
#
#Distance restraints for Peptoid 6i from NMR data
#
#    ac1- C(alpha)    ac2-C(alpha)       < 5.0 Å
 &rst
  ixpk= 0, nxpk= 0, iat=  67,  77, r1= 2.00, r2= 2.50, r3= 5.00, r4= 5.50,
      rk2=0.0, rk3=32.0, ir6=1, ialtd=0,        &end
#    ac2-C(alpha)      N3-C(gamma1)       < 5.0 Å
 &rst
  ixpk= 0, nxpk= 0, iat= 77,  73, r1= 2.00, r2= 2.50, r3= 5.00, r4= 5.50,  &end
#
#    N2-C(beta1)       N3-C(gamma1)       < 6.0 Å
 &rst
  ixpk= 0, nxpk= 0, iat=  38,  73, r1= 3.00, r2= 3.50,  r3= 6.00, r4= 6.50,  &end
#
#    N1-C(delta1)      N4-H(alpha)        < 5.0 Å
 &rst
  ixpk= 0, nxpk= 0, iat=  41,  90, r1= 2.00, r2= 2.50,  r3= 5.00, r4= 5.50,  &end
#
#    N3-H(delta)       N6-H(alpha)        < 5.0 Å
 &rst
  ixpk= 0, nxpk= 0, iat=  103,  99, r1= 2.00, r2= 2.50, r3= 5.00, r4= 5.50,  &end
#
#    N3-C(gamma1)      N6-H(alpha)        < 5.0 Å
 &rst
  ixpk= 0, nxpk= 0, iat= 73, 99, r1= 2.00, r2= 2.50, r3= 5.00, r4= 5.50,  &end
#
#    N6-H(gamma)       ac2-C(alpha)       < 5.0 Å
 &rst
  ixpk= 0, nxpk= 0, iat=  133,  18, r1= 2.00, r2= 2.50, r3= 5.00, r4= 5.50,  &end
#
#    N6-H(gamma)       CT-H(1-3)          < 6.0 Å
 &rst
  ixpk= 0, nxpk= 0, iat= 133, 21, r1= 3.00, r2= 3.50, r3= 6.00, r4= 6.50,  &end
#
#    CT-C(1)         ac2-C(alpha)       < 5.0 Å
 &rst
  ixpk= 0, nxpk= 0, iat=  21,  18, r1= 1.00, r2= 1.50, r3= 5.00, r4= 5.50,  &end
```

Command file for AMBER simulated annealing calculations:

```
simulated annealing protocol, 200 ps

 &cntrl
    ig=-1, nstlim=240000, pencut=0.01,
    ipnlty=1, nmropt=1, tempi=1
    ntpr=200, ntt=1, ntwx=200,
    cut=15.0, ntb=0, vlimit=12,
 /
 &ewald
    eedmeth=5,
 /
#
#Simulated annealing:
#
##
 &wt type='TEMP0', istep1=0,istep2=50000,value1=1200.0,
            value2=1200.0,    /
 &wt type='TEMP0', istep1=50001, istep2=60000, value1=1200.0,
            value2=1000.0,     /
 &wt type='TEMP0', istep1=60001, istep2=120000, value1=1000.0,
            value2=800.0,     /
 &wt type='TEMP0', istep1=120001, istep2=140000, value1=800.0,
            value2=800.0,     /
 &wt type='TEMP0', istep1=140001, istep2=160000, value1=800.0,
            value2=600.0,     /
 &wt type='TEMP0', istep1=160001, istep2=180000, value1=600.0,
            value2=600.0,     /
&wt type='TEMP0', istep1=180001, istep2=200000, value1=600.0,
            value2=298.0,     /
 &wt type='TEMP0', istep1=200001, istep2=220000, value1=298.0,
            value2=298.0,     /
 &wt type='TEMP0', istep1=220001, istep2=240000, value1=298.0,
            value2=0.0,       /


 &wt type='TAUTP', istep1=0,istep2=50000,value1=0.4,
            value2=0.4,     /
 &wt type='TAUTP', istep1=50001,istep2=160000,value1=4.0,
            value2=4.0,     /
 &wt type='TAUTP', istep1=160001,istep2=180000,value1=2.0,
            value2=1.0,     /
 &wt type='TAUTP', istep1=180001,istep2=200000,value1=1.0,
            value2=0.1,     /
 &wt type='TAUTP', istep1=200001,istep2=240000,value1=0.1,
            value2=0.05,    /
 &wt type='REST', istep1=0,istep2=40000,value1=0.1,
            value2=1.0,  /
 &wt type='REST', istep1=40001,istep2=240000,value1=1.0,
            value2=1.0,  /

 &wt type='END'  /
LISTOUT=POUT
DISANG=RST
```

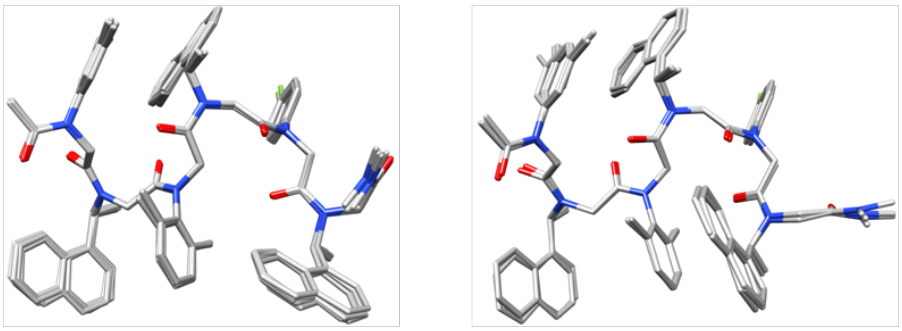

Figure S-10. View of two low energy populations of peptoid **6*i*** (termed **6*i*-A** and **6*i*-B**) as determined by NMR-restrained AMBER calculations.

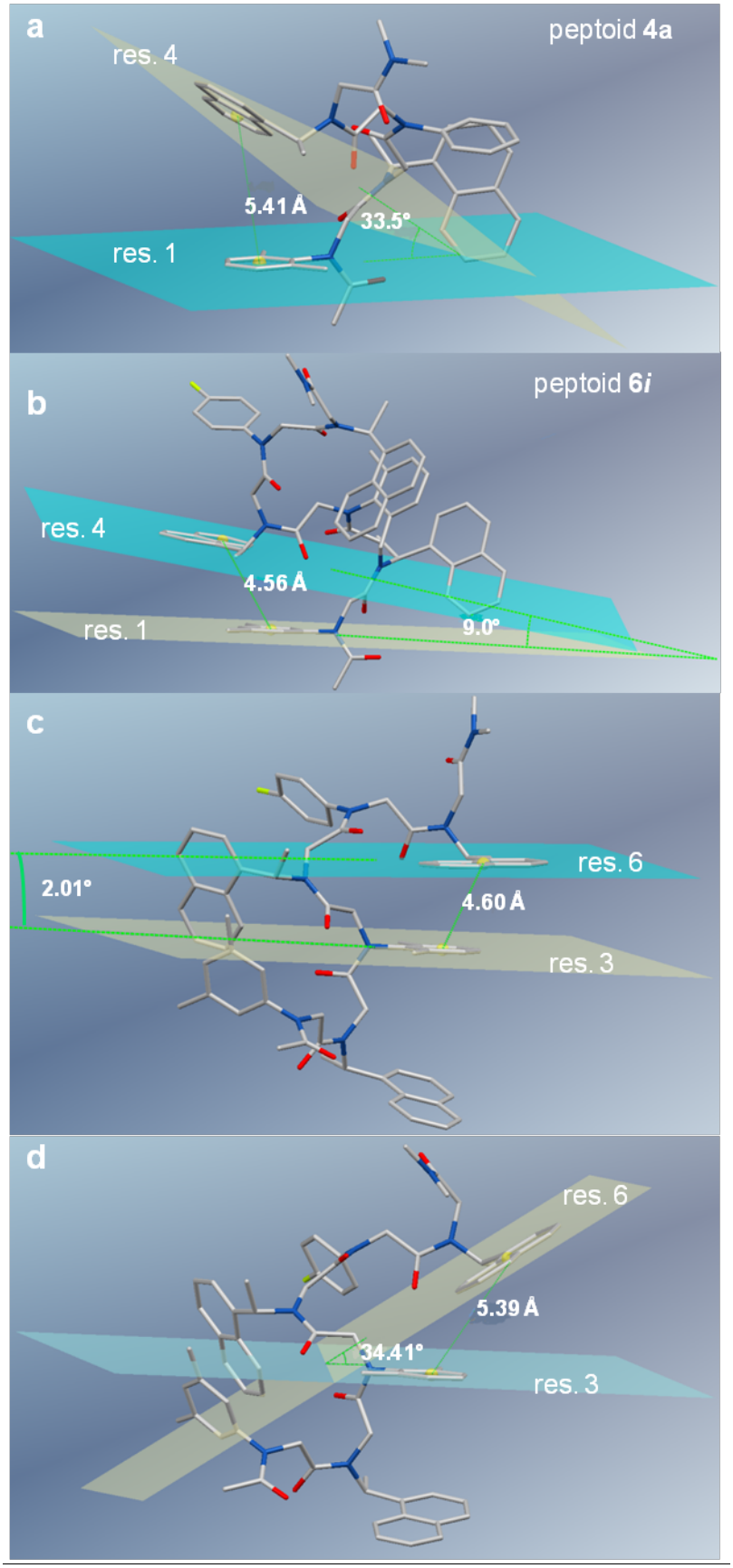

Figure S-11. (a) An aromatic-aromatic stacking interactions detected between the side chains of residues 1 and 4 in the X-ray crystal structure of **4a**. (b) An aromatic-aromatic stacking interactions detected between the side chains of residues 1 and 4 in all low energy structures of **6*i***. The side chain aryl rings of residues 1 and 4 were oriented in a parallel displaced stacking fashion (angle between aromatic planes = 9.0°) with a centroid–centroid distance of 4.6 Å and nearest interresidue C–C distance of 3.4 Å. (c) An aromatic-aromatic stacking interactions detected between the side chains of residues 3 and 6 in the population of structures of **6*i*-B**. In this ensemble, the aryl side chains were oriented in a parallel displaced stacking fashion (angle between aromatic planes = 2.1°) with a centroid–centroid distance of 4.6 Å and nearest interresidue C–C distance of 3.5 Å. (d) Aromatic-aromatic stacking interactions detected between the side chains of residues 3 and 6 in the population of structures of **6*i*-A**. In this ensemble of structures the side chains were oriented in an oblique displaced stacking fashion (angle between aromatic planes = 34.4°) with a centroid-centroid distance of 5.4 Å and nearest interresidue C–C distance of 3.3 Å.

***Note*: Mercury 3.0 was used to measure all distances and angles, and to generate the images in this figure.

Supplemental X-ray crystallographic data and crystal packing diagrams for Br-Nph-Ns1npe-dma, 3, and 4a.

General. A small quantity (~10 mg) of each peptoid was dissolved in reagent–grade 1-propanol. Slow evaporation after ~10-12 days at rt afforded crystals of **Br-Nph-Ns1npe-dma**, **3**, and **4a** that were suitable for X-ray analysis.

The coordinates for the structures of **Br-Nph-Ns1npe-dma**, **3**, and **4a** are deposited at the Cambridge Crystallographic Data Centre with deposition numbers 868892, 868891, and 868890, respectively.

Peptoid intermediate Br-Nph-Ns1npe-dma

Data collection. A colorless crystal with approximate dimensions 0.80 x 0.16 x 0.05 mm^3 was selected under oil under ambient conditions and attached to the tip of a MiTeGen MicroMount©. The crystal was mounted in a stream of cold nitrogen at 100(1) K and centered in the X-ray beam by using a video camera.

The crystal evaluation and data collection were performed on a Bruker Quazar SMART APEXII diffractometer with Mo K_α (λ = 0.71073 Å) radiation and the diffractometer to crystal distance of 4.96 cm. The initial cell constants were obtained from three series of ω scans at different starting angles. Each series consisted of 12 frames collected at intervals of 0.5º in a 6º range about ω with the exposure time of 10 sec per frame. The reflections were successfully indexed by an automated indexing routine built in the APEXII program suite. The final cell constants were calculated from a set of 9205 strong reflections from the actual data collection.

The data were collected by using the full sphere data collection routine to survey the reciprocal space to the extent of a full sphere to a resolution of 0.70 Å. A total of 95464 data were harvested by collecting 6 sets of frames with 0.4 and 0.5º scans in ω and ϕ with exposure times of 70 sec per frame. These highly redundant datasets were corrected for Lorentz and polarization effects. The absorption correction was based on fitting a function to the empirical transmission surface as sampled by multiple equivalent measurements.[13]

Structure solution and refinement. The systematic absences in the diffraction data and *E*-statistics were uniquely consistent for the space group *C*2 that yielded chemically reasonable and computationally stable results of refinement.[14-16] A successful solution by the direct methods provided most non-hydrogen atoms from the *E*-map. The remaining non-hydrogen atoms were located in an alternating series of least-squares cycles and difference Fourier maps. All non-hydrogen atoms were refined with anisotropic displacement coefficients. All hydrogen atoms were included in the structure factor calculation at idealized positions and were allowed to ride on the neighboring atoms with relative isotropic displacement coefficients.

The only crystal large enough for the single-crystal X-ray diffraction experiment proved to be a non-merohedral twin with a 9.37(3)% second component contribution. The twin components were related by a 179.9° rotation about *a* axis. There were two symmetry independent molecules

with the same composition and handedness in the asymmetric unit. The chiral centers at C15 and C15a were determined to be S. The final least-squares refinement of 602 parameters against 40060 data resulted in residuals *R* (based on F^2 for $I \geq 2\sigma$) and *wR* (based on F^2 for all data) of 0.0507 and 0.1210, respectively. The final difference Fourier map was featureless.

Crystal data and structure refinement for Br-*N*ph-*N*s1npe-dma:

Empirical formula	$C_{26}\,H_{28}\,Br\,N_3\,O_3$	
Formula weight	510.42	
Temperature	100(1) K	
Wavelength	0.71073 Å	
Crystal system	Monoclinic	
Space group	C2	
Unit cell dimensions	a = 17.8626(9) Å	a= 90°
	b = 9.9686(5) Å	b= 103.580(3)°
	c = 27.3919(13) Å	g = 90°
Volume	4741.2(4) $Å^3$	
Z	8	
Density (calculated)	1.430 Mg/m^3	
Absorption coefficient	1.767 mm^{-1}	
F(000)	2112	
Crystal size	0.80 x 0.16 x 0.05 mm^3	
Theta range for data collection	2.29 to 27.50°.	
Index ranges	-23<=h<=23, -12<=k<=12, -35<=l<=35	
Reflections collected	40006	
Independent reflections	10875 [R(int) = 0.0308]	
Completeness to theta = 25.00°	99.8%	
Absorption correction	Numerical with SADABS	
Max. and min. transmission	0.9168 and 0.3322	
Refinement method	Full-matrix least-squares on F^2	
Data / restraints / parameters	40060 / 1 / 602	
Goodness-of-fit on F^2	0.975	
Final R indices [I>2sigma(I)]	R1 = 0.0507, wR2 = 0.1169	
R indices (all data)	R1 = 0.0615, wR2 = 0.1210	
Absolute structure parameter	0.0937(3)	
Largest diff. peak and hole	1.281 and -1.024 $e.Å^{-3}$	

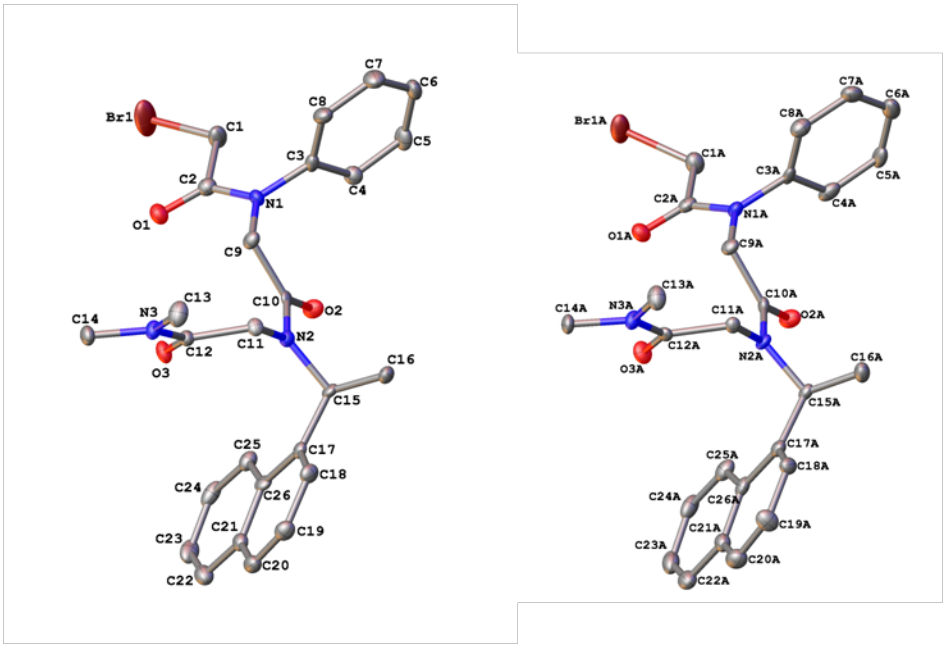

Figure S-12. A molecular drawing of the two independent molecules of **Br-*N*ph-*N*s1npe-dma**. All hydrogen atoms are omitted and the molecules are drawn with 50% probability ellipsoids.

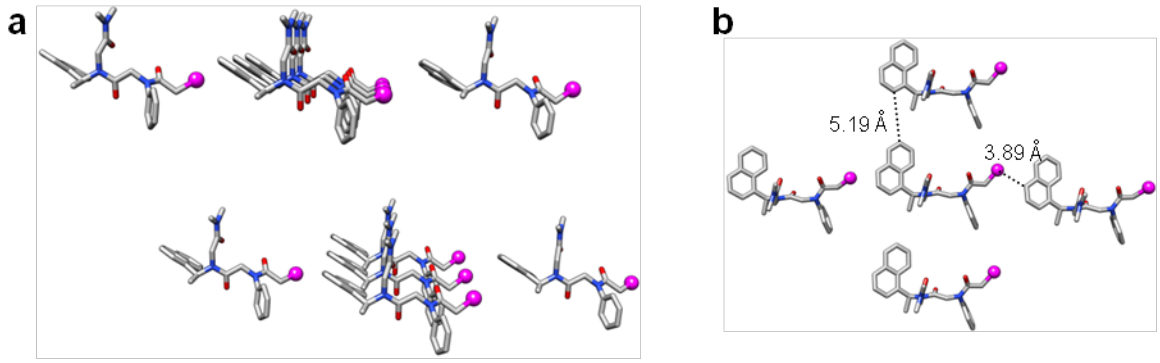

Figure S-13. (a) A stereoview of the crystal packing of the two symmetry independent molecules in the crystal structure of **Br-*N*ph-*N*s1npe-dma**. (b) A view of one of the symmetry independent molecules looking down from the C-termini. The black dashed lines indicate selected intermolecular distances. Hydrogen atoms have been omitted in both (a) and (b).

Peptoid 3

Data collection. A colorless crystal with approximate dimensions 0.51 x 0.40 x 0.23 mm^3 was selected under oil under ambient conditions and attached to the tip of a MiTeGen MicroMount©. The crystal was mounted in a stream of cold nitrogen at 100(1) K and centered in the X-ray beam by using a video camera. The crystal evaluation and data collection were performed on a Bruker SMART APEXII diffractometer with Cu Kα (λ = 1.54178 Å) radiation and the diffractometer to crystal distance of 4.03 cm.

The initial cell constants were obtained from three series of scans at different starting angles. Each series consisted of 50 frames collected at intervals of 0.5º in a 25º range about with the exposure time of 5 sec per frame. The reflections were successfully indexed by an automated indexing routine built in the APEXII program. The final cell constants were calculated from a set of 9936 strong reflections from the actual data collection.

The data were collected by using the full sphere data collection routine to survey the reciprocal space to the extent of a full sphere to a resolution of 0.8 Å. A total of 14291 data were harvested by collecting 21 sets of frames with 0.65º scans in with an exposure time 5–10 sec per frame. These highly redundant datasets were corrected for Lorentz and polarization effects. The absorption correction was based on fitting a function to the empirical transmission surface as sampled by multiple equivalent measurements.[13]

Structure solution and refinement. The systematic absences in the diffraction data were consistent for the space groups *P*21 and *P*21/*m*. The *E*-statistics suggested the centrosymmetric space group *P21/m* which was inconsistent with the chiral nature of the compound, thus the chiral space group *P*21 was selected. A refinement in this space group yielded chemically reasonable and computationally stable results of refinement.[14-16] A successful solution by the direct methods provided most non-hydrogen atoms from the *E*-map. The remaining non-hydrogen atoms were located in an alternating series of least-squares cycles and difference Fourier maps. All non-hydrogen atoms were refined with anisotropic displacement coefficients. All hydrogen atoms were included in the structure factor calculation at idealized positions and were allowed to ride on the neighboring atoms with relative isotropic displacement coefficients.

There is also one molecule of solvate 1-propanol per one molecule of trimer in the lattice. The asymmetric unit contains two molecules of the trimer with very similar geometries and two molecules of 1-propanol in somewhat different conformations. The absolute configuration has been independently confirmed by the results of the single-crystal X-ray analysis – all chiral centers are *S*. The final least-squares refinement of 952 parameters against 14291 data resulted in residuals *R* (based on *F*2 for $I \geq 2\sigma$) and *wR* (based on *F*2 for all data) of 0.0317 and 0.0858, respectively. The final difference Fourier map was featureless. The molecular diagrams are drawn with 50% probability ellipsoids.

Crystal data and structure refinement for peptoid 3:

Empirical formula	$C_{40}H_{42}N_4O_4 \cdot C_3H_8O$
Formula weight	702.87
Temperature	100(1) K
Wavelength	1.54178 Å
Crystal system	Monoclinic
Space group	*P*21
Unit cell dimensions	a = 9.771(7) Å = 90°
	b = 18.070(10) Å = 95.90 (4)°
	c = 21.395(15) Å = 90°
Volume	3758(4) $Å^3$
Z	4
Density (calculated)	1.242 Mg/m^3
Absorption coefficient	0.650 mm^{-1}
F(000)	1504
Crystal size	0.51 x 0.40 x 0.23 mm^3
Theta range for data collection	2.08 to 72.35°
Index ranges	-12<=h<=12, -21<=k<=22, -24<=l<=26
Reflections collected	69154
Independent reflections	14291 [R(int) = 0.0245]
Completeness to theta = 67.00°	99.8 %
Absorption correction	Numerical with SADABS
Max. and min. transmission	0.8648 and 0.7326
Refinement method	Full-matrix least-squares on F^2
Data / restraints / parameters	14291 / 1 / 952
Goodness-of-fit on F^2	1.006
Final R indices [I > 2 sigma (I)]	R1 = 0.0317, wR2 = 0.0854
R indices (all data)	R1 = 0.0320, wR2 = 0.0858
Absolute structure parameter	Flack x 0.03(8)
Absolute structure parameter	Hooft y 0.03(2)
Largest diff. peak and hole	0.416 and -0.210 e.$Å^{-3}$

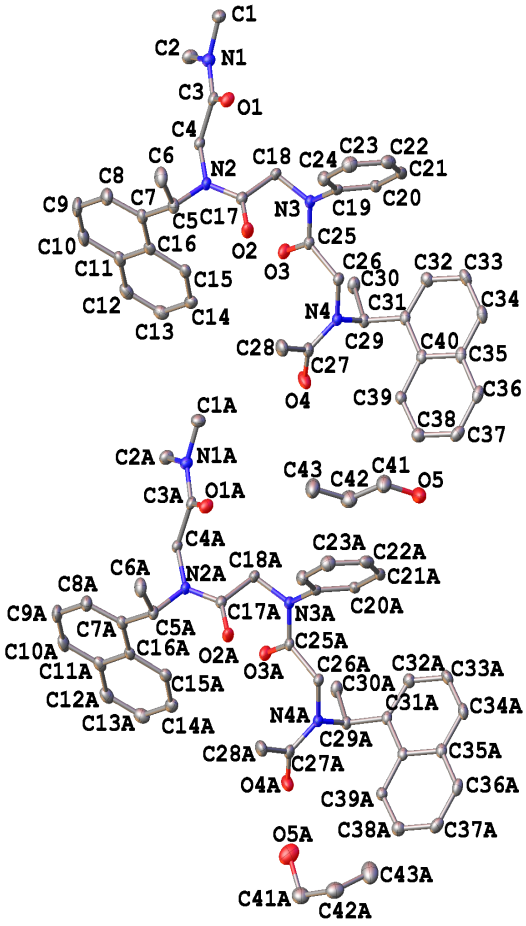

Figure S-14. The content of the asymmetric unit of peptoid **3**. All hydrogen atoms are omitted.

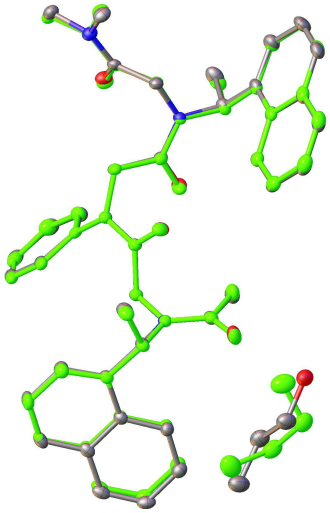

Figure S-15. An overlay of the symmetry-independent molecules of **3**. All hydrogen atoms are omitted.

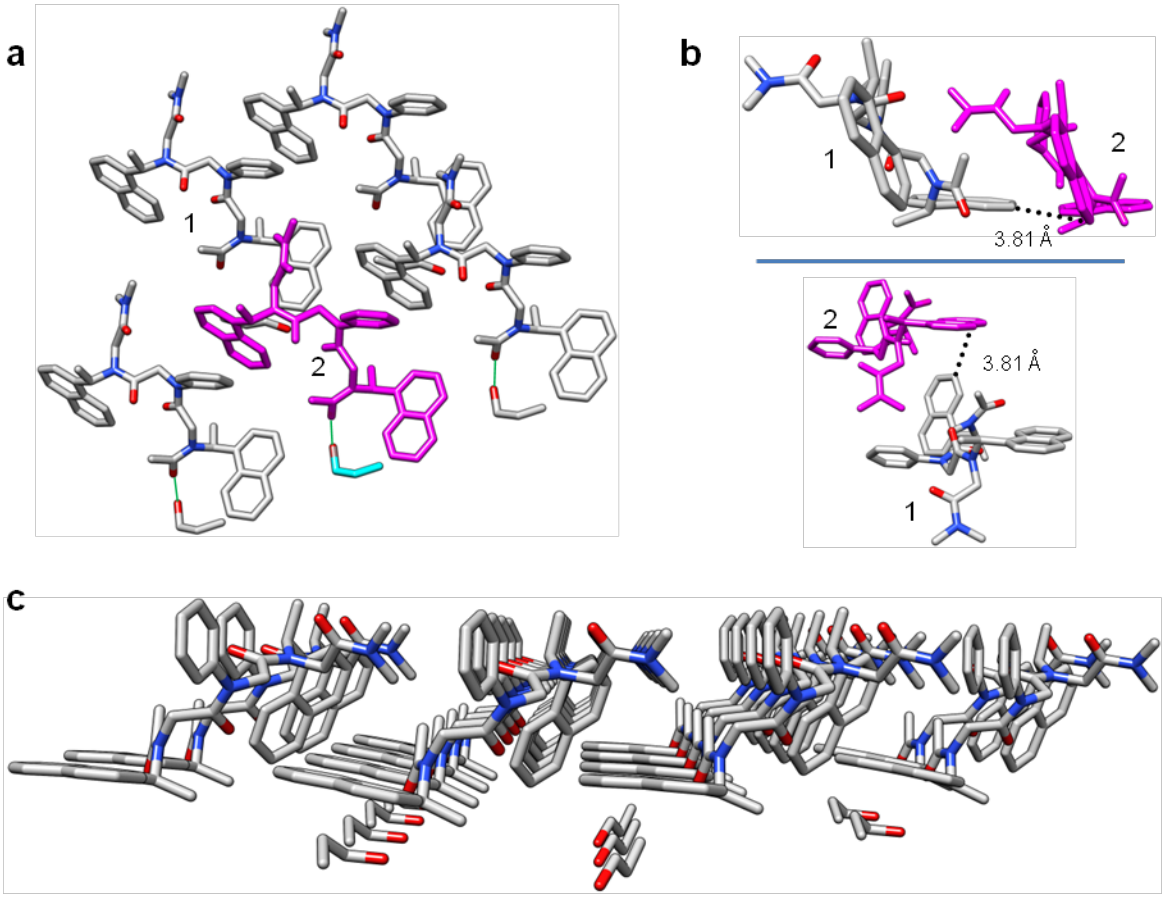

Figure S-16. (a) A view of the tight crystal packing in the solid state structure of peptoid **3**. The green lines indicate hydrogen bonds to co-crystallized 1-propanol molecules. (b) Two views illustrating the same potential intermolecular aromatic edge-to-face interaction for **3**. The molecules are numbered and colored in accordance with the image displayed in part (a). The black dashed lines indicate intermolecular distances. (c) A stereoview showing one layer of the crystal packing of **3**. Hydrogen atoms have been omitted in all cases.

Peptoid 4a

Data collection. A colorless crystal with approximate dimensions 0.51 x 0.28 x 0.22 mm^3 was selected under oil under ambient conditions and attached to the tip of a MiTeGen MicroMount©. The crystal was mounted in a stream of cold nitrogen at 100(1) K and centered in the X-ray beam by using a video camera. The crystal evaluation and data collection were performed on a Bruker SMART APEXII diffractometer with Cu K_α (λ = 1.54178 Å) radiation and the diffractometer to crystal distance of 4.03 cm.

The initial cell constants were obtained from three series of ω scans at different starting angles. Each series consisted of 50 frames collected at intervals of 0.5º in a 25º range about ω with the exposure time of 5 sec per frame. The reflections were successfully indexed by an automated indexing routine built in the APEXII program. The final cell constants were calculated from a set of 9855 strong reflections from the actual data collection.

The data were collected by using the full sphere data collection routine to survey the reciprocal space to the extent of a full sphere to a resolution of 0.82 Å. A total of 68014 data were harvested by collecting 19 sets of frames with 0.6º scans in ω with an exposure time 5/7/10/15 sec per frame. These highly redundant datasets were corrected for Lorentz and polarization effects. The absorption correction was based on fitting a function to the empirical transmission surface as sampled by multiple equivalent measurements.[13]

Structure solution and refinement. The systematic absences in the diffraction data were uniquely consistent for the space group $P2_12_12_1$ that yielded chemically reasonable and computationally stable results of refinement.[14-16] A successful solution by the direct methods provided most non-hydrogen atoms from the *E*-map. The remaining non-hydrogen atoms were located in an alternating series of least-squares cycles and difference Fourier maps. All non-hydrogen atoms were refined with anisotropic displacement coefficients. All hydrogen atoms were included in the structure factor calculation at idealized positions and were allowed to ride on the neighboring atoms with relative isotropic displacement coefficients.

The 2,6-dimethylphenyl group was disordered over two positions (the major component contribution is 51.9(4)% and was refined with an idealized geometry based on a DFT geometry optimization. The final least-squares refinement of 538 parameters against 8374 data resulted in residuals *R* (based on F^2 for $I \geq 2\sigma$) and *wR* (based on F^2 for all data) of 0.0392 and 0.0959, respectively. The final difference Fourier map was featureless.

Crystal data and structure refinement for peptoid 4a:

Empirical formula	$C_{50}\ H_{53}\ N_5\ O_5$	
Formula weight	803.97	
Temperature	100(1) K	
Wavelength	1.54178 Å	
Crystal system	Orthorhombic	
Space group	$P2_12_12_1$	
Unit cell dimensions	a = 10.3233(14) Å	a= 90°
	b = 15.429(2) Å	b= 90°
	c = 27.118(4) Å	g = 90°
Volume	4319.2(11) $Å^3$	
Z	4	
Density (calculated)	1.236 Mg/m^3	
Absorption coefficient	0.640 mm^{-1}	
F(000)	1712	
Crystal size	0.51 x 0.28 x 0.22 mm^3	
Theta range for data collection	3.26 to 71.84°.	
Index ranges	-12<=h<=12, -18<=k<=19, -29<=l<=32	
Reflections collected	68014	
Independent reflections	8374 [R(int) = 0.0231]	
Completeness to theta = 67.00°	100.0 %	
Absorption correction	Numerical with SADABS	
Max. and min. transmission	0.8693 and 0.7356	
Refinement method	Full-matrix least-squares on F^2	
Data / restraints / parameters	8374 / 6 / 538	
Goodness-of-fit on F^2	1.041	
Final R indices [I>2sigma(I)]	R1 = 0.0392, wR2 = 0.0955	
R indices (all data)	R1 = 0.0396, wR2 = 0.0959	
Absolute structure parameter (Flack x)	-0.01(15)	
Absolute structure parameter (Hooft y)	-0.01(2)	
Largest diff. peak and hole	0.474 and -0.334 $e.Å^{-3}$	

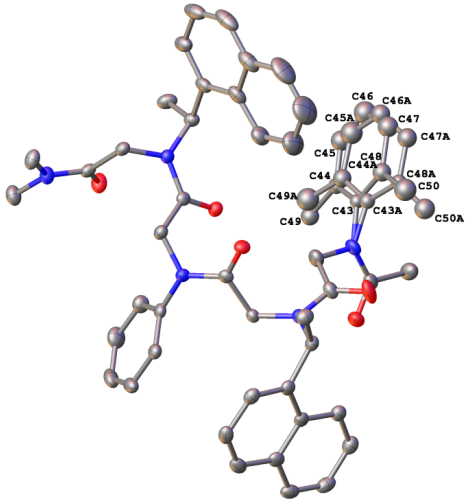

Figure S-17. A molecular drawing of peptoid **4a** showing both components of the disordered group. All hydrogen atoms are omitted. The molecular diagram is drawn with 50% probability ellipsoids.

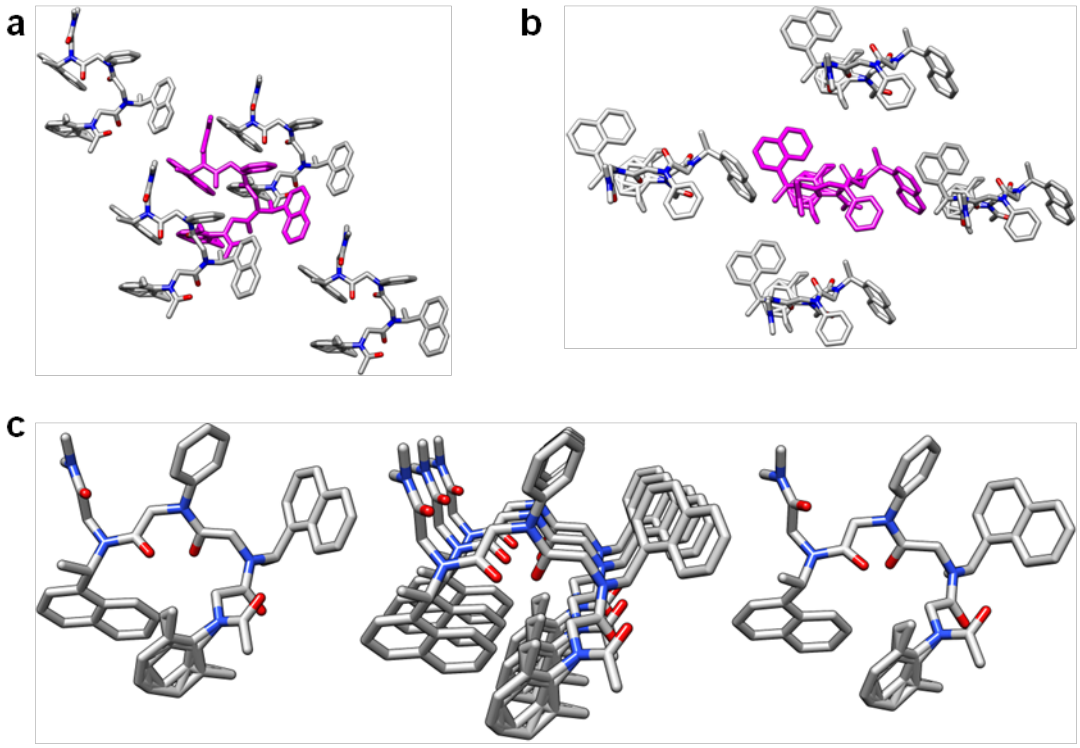

Figure S-18. The crystal packing in the solid state structure of **4a** is illustrated by (a) a side-on view, (b) a view looking down from the C-termini, and (c) a stereoview. The molecule in the center of (a) and (b) is colored magenta for clarity purposes. Hydrogen atoms have been omitted in all cases. No non-covalent intermolecular interactions of significance were observed.

Main chain dihedral angles for Br-Nph-Ns1npe-dma, 3, 4a, and 6*i* as determined by X-ray crystallography or NMR.

Table S-4. Main chain dihedral angles of **Br-*N*ph-*N*s1npe-dma**, **3**, and **4a** as determined by X-ray crystallography, and ensemble averages (± standard deviation) for main chain dihedral angles of the two populations of the NMR determined structure of **6*i***.

peptoid	residue	ω	ϕ	ψ
Br-*N*ph-*N*s1npe-dma[†]	*i* (*ph*)	175.35	108.52	176.32
	i+1 (*s1npe*)	0.75	77.53	179.18
3[†]	*i* (*s1npe*)	-13.44	-71.84	-174.34
	i+1 (*ph*)	-161.92	64.61	-163.37
	i+2 (*s1npe*)	-8.81	-63.69	176.98
4a	*i* (2,6m*ph*)	-178.75	63.62	-154.90
	i+1 (*s1npe*)	0.86	-77.52	178.47
	i+2 (*ph*)	-158.97	62.85	-175.26
	i+3 (*s1npe*)	-22.80	-63.79	164.80
6*i*-A*	*i* (3,5m*ph*)	-175.08 ± 0.7	69.82 ± 2.2	-165.47 ± 1.9
	i+1 (*s1npe*)	-15.33 ± 1.3	-56.24 ± 1.8	159.07 ± 2.1
	i+2 (2,6m*ph*)	-167.23 ± 0.5	58.39 ± 0.6	-146.65 ± 2.3
	i+3 (*s1npe*)	-1.48 ± 1.5	-51.61 ± 1.5	162.04 ± 1.9
	i+4 (*ph*)	-168.67 ± 0.9	78.57 ± 1.5	174.33 ± 1.1
	i+5 (*s1npe*)	-4.25 ± 1.7	40.64 ± 2.5	56.82 ± 3.2
6*i*-B*	*i* (3,5m*ph*)	-175.51 ± 0.3	73.47 ± 7.1	-169.60 ± 6.6
	i+1 (*s1npe*)	-12.83 ± 4.2	-55.33 ± 3.7	162.97 ± 1.1
	i+2 (2,6m*ph*)	-166.61 ± 0.7	56.35 ± 2.7	-159.74 ± 1.7
	i+3 (*s1npe*)	-12.55 ± 0.5	-55.83 ± 1.1	158.52 ± 1.0
	i+4 (*ph*)	-162.73 ± 1.1	62.35 ± 1.1	-148.22 ± 2.2
	i+5 (*s1npe*)	-7.12 ± 1.8	-59.33 ± 4.1	-175.08 ± 7.5

[†] Values reported are an average of angles measured for two nearly identical, but symmetry independent, molecules in the unit cell of the X-ray crystal structure. *Averages and S.D. for **6*i*-A** are for seven calculated structures, and the same values for **6*i*-B** are for three calculated structures (see Figure S-10 for structures of **6*i*-A** and **6*i*-B**).

Supplemental CD data.

Protocol for CD analysis. Peptoid stock solutions were prepared by dissolving at least 2 mg of peptoid in ~4 mL spectroscopic grade acetonitrile. A volume of the stock solutions (100 μL) was weighed using a high-precision balance (Mettler-Toledo XS105) and diluted to close to the desired concentration using spectroscopic grade acetonitrile. The final concentrations were accurately determined by the mass of the final dilution using a high-precision balance. Spectra were obtained in a square quartz cell (path length 0.1 cm) with a step size of 1 nm and an averaging time of 5 sec from 260 nm to 190 nm. Solvent spectra were subtracted from the raw data, and experimental spectra were plotted as molar ellipticity (deg cm^2/dmol) per-amide.

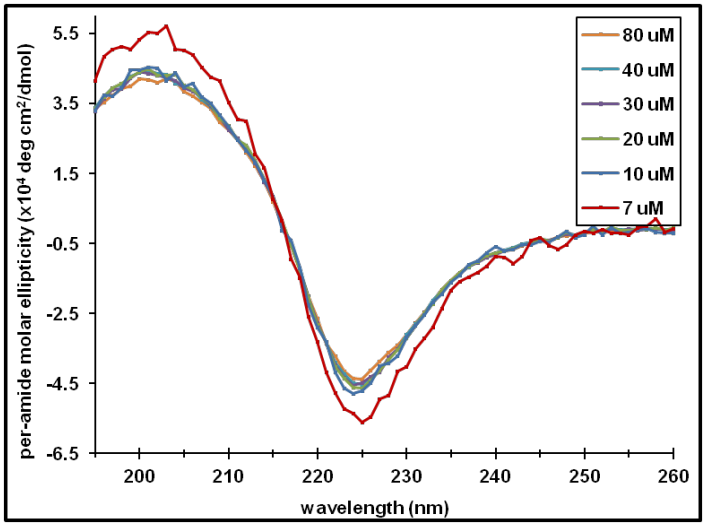

Figure S-19. CD spectra of **8** at 20 °C in acetonitrile at various concentrations.

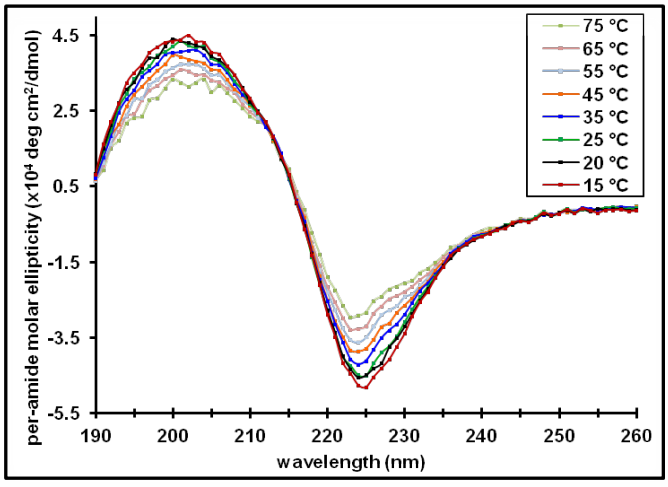

Figure S-20. CD spectra of peptoid **8** at 30 μM in acetonitrile at various temperatures.

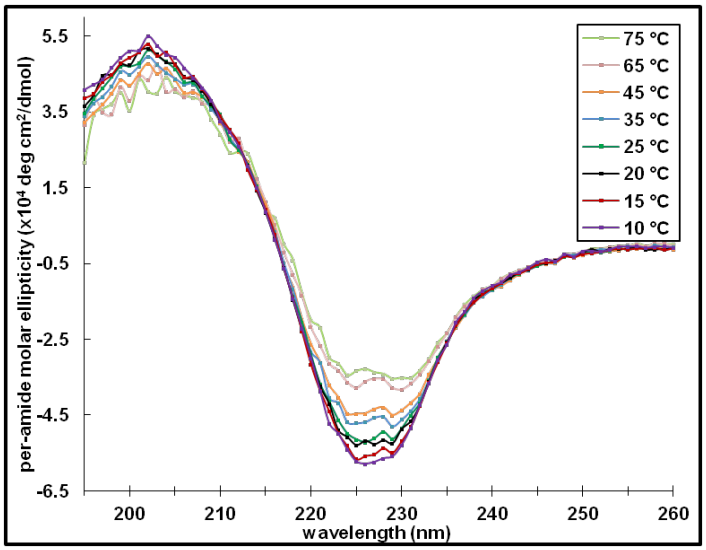

Figure S-21. CD spectra of peptoid **8** at 30 μM in 1:1 acetonitrile:water at various temperatures.

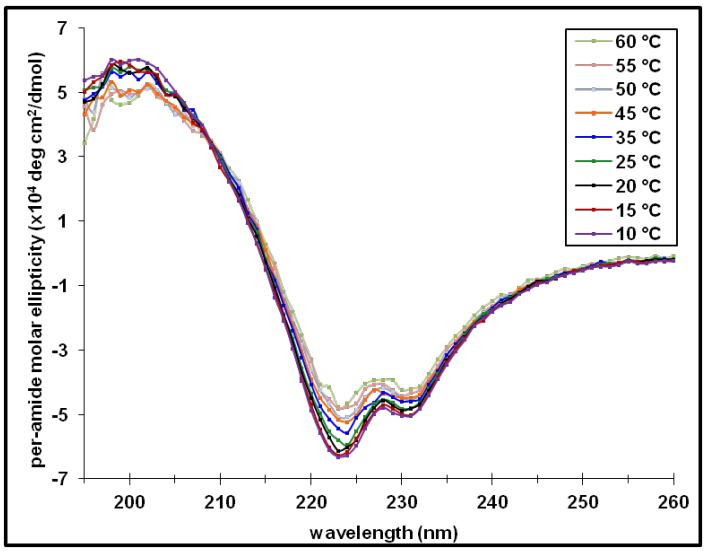

Figure S-22. CD spectra of peptoid **8** at 30 μM in methanol at various temperatures.

Characterization data for all synthetic intermediates.

Br-dma. After aqueous workup, the crude brown oil was loaded onto a column of silica gel (equilibrated with 3:2 EtOAc/hexanes) and eluted by flash column chromatography using a 3:2 mixture of EtOAc/hexanes to afford a transparent, faintly-orange oil. Isolated yield = 39%; TLC: R_f = 0.18 (3:2 EtOAc/hexanes); ^{1}H NMR ($CDCl_3$, 300 MHz): δ 3.87 (s, 2H), 3.11 (s, 3H), 2.99 (s, 3H); ^{13}C NMR (75 MHz, $CDCl_3$, ^{1}H broadband-decoupled): δ 166.9, 38.3, 36.2, 26.3; IR (ATR, cm^{-1}): brd 2935, 1645, 1497, 1438, 1398, 1263, 1219, 1193, 1135, 1092, 1061, 976, 898, 782, 616; HR-MS (ESI): C_4H_9BrNO, $[M+H]^+$ calcd *m/z* = 165.9863, observed *m/z* =165.9872.

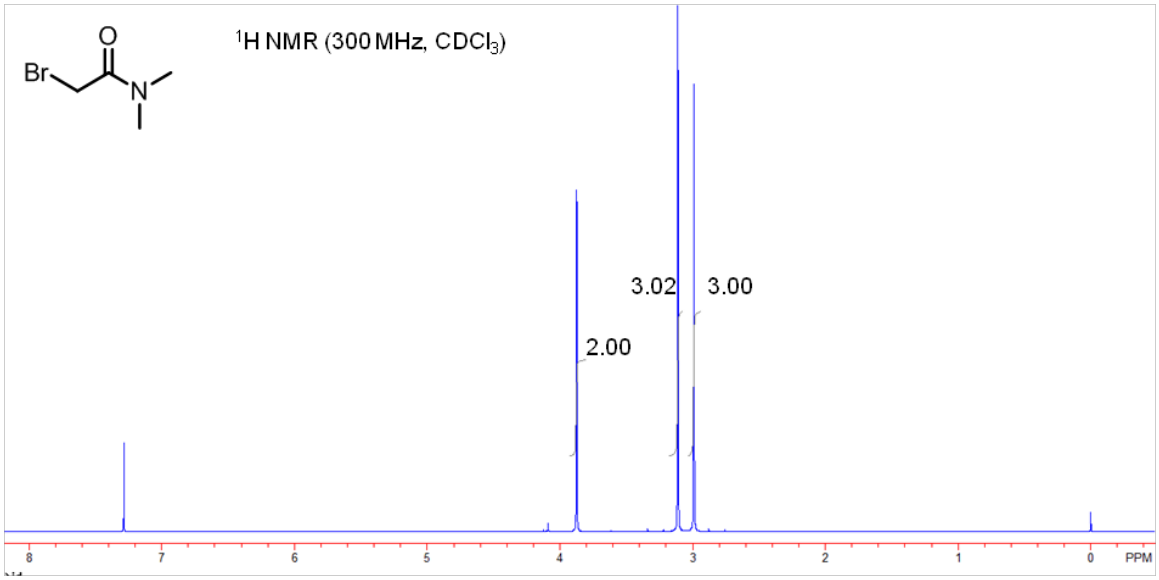

H-*N*s1npe-dma. After aqueous work-up, the crude brownish orange oil was loaded onto a column of silica gel (equilibrated with EtOAc) and eluted by flash column chromatography using EtOAc containing 2% MeOH and 1% TEA for two column volumes and then EtOAc containing 4% MeOH and 2% TEA; two rounds of chromatography required to afford a yellow oil. Isolated yield = 75%; TLC: R_f = 0.27 (2% MeOH/ EtOAc); ^{1}H NMR ($CDCl_3$, 300 MHz): δ 8.20 (m, 1H), 7.85 (m, 1H) 7.73 (m, 2H), 7.55–7.40 (m, 3H), 4.65 (q, J = 6.7 Hz, 1H), 3.30 (ABq, 2H, $\Delta\nu_{AB}$ = 30.4 Hz, J_{AB} = 16.1 Hz), 2.94 (s, 3H), 2.71 (s, 3H), 2.49 (s, 1H), 1.53 (d, J = 6.7 Hz, 3H); ^{13}C NMR (75 MHz, $CDCl_3$, ^{1}H broadband-decoupled): δ 171.4, 140.9, 134.1, 131.6, 129.0, 127.3, 125.9, 125.9, 125.4, 123.2, 123.2, 54.0, 48.7, 36.0, 35.6, 24.3; IR (ATR, cm^{-1}): 3325, 3050, 2964, 2927, 1649, 1595, 1508, 1452, 1396, 1323, 1266, 1226, 1173, 1126, 1069, 996, 910, 802, 780, 731, 699, 645; HR-MS (ESI): $C_{16}H_{21}N_2O$, $[M+H]^+$ calcd m/z = 257.1649, observed m/z = 257.1648.

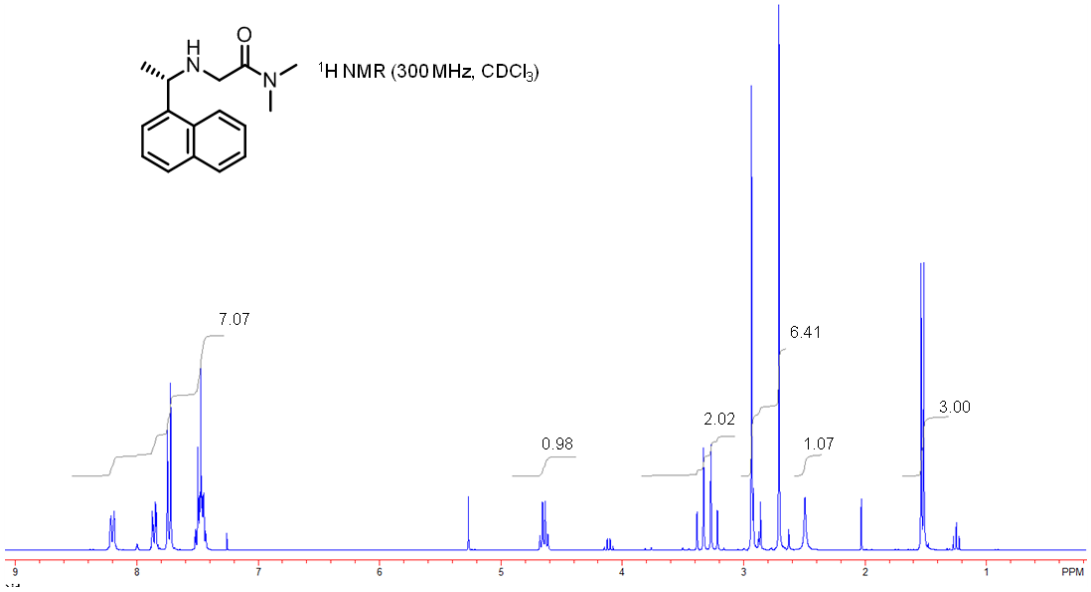

H-*N*ph-dma. After aqueous work-up, the crude brownish orange oil was loaded onto a column of silica gel (equilibrated with 5:4 EtOAc/hexanes) and eluted by flash column chromatography using 5:4 EtOAc/hexanes to afford a white solid. Isolated yield = 71%; TLC: R_f = 0.22 (2.5:2 EtOAc/hexanes); ^{1}H NMR ($CDCl_3$, 300 MHz): δ 7.17 (t, J = 7.9 Hz, 2H), 6.69 (t, J = 7.3 Hz, 1H), 6.63 (d, J = 7.9 Hz, 2H), 4.89 (brd s, 1H), 3.85 (s, 2H), 3.01 (s, 3H), 3.00 (s, 3H); ^{13}C NMR (75 MHz, $CDCl_3$, ^{1}H broadband-decoupled): δ 168.9, 147.4, 129.1, 117.1, 116.5, 112.7, 44.9, 35.5, 35.3; IR (ATR, cm^{-1}): 3363, 3051, 2931, 1644, 1606, 1580, 1510,1455, 1412, 1402, 1322, 1263, 1175, 1125, 1062, 993, 868, 741, 691; HR-MS (ESI): $C_{10}H_{15}N_2O$, $[M+H]^+$ calcd m/z = 179.1179, observed m/z = 179.1185.

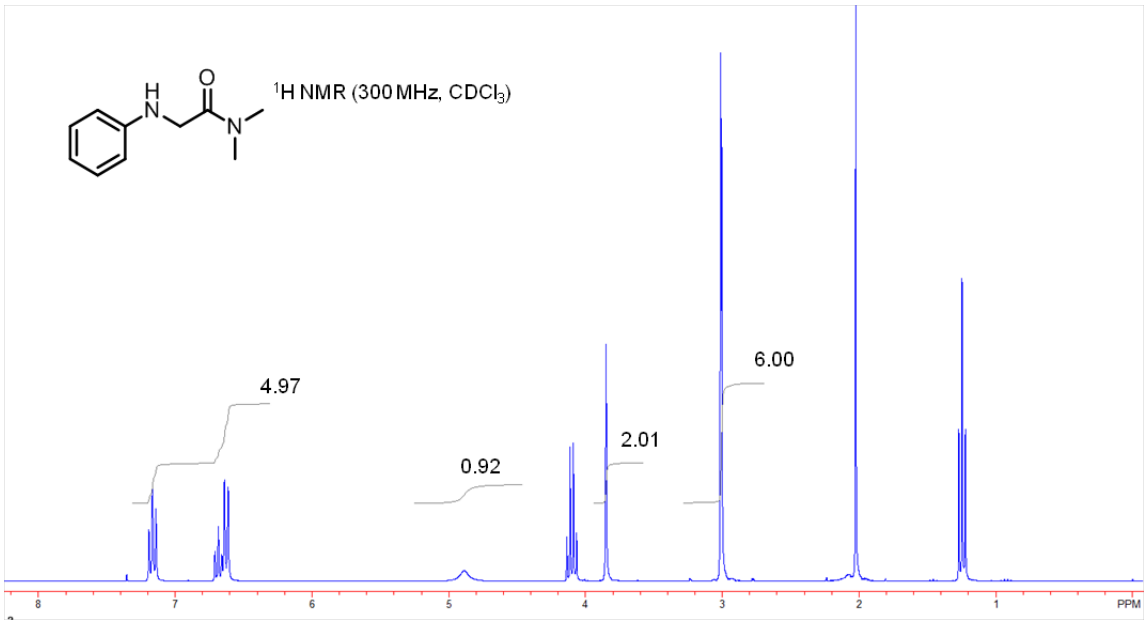

Br-*N*s1npe-dma. After a general acylation of H-*N*s1npe-Dma and aqueous work-up, the crude dark brown liquid was loaded onto a column of silica gel (equilibrated with 4:1 EtOAc/hexanes) and eluted by flash column chromatography using 4:1 EtOAc/hexanes to afford a white crystalline solid. (*Note*, product can also be isolated in low to moderate yield by crystallization from the crude reaction mixture). Isolated yield = 81%; TLC: R_f = 0.27 (4:1 EtOAc/hexanes); HR-MS (ESI): $C_{18}H_{22}BrN_2O_2$ $[M+H]^+$ calcd m/z = 399.0679, observed m/z = 399.0662.

HPLC (220 nm)

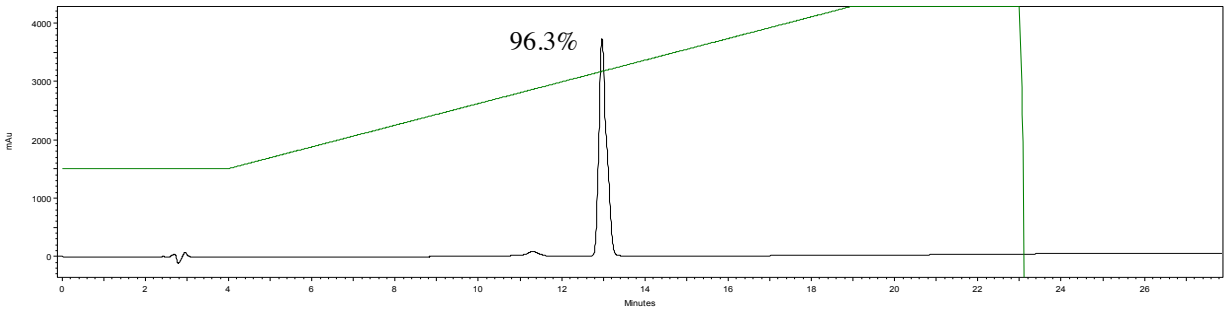

^{1}H NMR (300 MHz, $CDCl_3$)

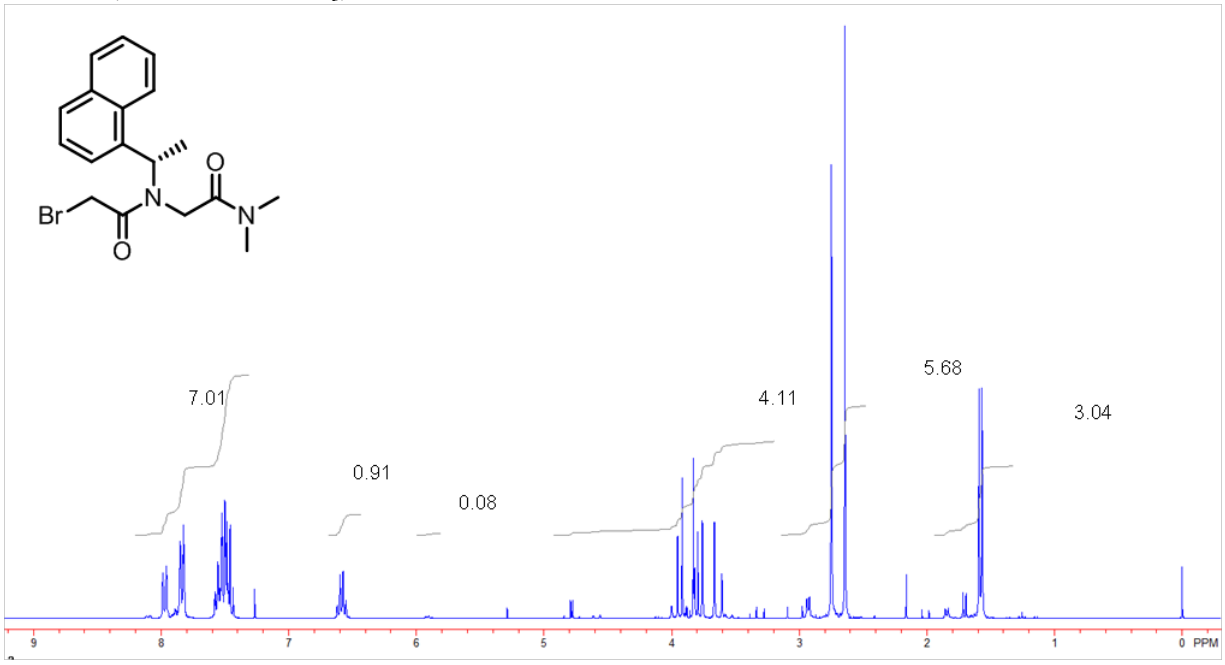

Br-*N*ph-dma. After a general acylation of H-*N*ph-Dma and aqueous work-up, the crude brown oil was loaded onto a column of silica gel (equilibrated with 7:3 EtOAc/hexanes) and eluted by flash column chromatography using 7:3 EtOAc/hexanes to afford a white solid. Isolated yield = 93%; TLC: R_f = 0.15 (7:3 EtOAc/hexanes); ^{1}H NMR ($CDCl_3$, 300 MHz): δ 7.65–7.48 (m, 2H), 7.48–7.32 (m, 3H), 4.47 (s, 2H), 3.74 (s, 2H), 3.00 (s, 3H), 2.96 (s, 3H); ^{13}C NMR (75 MHz, $CDCl_3$, ^{1}H broadband-decoupled): δ 167.0, 142.5, 129.9, 128.9, 128.4, 52.7, 36.5, 36.0, 26.9; HR-MS (ESI): $C_{12}H_{16}BrN_2O_2$, $[M+H]^+$ calcd *m/z* = 321.0210, observed *m/z* =321.0209.

HPLC (220 nm)

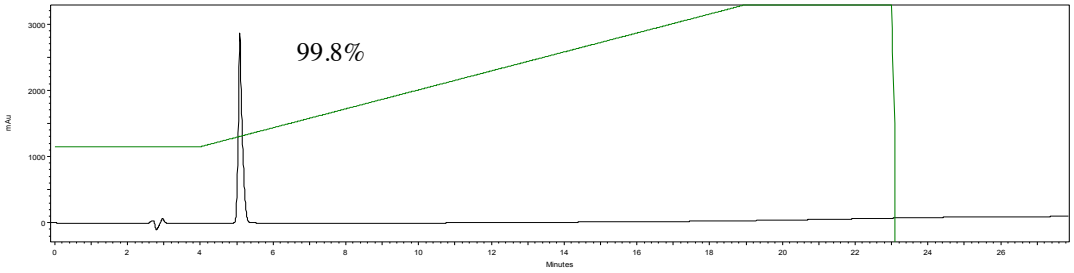

^{1}H NMR (300 MHz, $CDCl_3$)

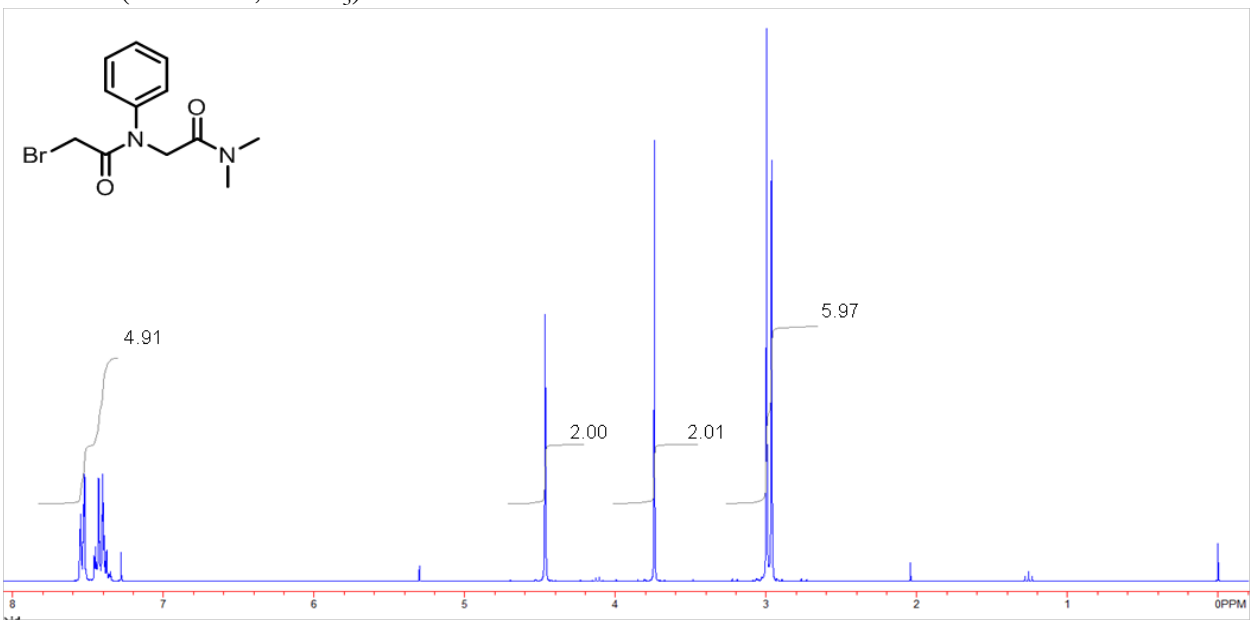

H-*N*ph-*N*s1npe-dma. After a general alkylation procedure from Br-*N*s1npe-Dma and aqueous work-up, the crude brown oil was loaded onto a column of silica gel (equilibrated with 4:1 EtOAc/hexanes) and eluted by flash column chromatography using 4:1 EtOAc/hexanes to afford a white foam. Isolated yield = 84%; TLC: R_f = 0.22 (4:1 EtOAc/hexanes with 2% TEA); HR-MS (ESI): $C_{24}H_{27}N_3NaO_2$, $[M+Na]^+$ calcd m/z = 412.1996, observed m/z = 412.1981.

HPLC (220 nm)

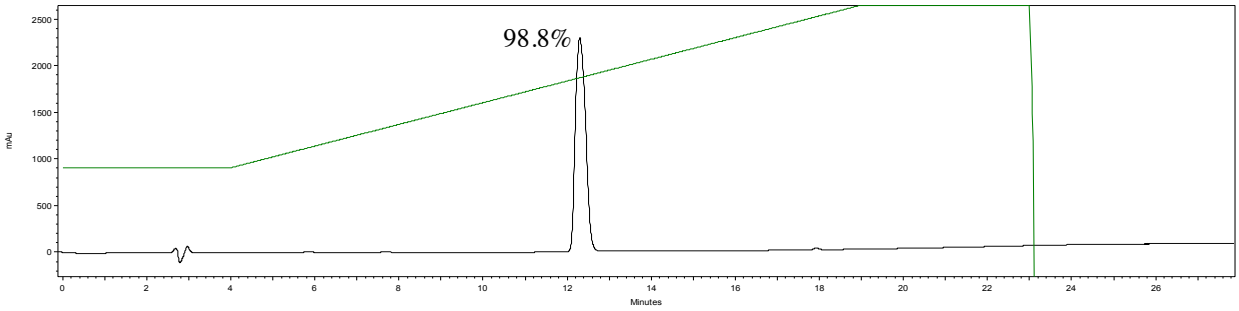

^{1}H NMR (300 MHz, $CDCl_3$)

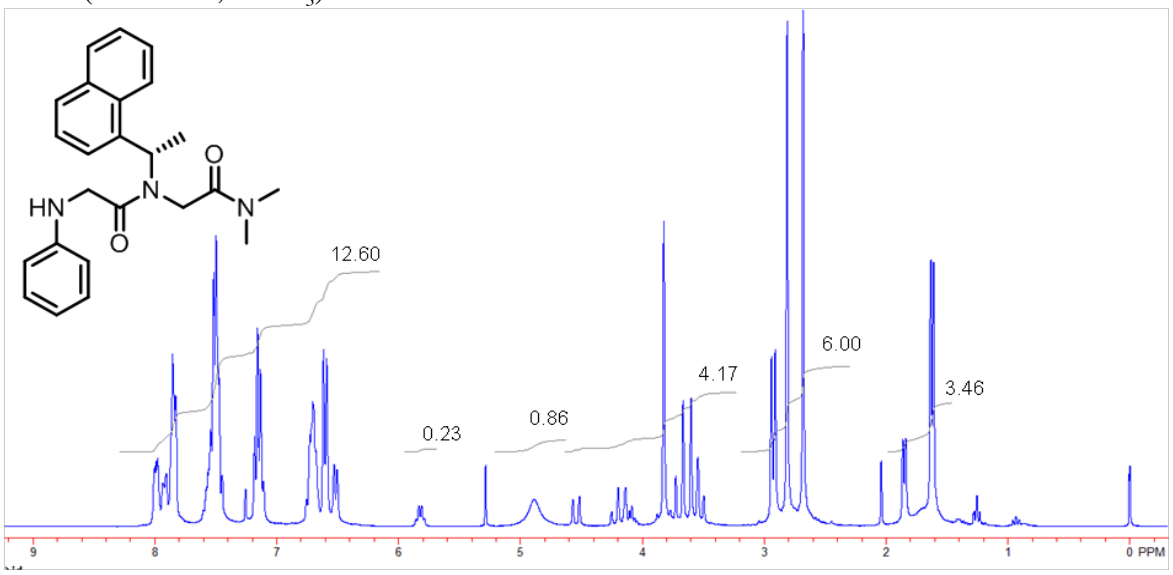

H-*N*s1npe-*N*ph-dma. After a general alkylation of Br-*N*ph-Dma and aqueous work-up, the crude brown oil was loaded onto a column of silica gel (equilibrated with 9:1 EtOAc/MeOH and 1% TEA) and eluted by flash column chromatography using 9:1 EtOAc/hexanes with 2% TEA to afford a clear, faintly yellow oil. Isolated yield = 86%; TLC: R_f = 0.27 (9:1 EtOAc/MeOH); ^{1}H NMR ($CDCl_3$, 300 MHz): δ 8.17 (brd d, J = 7.9 Hz, 1H), 7.90–7.76 (m, 1H), 7.68 (d, J = 8.2 Hz 1H), 7.61 (d, J = 7.0 Hz 1H), 7.55–7.30 (m, 3H), 7.24–7.05 (m, 5H), 4.58 (q, J = 6.5 Hz 1H), 4.42 (ABq, 2H, $\Delta\nu_{AB}$ = 44.7 Hz, J_{AB} = 15.9 Hz), 3.14 (ABq, 2H, $\Delta\nu_{AB}$ = 34.5 Hz, J_{AB} = 16.5 Hz), 2.96 (s, 3H), 2.95 (s, 3H), 2.44 (s, 1H), 1.44 (d, J = 6.5 Hz, 3H); ^{13}C NMR (75 MHz, $CDCl_3$, ^{1}H broadband-decoupled): δ 172.4, 167.5, 142.1, 140.9, 134.1, 131.6, 129.7, 129.0, 128.4, 128.3, 127.3, 126.0, 125.9, 125.4, 123.4, 123.2, 53.5, 51.6, 49.2, 36.5, 36.0, 24.1; HR-MS (ESI): $C_{24}H_{28}N_3O_2$ $[M+H]^+$ calcd m/z = 390.2177, observed m/z =390.2188.

HPLC (220 nm)

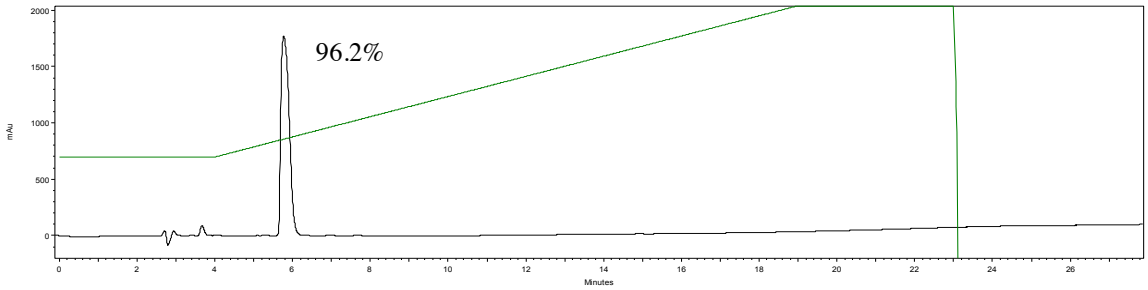

^{1}H NMR (300 MHz, $CDCl_3$)

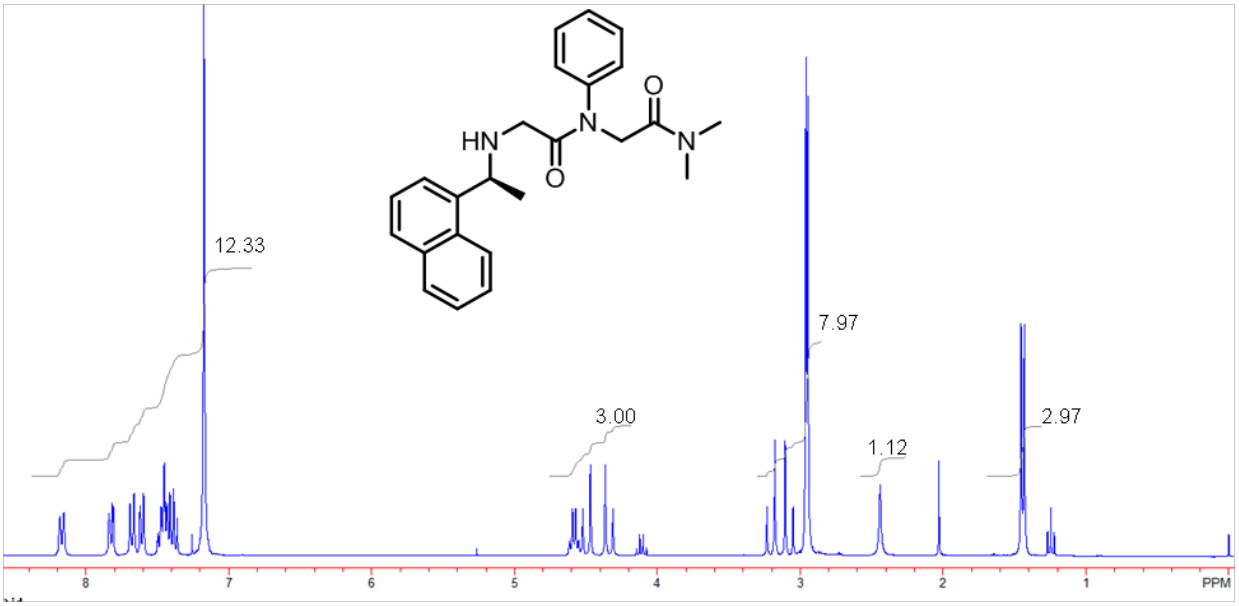

H-*N*4fph-*N*s1npe-dma. After a general alkylation procedure from Br-*N*s1npe-Dma and aqueous work-up, the crude brown oil was loaded onto a column of silica gel (equilibrated with 3:2 EtOAc/hexanes) and eluted by flash column chromatography using 3:2 EtOAc/hexanes to afford a white foam. Isolated yield = 93%; TLC: R_f = 0.14 (3:2 EtOAc/hexanes); HR-MS (ESI): $C_{24}H_{26}FN_3NaO_2$, $[M+Na]^+$ calcd m/z = 408.2082, observed m/z = 408.2090.

HPLC (218 nm)

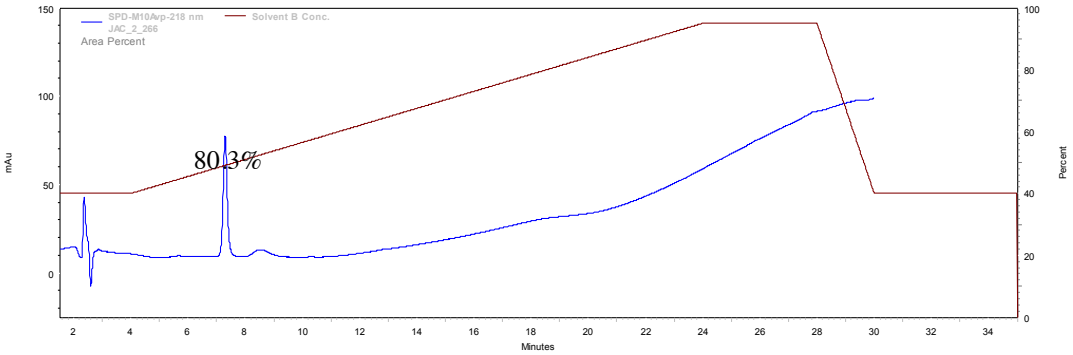

^{1}H NMR (300 MHz, $CDCl_3$)

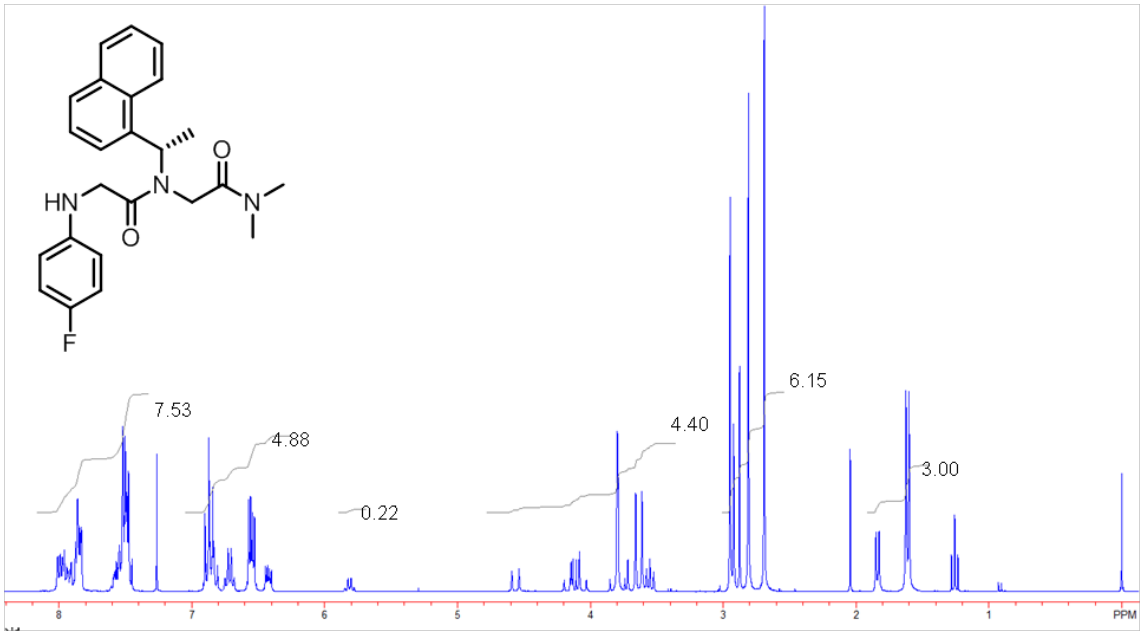

Br-*N*ph-*N*s1npe-dma. After a general acylation procedure from H-*N*ph-*N*s1npe-Dma and aqueous work-up, the crude tan oil was loaded onto a column of silica gel (equilibrated with 4:1 EtOAc/hexanes) and eluted by flash column chromatography using 4:1 EtOAc/hexanes to afford a white foam. Isolated yield = 87%; TLC: R_f = 0.29 (4:1 EtOAc/hexanes); HR-MS (ESI): $C_{26}H_{29}BrN_3O_3$, $[M+H]^+$ calcd m/z = 532.1207, observed m/z = 532.1185.

HPLC (220 nm)

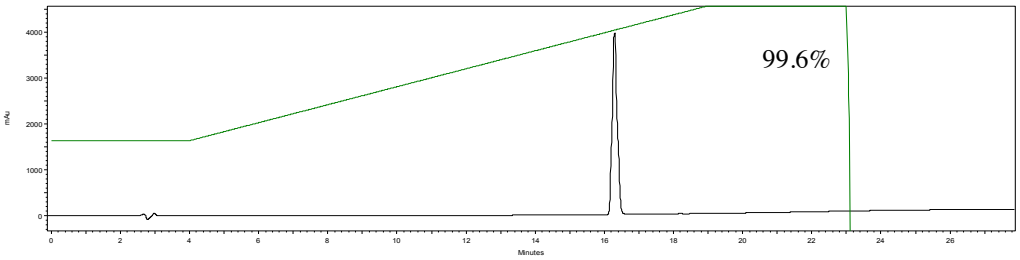

^{1}H NMR (300 MHz, $CDCl_3$)

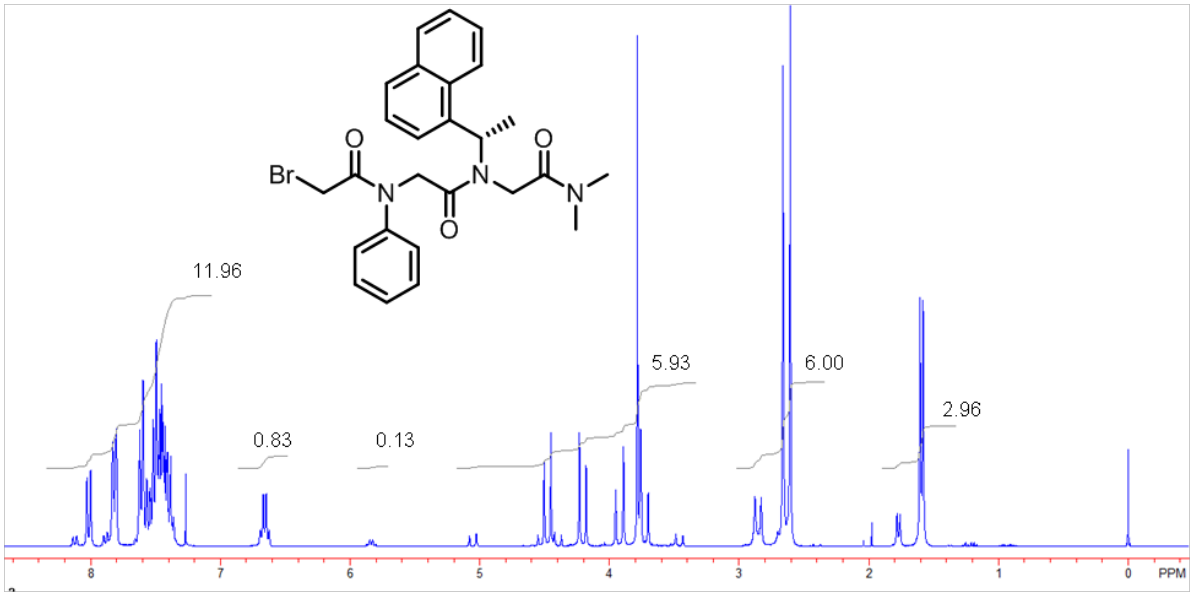

Br-*N*4fph-*N*s1npe-dma. After a general acylation procedure from H-*N*4fph-*N*s1npe-Dma and aqueous work-up, the crude tan oil was loaded onto a column of silica gel (equilibrated with 4:1 EtOAc/hexanes) and eluted by flash column chromatography using 4:1 EtOAc/hexanes to afford a white foam. Isolated yield = 87%; TLC: R_f = 0.29 (4:1 EtOAc/hexanes); HR-MS (ESI): $C_{26}H_{28}BrFN_3O_3$, $[M+H]^+$ calcd m/z = 532.1207, observed m/z = 532.1185.

HPLC (218 nm)

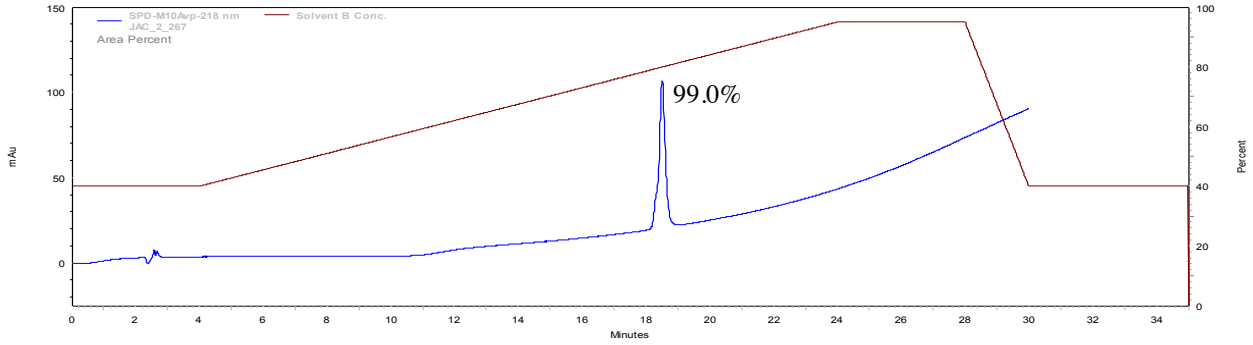

^{1}H NMR (300 MHz, $CDCl_3$)

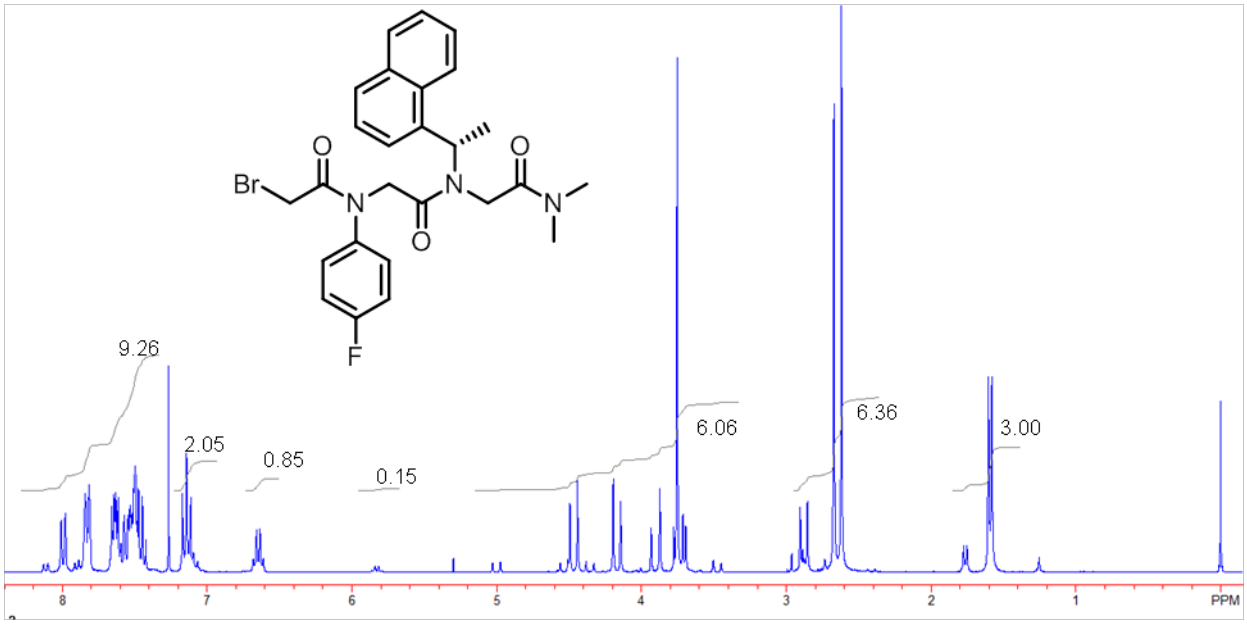

H-*N*s1npe-*N*ph-*N*s1npe-dma. After a general alkylation procedure from Br-*N*ph-*N*s1npe-Dma and aqueous work-up, the crude brown oil was loaded onto a column of silica gel (equilibrated with 9:1 EtOAc/MeOH) and eluted by flash column chromatography using 9:1 EtOAc/MeOH to afford a white foam. Isolated yield = 96%; TLC: R_f = 0.23 (9:1 EtOAc/MeOH, *note:* no TEA); HR-MS (ESI): $C_{38}H_{41}N_4O_3$, $[M+H]^+$ 601.3174, observed *m/z* = 601.3178.

HPLC (220 nm)

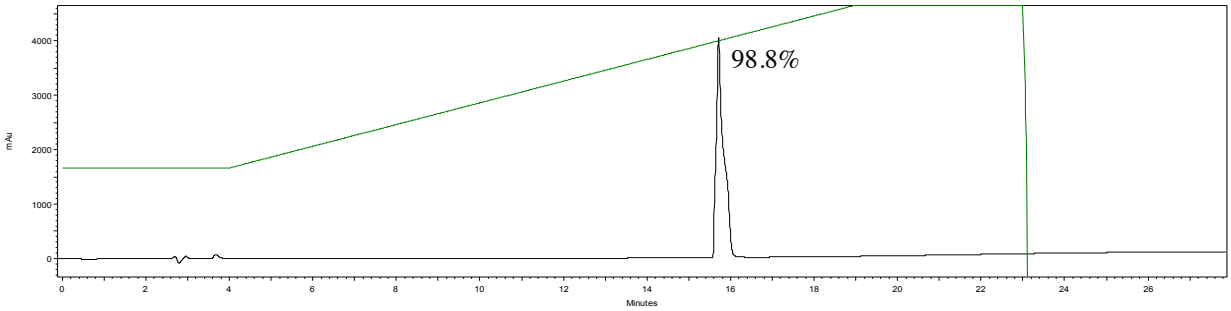

^{1}H NMR (300 MHz, $CDCl_3$) – "X" marks trace solvent peak (EtOAc).

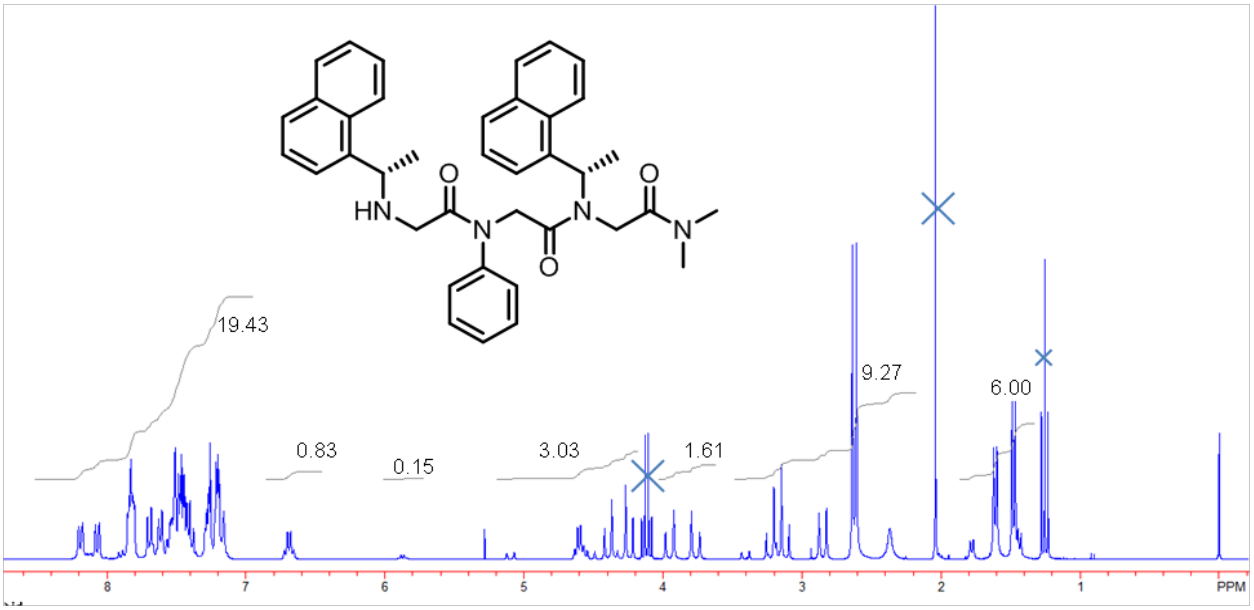

H-*N*s1npe-*N*4fph-*N*s1npe-dma. After a general alkylation procedure from Br-*N*4fph-*N*s1npe-Dma and aqueous work-up, the crude brown oil was loaded onto a column of silica gel (equilibrated with 9:1 EtOAc/MeOH) and eluted by flash column chromatography using 9:1 EtOAc/MeOH to afford a white foam. Isolated yield = 90%; TLC: R_f = 0.23 (9:1 EtOAc/MeOH, *note*: no TEA); HR-MS (ESI): $C_{38}H_{39}FN_4NaO_3$ $[M+Na]^+$, calcd *m/z* = 641.2899, observed *m/z* = 641.2881.

HPLC (220 nm)

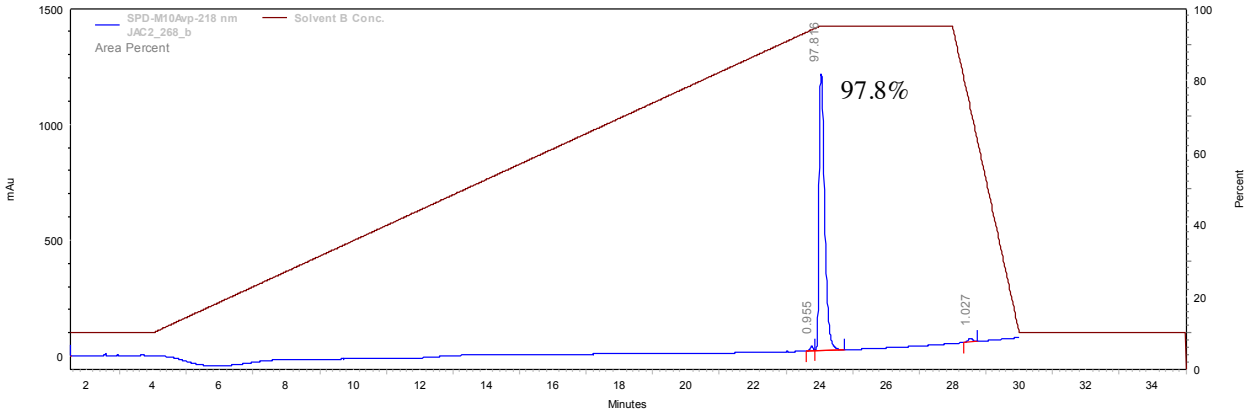

^{1}H NMR (300 MHz, $CDCl_3$)

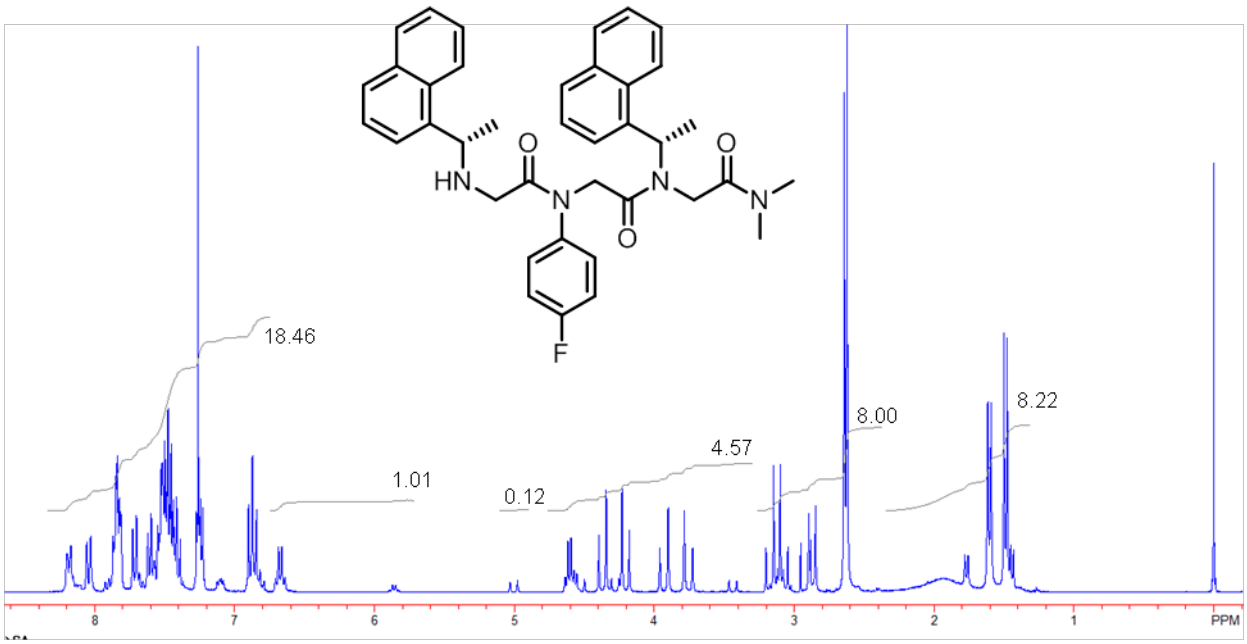

Br-*N*s1npe-*N*ph-*N*s1npe-dma. After a general acylation procedure from H-*N*s1npe-*N*ph-*N*s1npe-Dma and aqueous work-up, the product precipitated as a white solid from the crude brown oil. (*Note*, the crude oil can also be dissolved in a small quantity of 5:2 EtOAc/MeOH, loaded onto a column of silica gel (equilibrated with 5% MeOH in EtOAc), and eluted by flash column chromatography using 9:1 EtOAc/MeOH). Isolated yield = 94%; TLC: R_f = 0.32 (EtOAc); HR-MS (ESI): $C_{40}H_{41}BrN_4NaO_4$ $[M+Na]^+$ calcd m/z = 743.2204, observed m/z = 743.2227.

HPLC (220 nm)

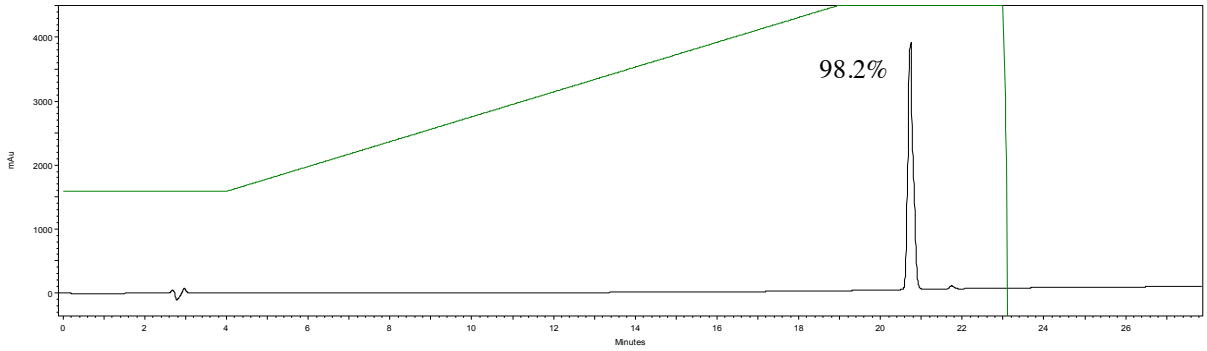

^{1}H NMR (300 MHz, $CDCl_3$)

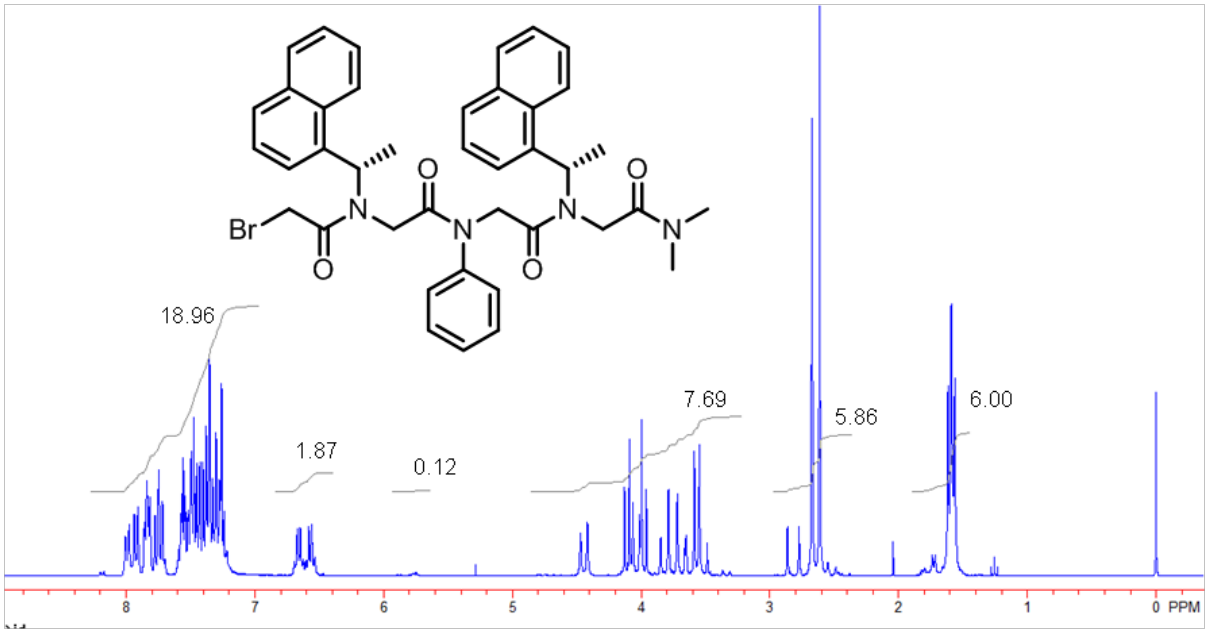

Br-Ac*^{13}C-*N*s1npe-*N*4fph-*N*s1npe-dma. After a general acylation procedure from H-*N*s1npe-*N*4fph-*N*s1npe-dma and aqueous workup, the crude brown oil was loaded onto a column of silica gel (equilibrated with 5% MeOH in EtOAc), and eluted by flash column chromatography using 5% MeOH in EtOAc; product not isolated completely from unidentified impurity. TLC: R_f = 0.20 (EtOAc); (ESI): $C_{38}C^{13}{}_2H_{40}BrFN_4NaO_4$, $[M+Na]^+$ calcd m/z = 763.2177, observed m/z = 763.2165.

HPLC (220 nm)

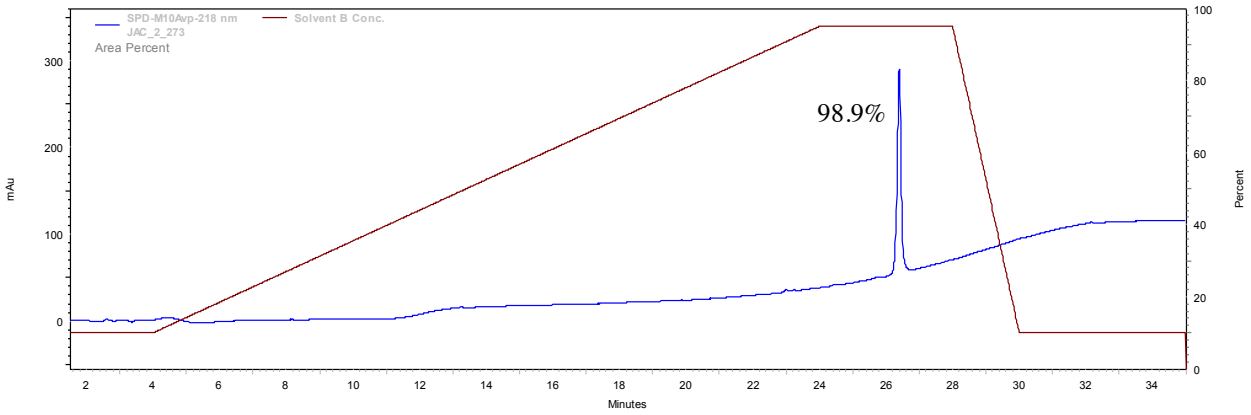

^{1}H NMR (300 MHz, $CDCl_3$) – "X" marks unidentified impurity.

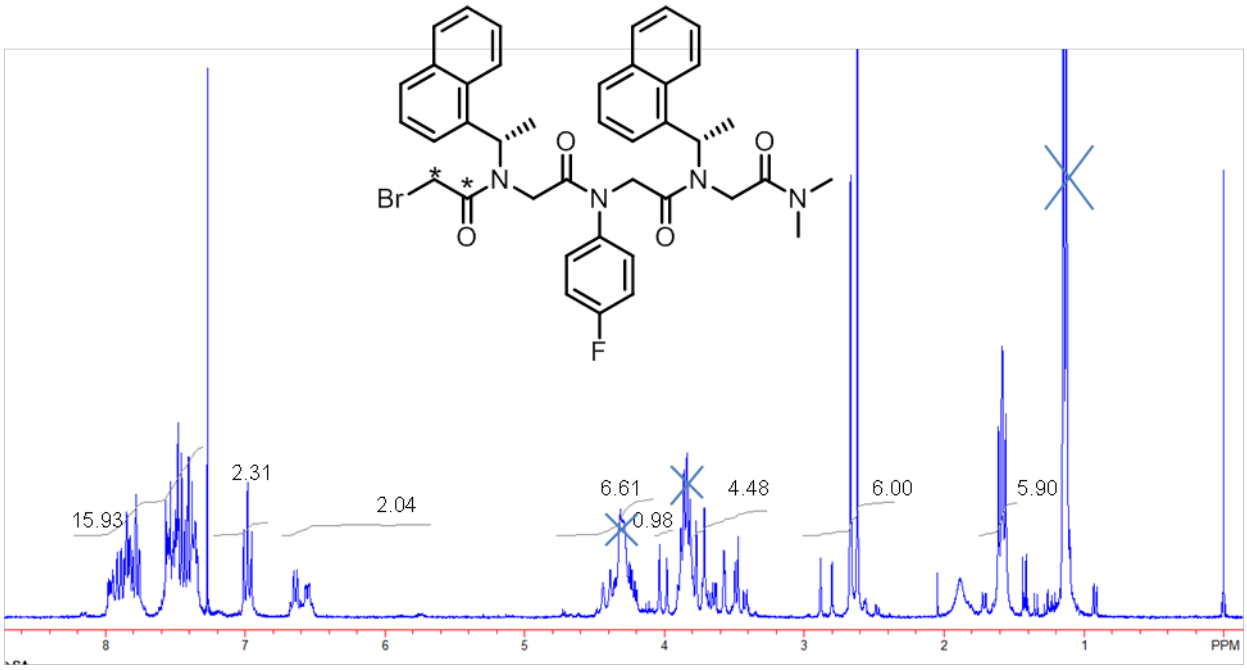

H-*N*ph-*N*s1npe-*N*ph-*N*s1npe-dma. After a general alkylation procedure from Br-*N*s1npe-*N*ph-*N*s1npe-Dma and aqueous work-up, the crude brown oil was loaded onto a column of silica gel (equilibrated with 9:1 EtOAc/hexanes) and eluted by flash column chromatography using 9:1 EtOAc/hexanes resulting in a off-white foam. Isolated yield = 88%; TLC: R_f = 0.23 (9:1 EtOAc/hexanes); HR-MS (ESI): $C_{46}H_{47}N_5NaO_4$ $[M+Na]^+$ calcd m/z = 756.3521, observed m/z = 756.3512.

HPLC (220 nm)

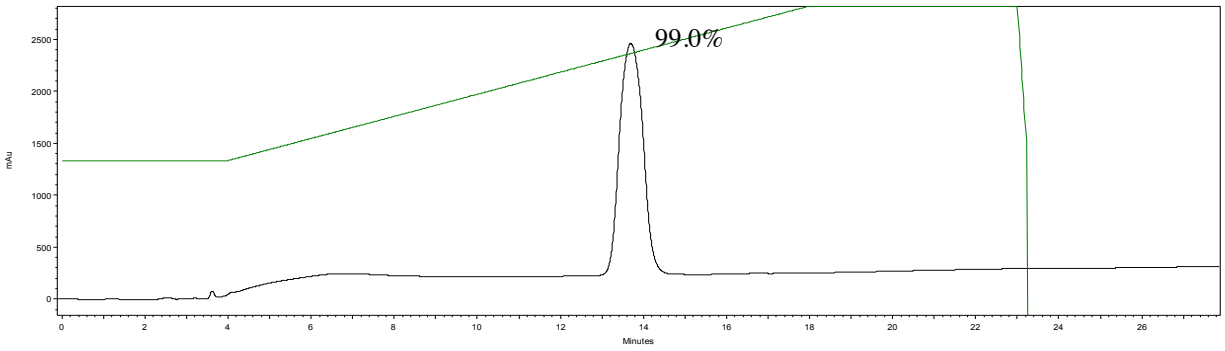

^{1}H NMR (300 MHz, $CDCl_3$)

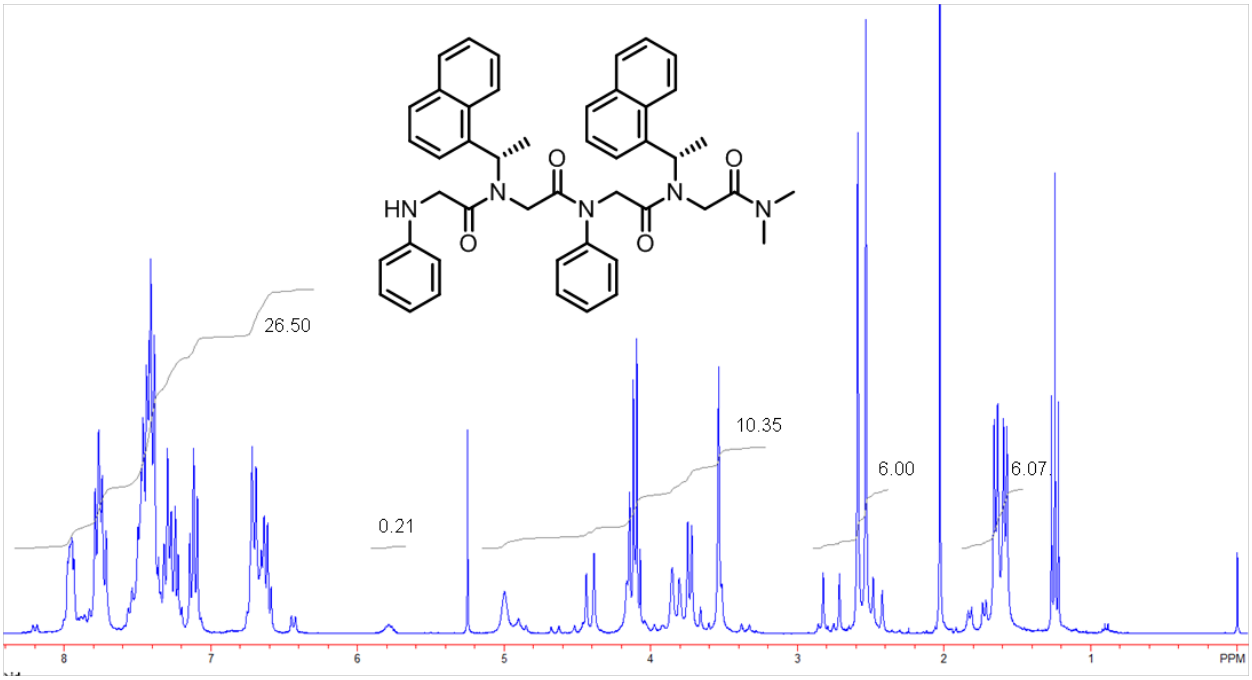

H-*N*2,6mph-*N*s1npe-*N*ph-*N*s1npe-dma. After a general alkylation procedure from Br-*N*s1npe-*N*ph-*N*s1npe-Dma and aqueous work-up, the crude brown oil was loaded onto a column of silica gel (equilibrated with 7:3 EtOAc/hexanes and 1% TEA) and eluted by flash column chromatography using 7:3 EtOAc/hexanes and 1% TEA to afford a white solid. Isolated yield = 94%; TLC: R_f = 0.24 (7:3 EtOAc/hexanes with 1% TEA); HR-MS (ESI): $C_{48}H_{52}N_5O_4$, $[M+H]^+$ calcd m/z = 762.4014, observed m/z = 762.3997.

HPLC (220 nm)

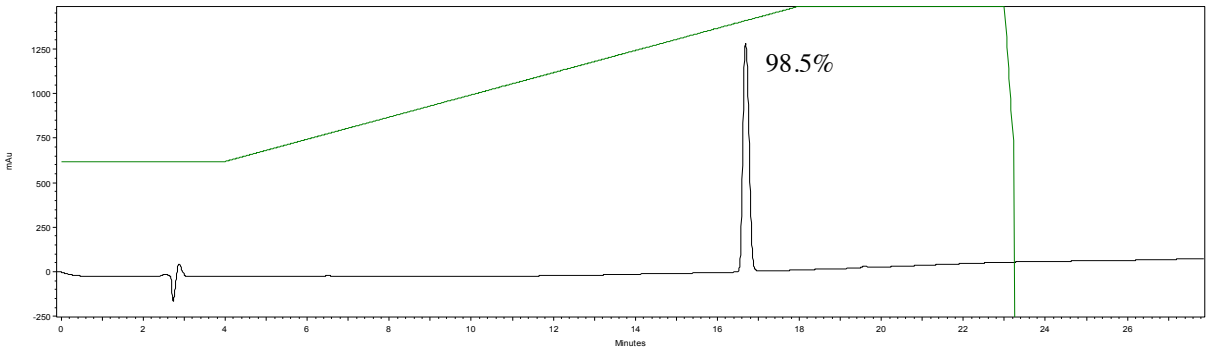

^{1}H NMR (300 MHz, $CDCl_3$) – "X" marks trace solvent peak (EtOAc).

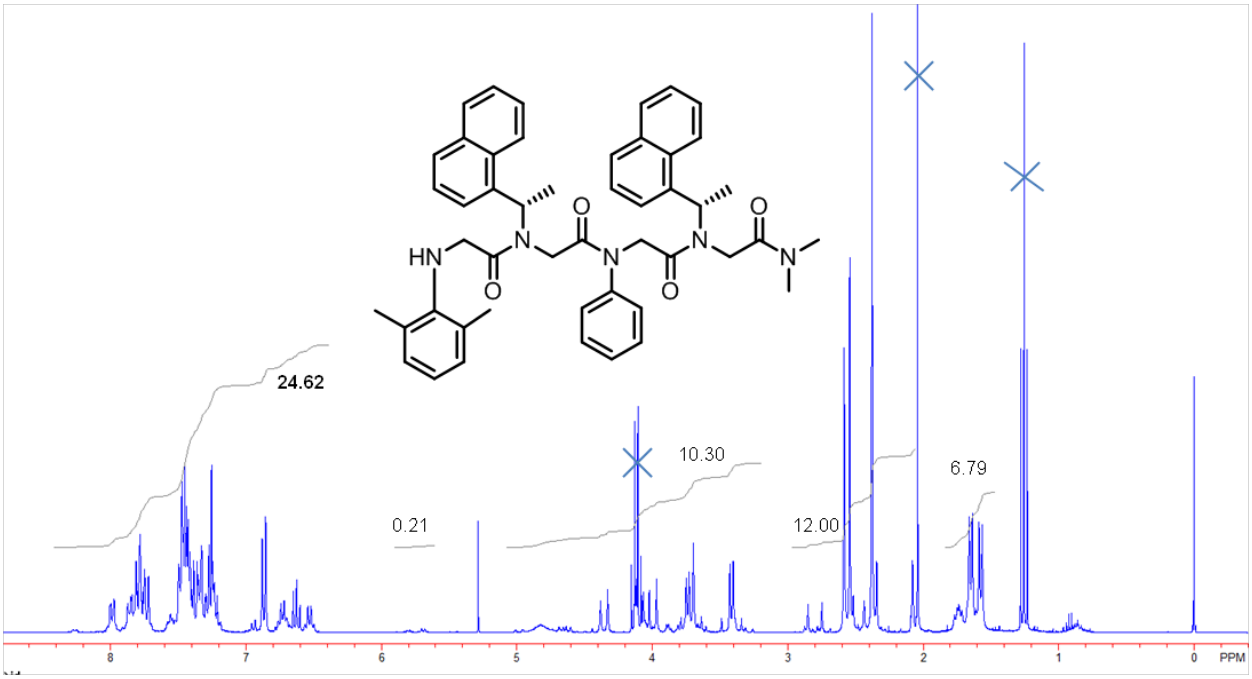

H-*N*2,6mph-Ac*^{13}C-*N*s1npe-*N*4fph-*N*s1npe-dma. After a general alkylation procedure from Br-Ac^{13}C-*N*s1npe-*N*ph-*N*s1npe-dma and aqueous work-up, the crude dark brown oil was loaded onto a column of silica gel (equilibrated with 4:1 EtOAc/hexanes) and eluted by flash column chromatography using 4:1 EtOAc/hexanes. The product was isolated as a white foam after two rounds of manual flash column chromatography. Isolated yield = 40% (over two steps from H-*N*s1npe-*N*4fph-*N*s1npe-dma); TLC: R_f = 0.33 (4:1 EtOAc/hexane), 0.53 (EtOAc); HR-MS (ESI): $C_{46}C^{13}{}_2H_{51}FN_5O_4$, $[M+H]^+$ calcd m/z = 782.3987, observed m/z = 782.3958.

HPLC (220 nm)

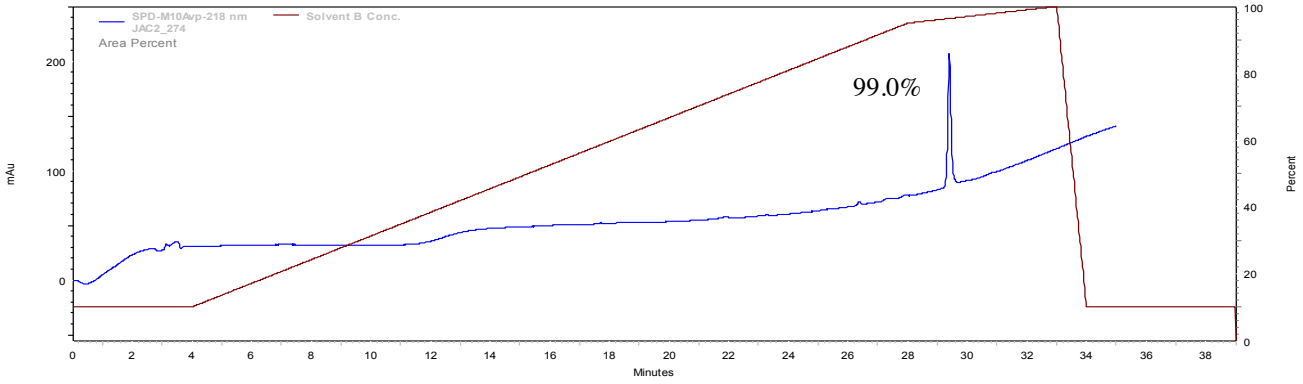

^{1}H NMR (300 MHz, $CDCl_3$)

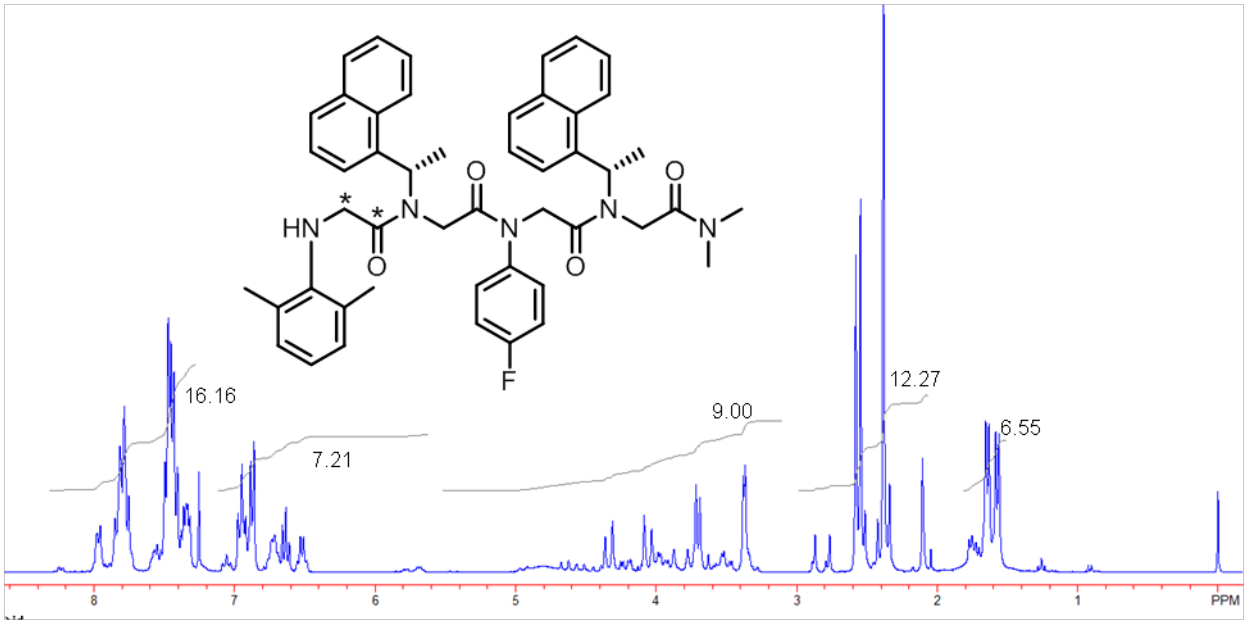

H-*N*3,5mph-*N*s1npe-*N*ph-*N*s1npe-dma. After a general alkylation procedure from Br-*N*s1npe-*N*ph-*N*s1npe-Dma and aqueous work-up, the crude brown oil was loaded onto a column of silica gel (equilibrated with 3:2 EtOAc/hexanes with 1% TEA) and eluted by flash column chromatography using 3:2 EtOAc/hexanes with 1% TEA to afford a white solid. yield = 89%; TLC: R_f = 0.25 (3:2 EtOAc/hexanes with 1% TEA); HR-MS (ESI): $C_{48}H_{52}N_5O_4$, $[M+H]^+$ calcd m/z = 762.4014, observed m/z = 762.4033.

HPLC (220 nm)

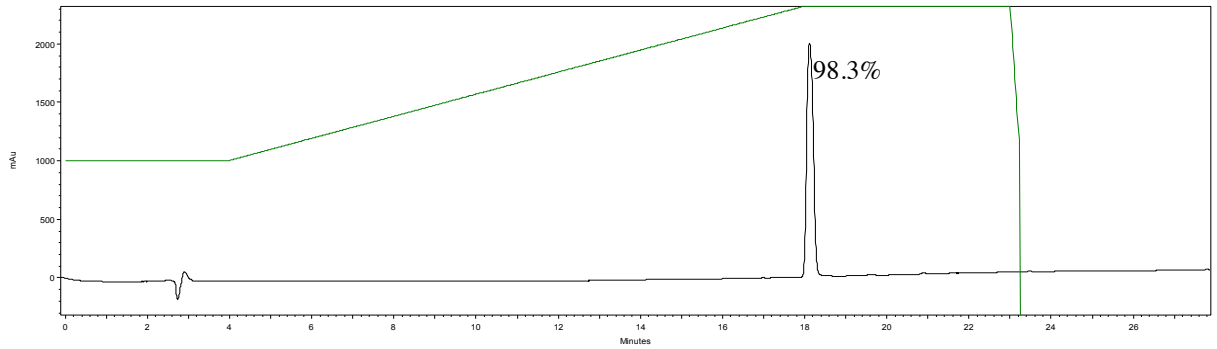

^{1}H NMR (300 MHz, $CDCl_3$)

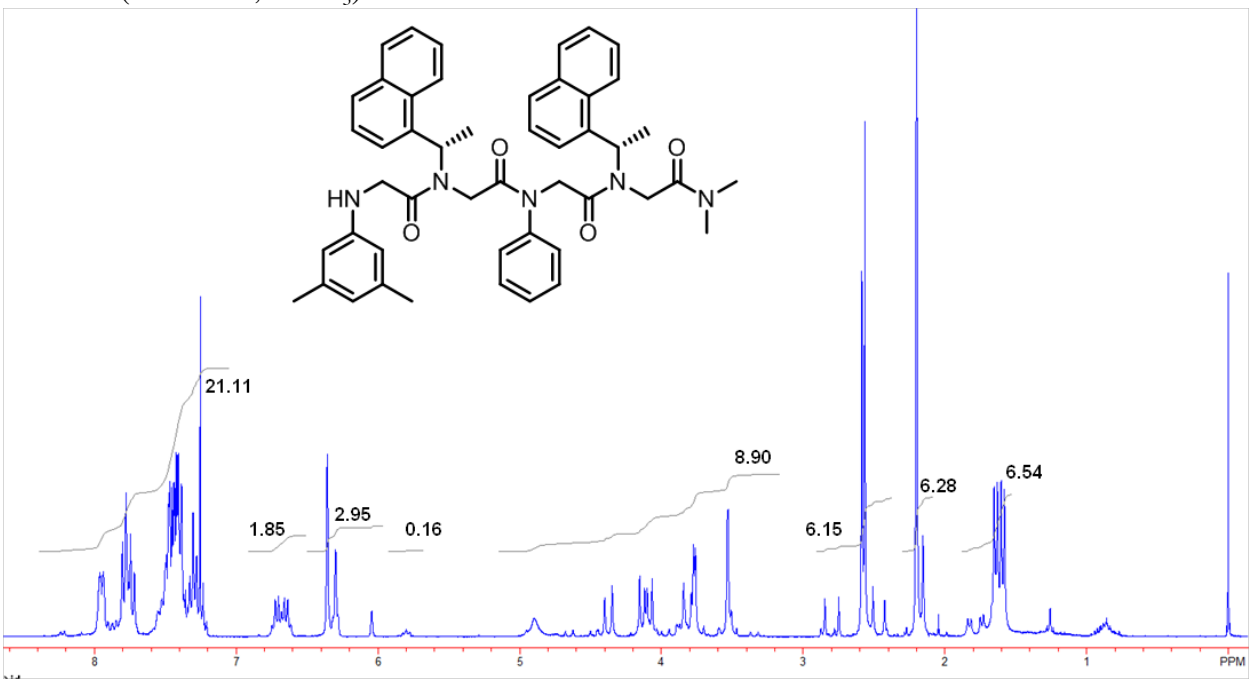

Br-*N*ph-*N*s1npe-*N*ph-*N*s1npe-dma. After a general acylation procedure of H-*N*ph-*N*s1npe-*N*ph-*N*s1npe-Dma and aqueous work-up, the crude tan oil was loaded onto a column of silica gel (equilibrated with 9:1 EtOAc/hexanes) and eluted by flash column chromatography using 9:1 EtOAc/hexanes to afford a white solid. Isolated yield = 93%; TLC: R_f = 0.22 (9:1 EtOAc/hexanes); HR-MS (ESI): $C_{48}H_{48}BrN_5NaO_5$, $[M+Na]^+$ calcd m/z = 876.2732, observed m/z = 876.2748.

HPLC (220 nm)

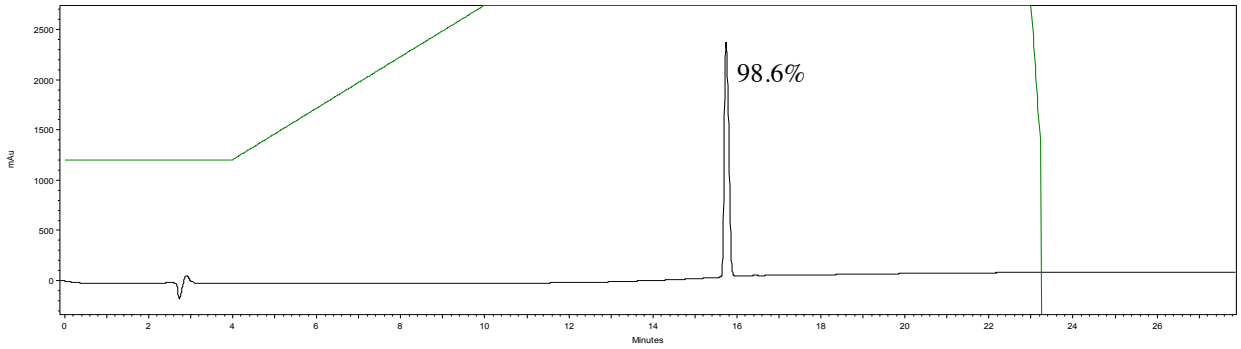

^{1}H NMR (300 MHz, $CDCl_3$)

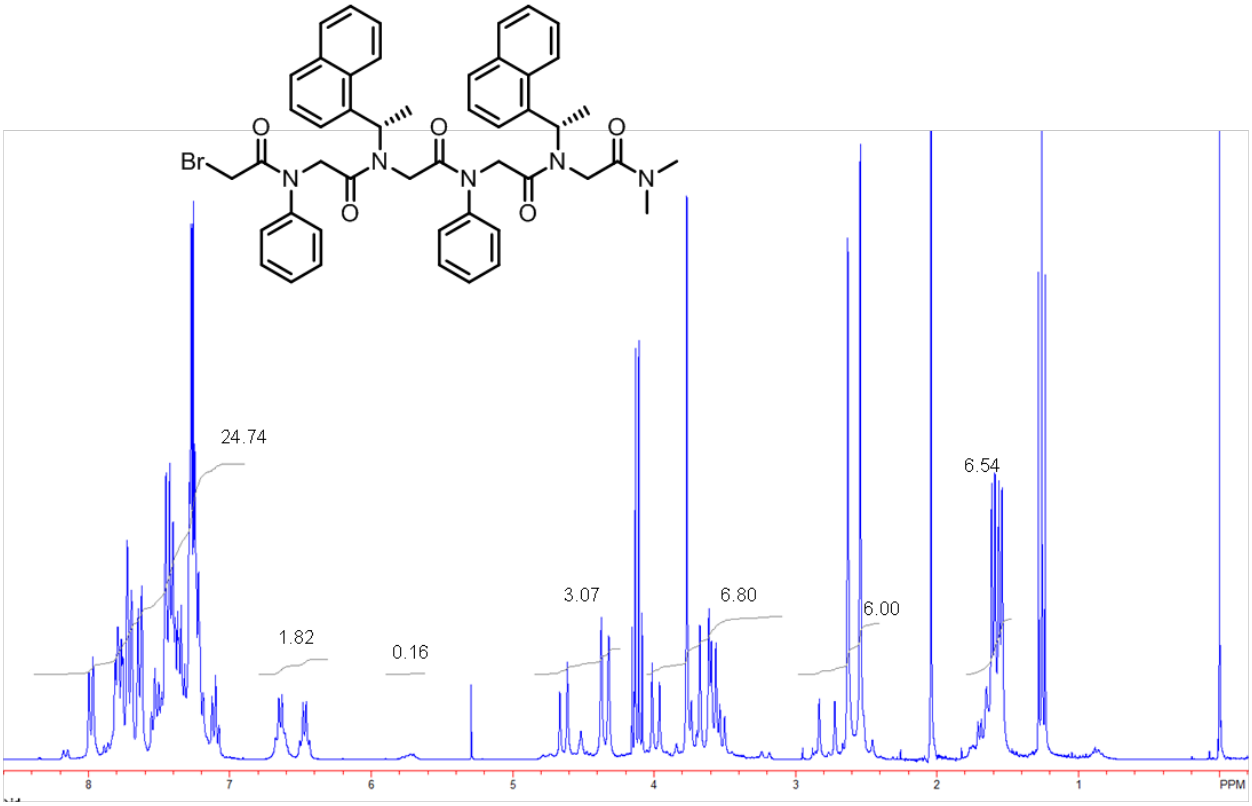

Br-*N*2,6mph-Ac*^{13}C-*N*s1npe-*N*4fph-*N*s1npe-dma. A general acylation procedure from H-*N*2,6mph-Ac^{13}C-*N*s1npe-*N*4fph-*N*s1npe-dma afforded a white foam. The crude product was carried on to the subsequent alkylation reaction after aqueous work-up; TLC: R_f = 0.30 (4:1 EtOAc/hexane), HR-MS (ESI): $C_{46}C^{13}{}_2H_{47}BrFN_5NaO_5$, $[M+Na]^+$ calcd m/z = 924.3017, observed m/z = 924.3031.

HPLC (220 nm)

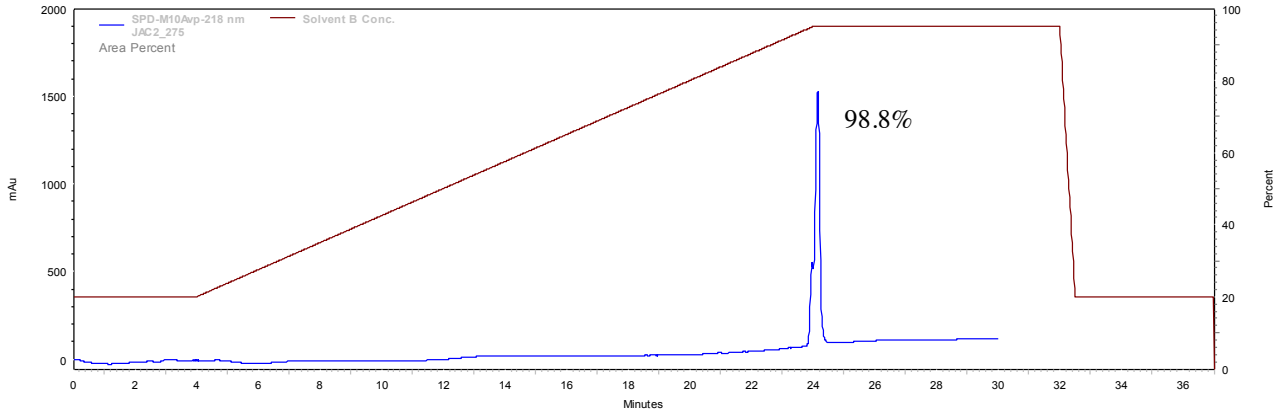

^{1}H NMR (300 MHz, $CDCl_3$)

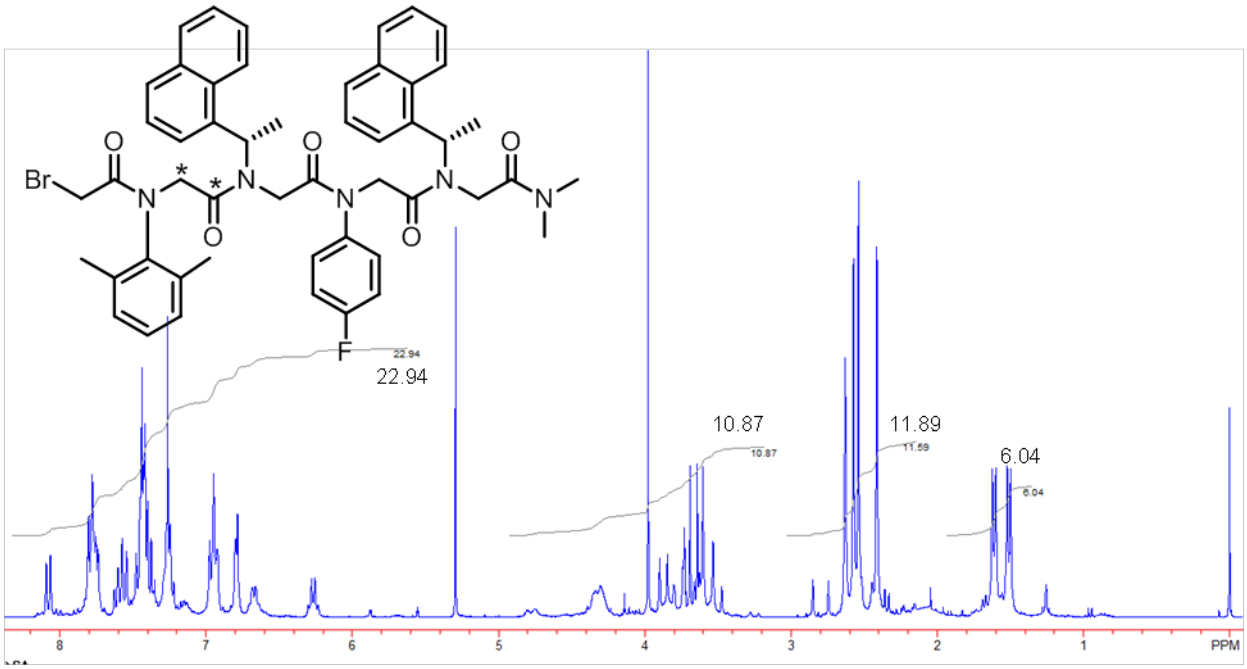

H-*N*s1npe-*N*ph-*N*s1npe-*N*ph-*N*s1npe-dma. After a general alkylation procedure from Br-*N*ph-*N*s1npe-*N*ph-*N*s1npe-Dma and aqueous work-up, the product was collected both by precipitation from EtOAc (as a white solid) and by column chromatography of the brown decantant solution. The latter solution was loaded onto a column of silica gel (equilibrated with 2% TEA/2% MeOH/CH_2Cl_2) and eluted by flash column chromatography using 2% TEA/2% MeOH/CH_2Cl_2 to afford a white powder. Isolated yield = 94%; TLC: R_f = 0.45 (2% TEA / 2% MeOH / CH_2Cl_2); HR-MS (ESI): $C_{60}H_{60}N_6NaO_5$, $[M+Na]^+$ calcd m/z = 967.4518, observed m/z = 967.4505.

HPLC (220 nm)

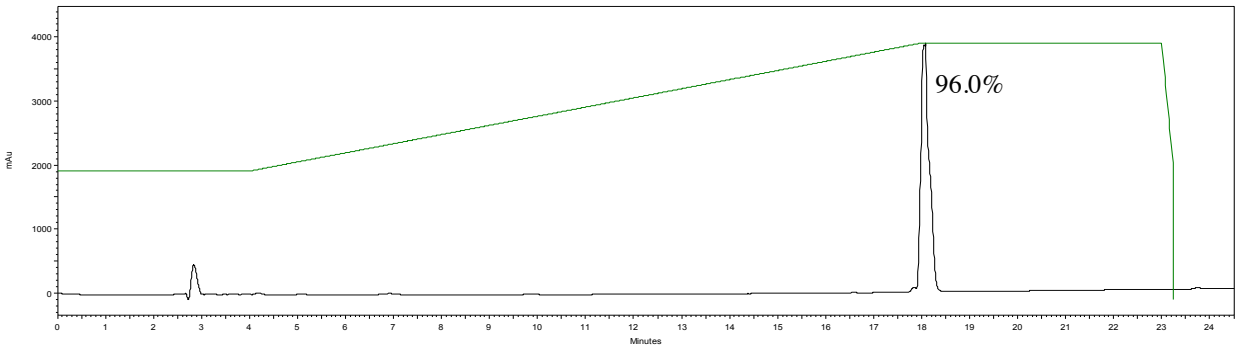

^{1}H NMR (300 MHz, $CDCl_3$) – "X" marks trace solvent peak (DMF).

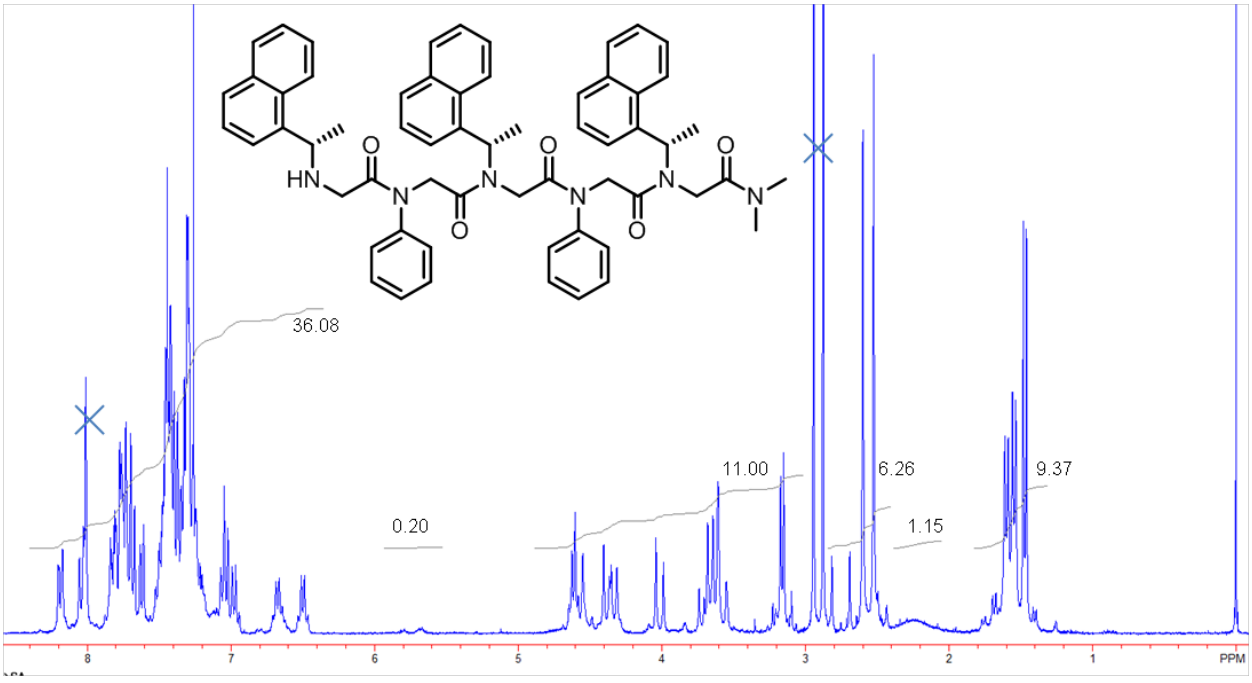

H-*N*s1npe-*N*2,6mph-Ac*^{13}C-*N*s1npe-*N*4fph-*N*s1npe-dma. After a general alkylation procedure from Br-*N*2,6mph-Ac^{13}C-*N*s1npe-*N*4fph-*N*s1npe-dma and aqueous work-up, the crude brown oil was loaded onto a column of silica gel (equilibrated with 5:1 EtOAc/hexanes) and eluted by flash column chromatography using 5:1 EtOAc/hexanes to afford a white foam. Isolated yield = 40% (over two steps from H-*N*2,6mph-Ac*^{13}C-*N*s1npe-*N*4fph-*N*s1npe-dma); TLC: R_f = 0.27 (5:1 EtOAc/hexane), HR-MS (ESI): $C_{60}C^{13}{}_2H_{63}FN_6NaO_5$, $[M+Na]^+$ calcd m/z = 1015.4843, observed m/z = 1015.4843.

HPLC (220 nm)

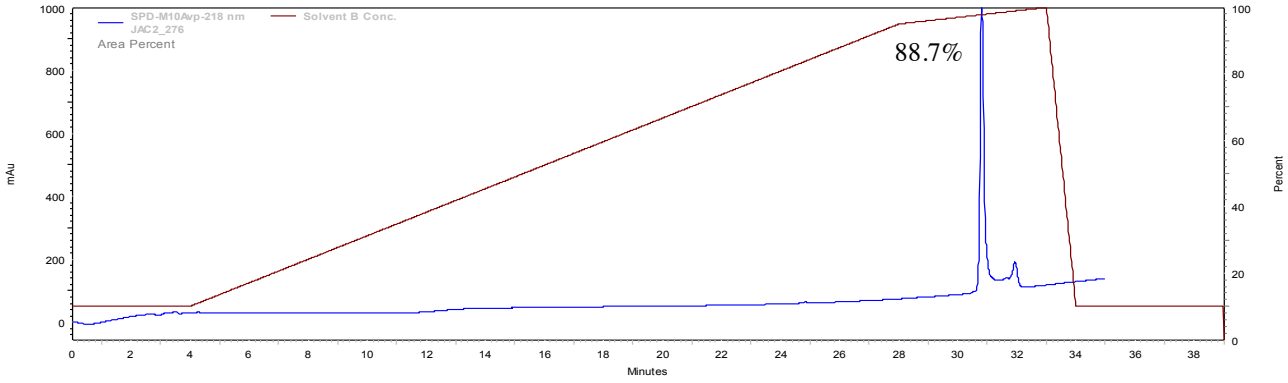

^{1}H NMR (300 MHz, $CDCl_3$) – "X" marks trace solvent peak (DMF).

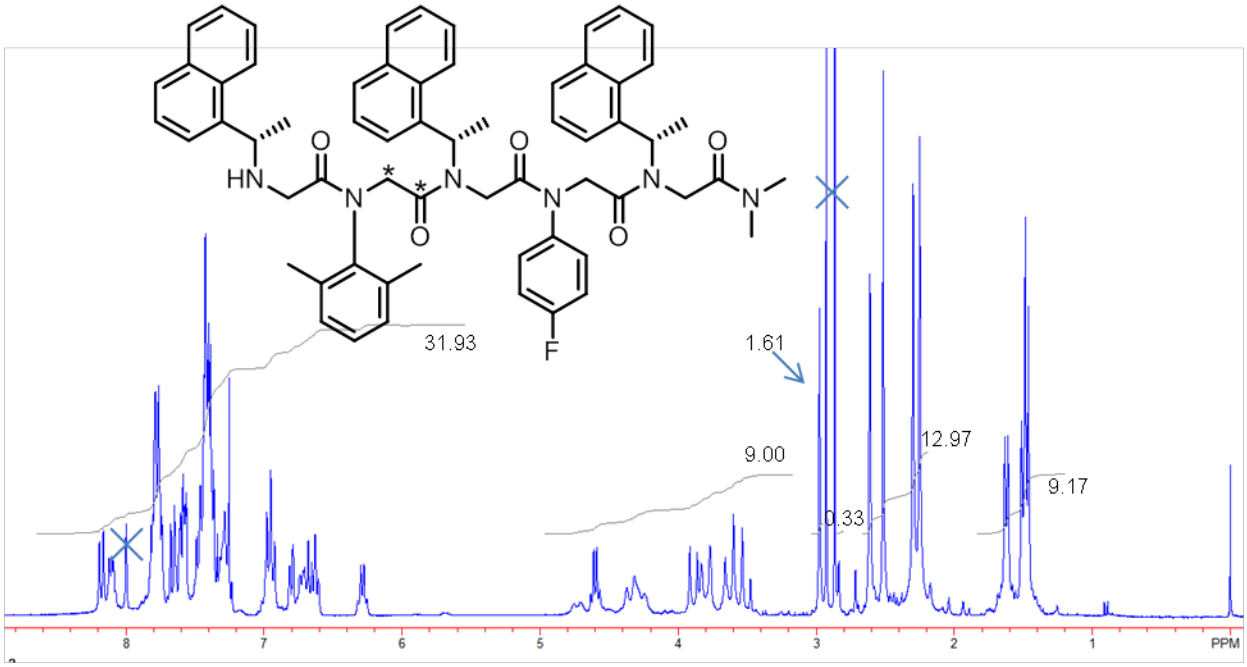

Br-*N*s1npe-*N*ph-*N*s1npe-*N*ph-*N*s1npe-dma. After a general acylation procedure from H-*N*s1npe-*N*ph-*N*s1npe-*N*ph-*N*s1npe-Dma and aqueous work-up, the crude tan oil was loaded onto a column of silica gel (equilibrated with EtOAc) and eluted by flash column chromatography using EtOAc to afford a white powder. Isolated yield = 63%; TLC: R_f = 0.39 (EtOAc); HR-MS (ESI): $C_{62}H_{61}BrN_6NaO_6$, $[M+Na]^+$ calcd m/z = 1087.3729, observed m/z = 1087.3696.

HPLC (220 nm)

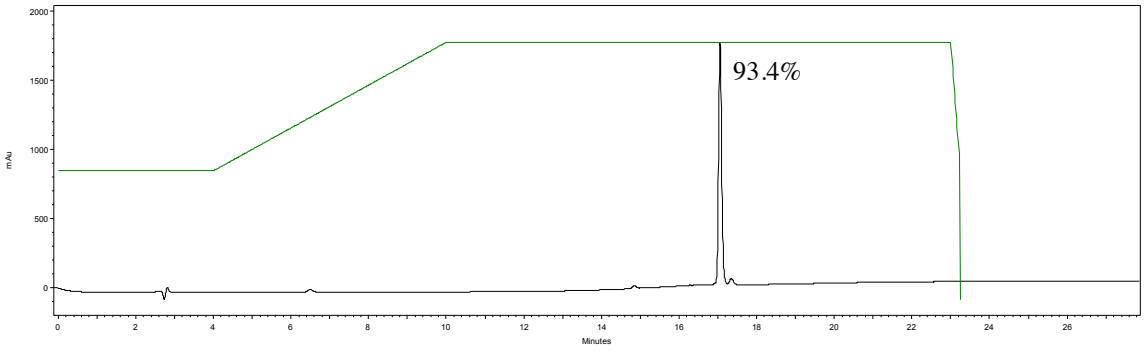

^{1}H NMR (300 MHz, $CDCl_3$) – "X" marks trace solvent peaks (CH_2Cl_2, acetone, and EtOAc).

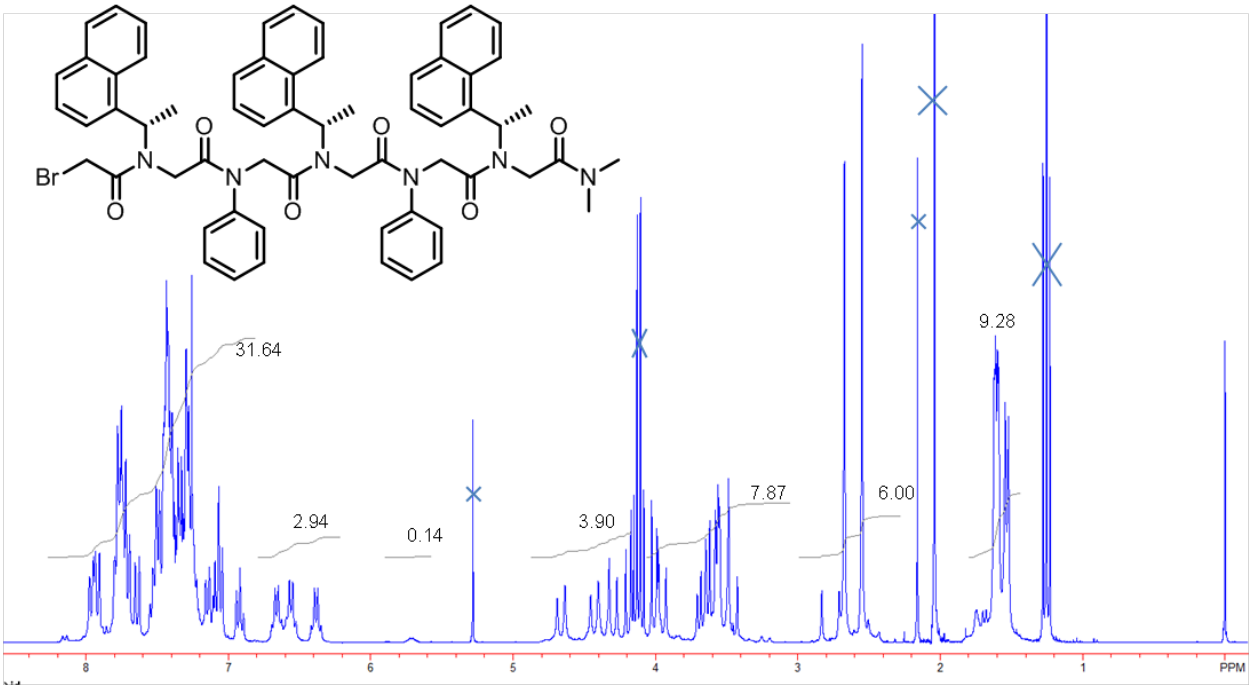

Br-*N*s1npe-*N*2,6mph-Ac*^{13}C-*N*s1npe-*N*4fph-*N*s1npe-dma. After a general acylation procedure from H-*N*s1npe-*N*2,6mph-Ac^{13}C-*N*s1npe-*N*4fph-*N*s1npe-dma and aqueous work-up, the crude tan oil was loaded onto a column of silica gel (equilibrated with 4:1 EtOAc/hexanes) and eluted by flash column chromatography using 4:1 EtOAc/hexanes to afford a white foam. Isolated yield = 91%; TLC: R_f = 0.27 (4:1 EtOAc/hexane), HR-MS (ESI): $C_{62}C^{13}{}_2H_{64}BrFN_6NaO_6$, $[M+Na]^+$ calcd m/z = 1135.4015, observed m/z = 1135.4044.

HPLC (220 nm)

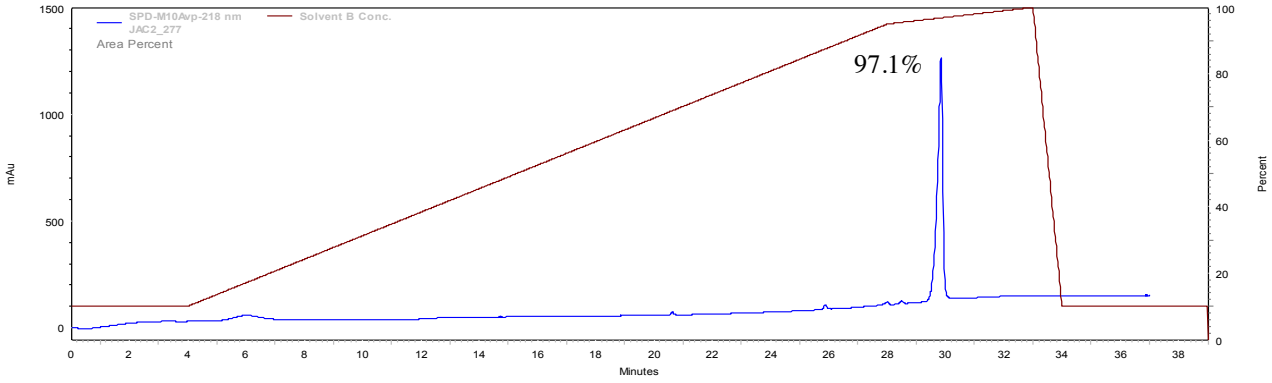

^{1}H NMR (300 MHz, $CDCl_3$) – "X" marks trace solvent peaks (CH_2Cl_2 and EtOAc).

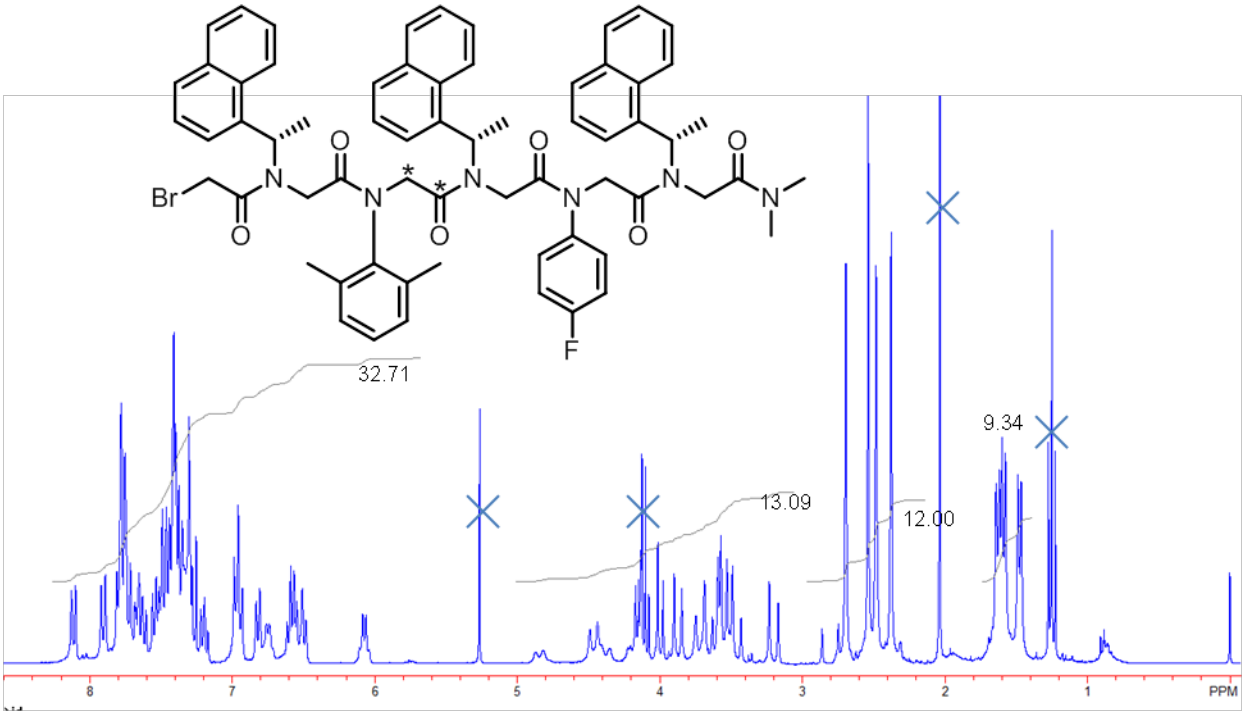

H-*N*ph-*N*s1npe-*N*ph-*N*s1npe-*N*ph-*N*s1npe-dma. After a general alkylation procedure from Br-*N*s1npe-*N*ph-*N*s1npe-*N*ph-*N*s1npe-Dma and aqueous work-up, the crude brown oil was loaded onto a column of silica gel (equilibrated with 9:1 EtOAc/hexanes) and eluted by flash column chromatography using 9:1 EtOAc/hexanes to afford a slightly yellow foam. Isolated yield = 95%; TLC: R_f = 0.29 (9:1 EtOAc/hexanes); HR-MS (ESI): $C_{68}H_{67}N_7NaO_6$, $[M+Na]^+$ calcd m/z = 1100.5046, observed m/z = 1100.5007.

HPLC (220 nm)

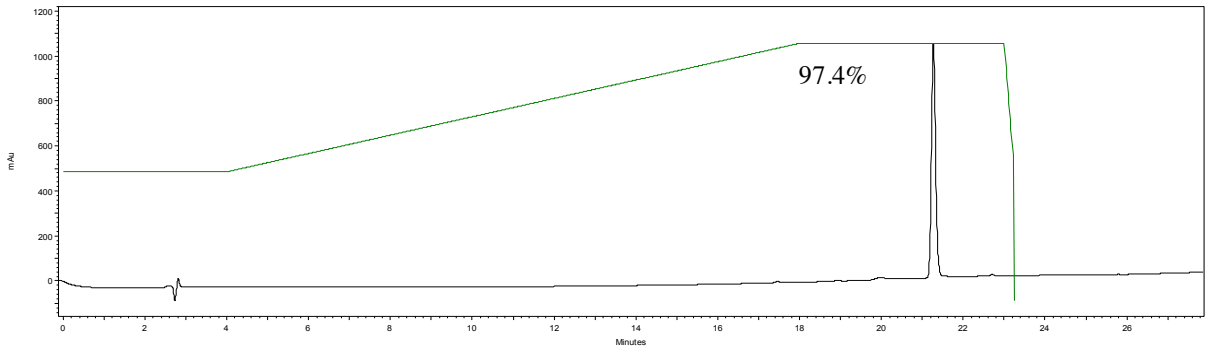

^{1}H NMR (300 MHz, $CDCl_3$)

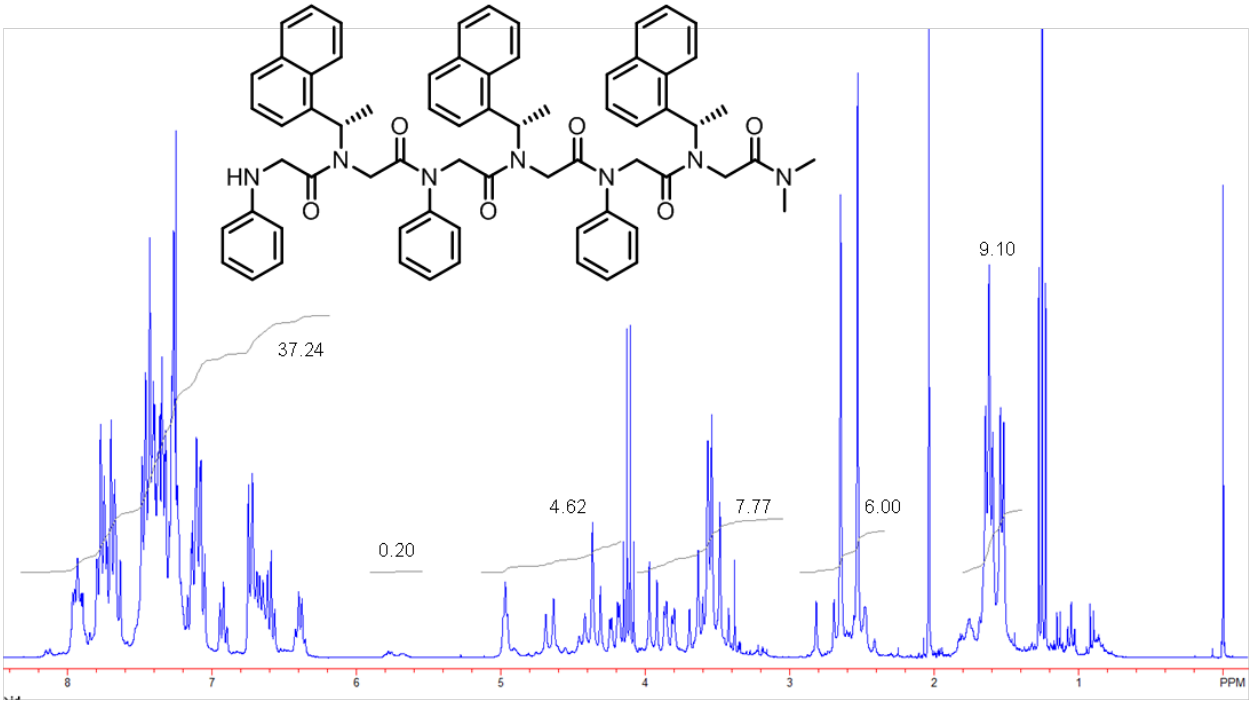

H-*N*3,5mph-*N*s1npe-*N*2,6mph-Ac*^{13}C-*N*s1npe-*N*4fph-*N*s1npe-dma. After a general alkylation procedure from Br-*N*s1npe-*N*2,6mph-Ac^{13}C-*N*s1npe-*N*4fph-*N*s1npe-dma and aqueous work-up, the crude light brown oil was loaded onto a column of silica gel (equilibrated with 4:1 EtOAc/hexanes) and eluted by flash column chromatography using 4:1 EtOAc/hexanes to afford a white powder. Isolated yield = 90%, TLC: R_f = 0.27 (4:1 EtOAc/hexane), HR-MS (ESI): $C_{70}C^{13}{}_2H_{75}FN_7O_6$, $[M+H]^+$ calcd m/z = 1154.5825, observed m/z = 1154.5870.

HPLC (220 nm)

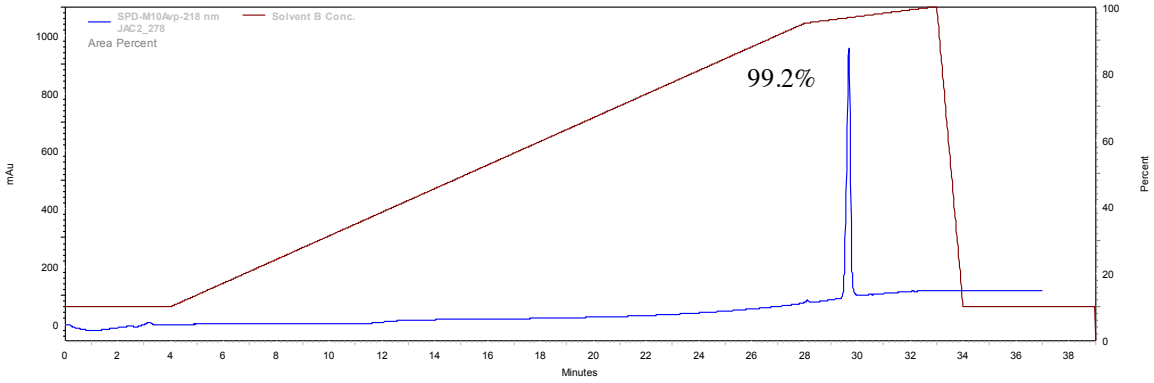

^{1}H NMR (300MHz, $CDCl_3$) – "X" marks trace solvent peak (EtOAc).

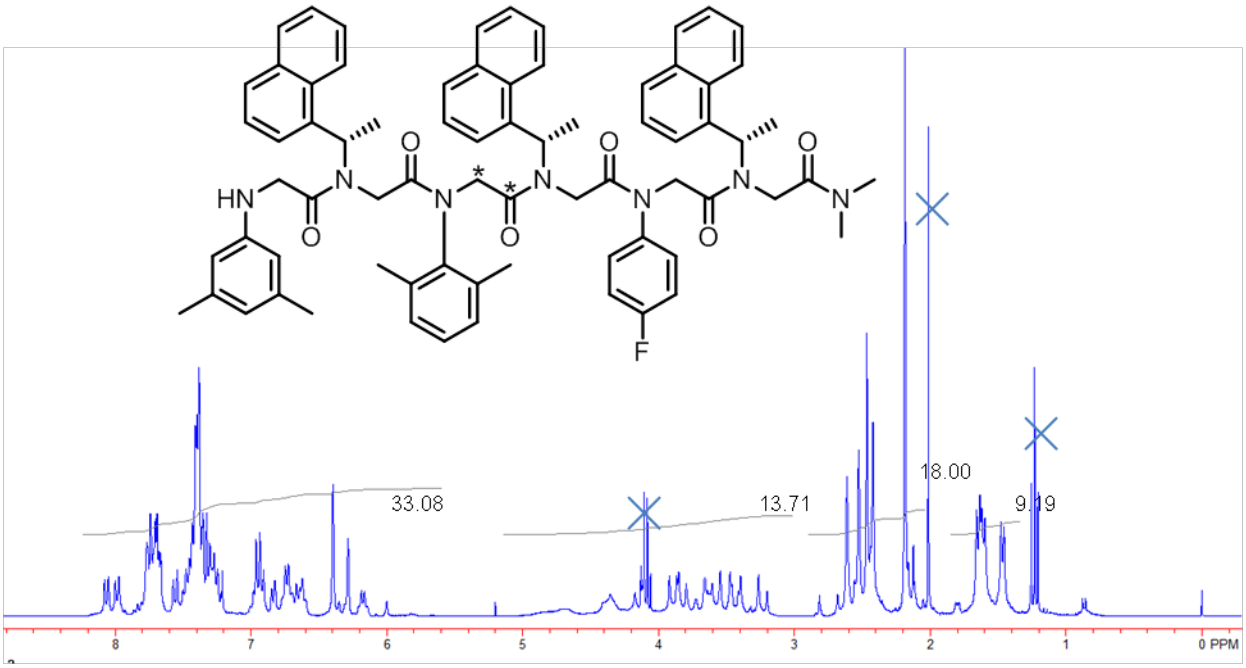

Br-*N*ph-*N*s1npe-*N*ph-*N*s1npe-*N*ph-*N*s1npe-dma. After a general acylation procedure from H-*N*ph-*N*s1npe-*N*ph-*N*s1npe-*N*ph-*N*s1npe-Dma and aqueous work-up, the crude brown oil was loaded onto a column of silica gel (equilibrated with EtOAc) and eluted by flash column chromatography using EtOAc to afford a white foam. Isolated yield = 79%; TLC: R_f = 0.31 (EtOAc); HR-MS (ESI): $C_{70}H_{68}BrN_7NaO_7$, $[M+Na]^+$ calcd m/z = 1220.4256, observed m/z = 1220.4249.

HPLC (220 nm)

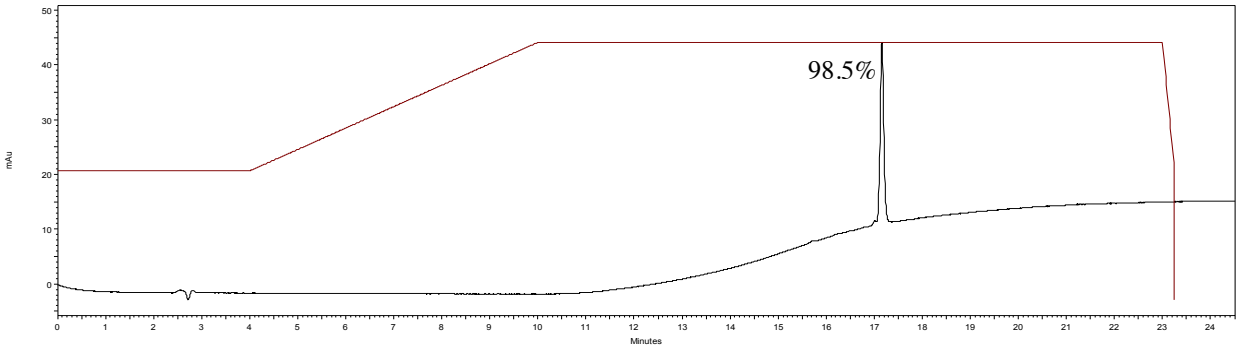

^{1}H NMR (300 MHz, $CDCl_3$)

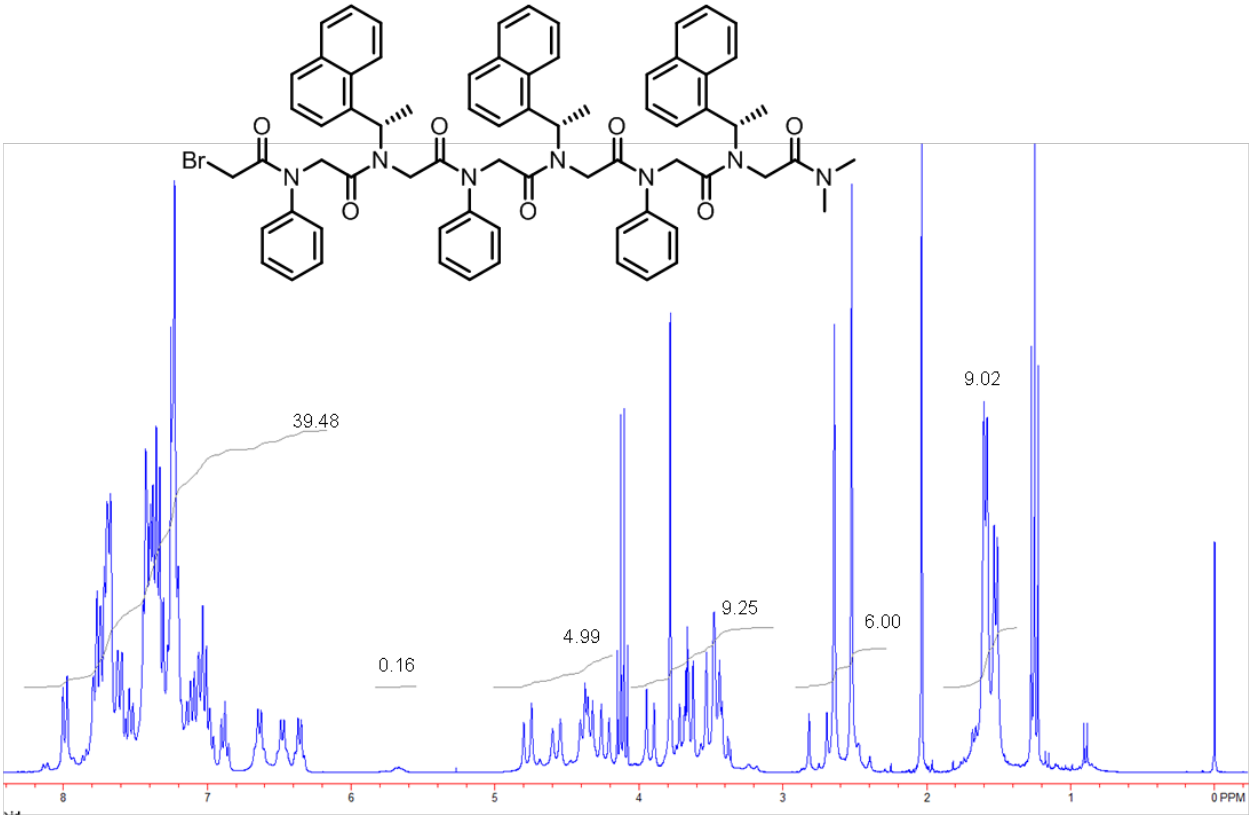

H-*N*s1npe-*N*ph-*N*s1npe-*N*ph-*N*s1npe-*N*ph-*N*s1npe-dma. A general alkylation procedure from Br-*N*ph-*N*s1npe-*N*ph-*N*s1npe-*N*ph-*N*s1npe-Dma afforded a white foam. Isolated yield = 84% (*note*, the impurity shown in the HPLC trace below is excess (*S*)-1-(1-naphthylethyl) amine that could not be separated fully after three attempts by column chromatography [the subsequent acylated peptoids were separated, as reported below; pages S-74 and S-84]); TLC: R_f = 0.34 (1:2:7 MeOH/CH_2Cl_2/EtOAc with 1% TEA), R_f = 0.15 (EtOAc with 1% TEA); HR-MS (ESI): $C_{82}H_{81}N_8O_7$, $[M+H]^+$ calcd m/z = 1289.6223, observed m/z = 1289.6232.

HPLC (220 nm)

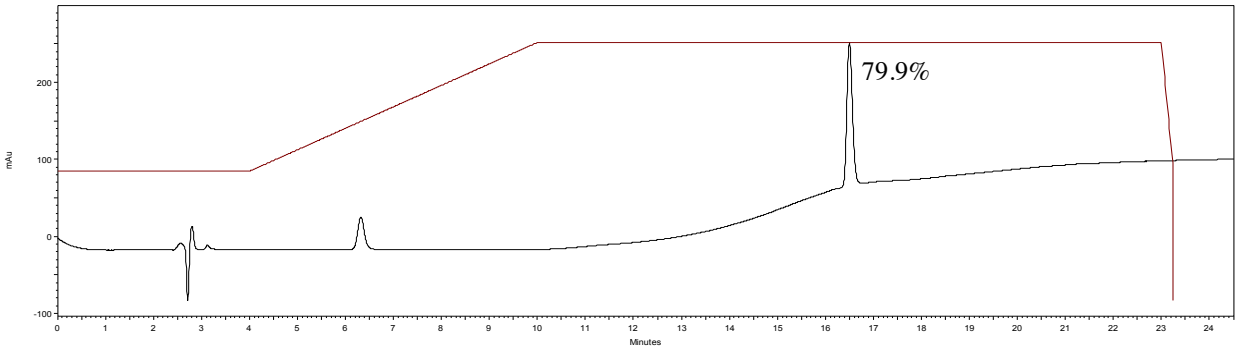

^{1}H NMR (300 MHz, $CDCl_3$)

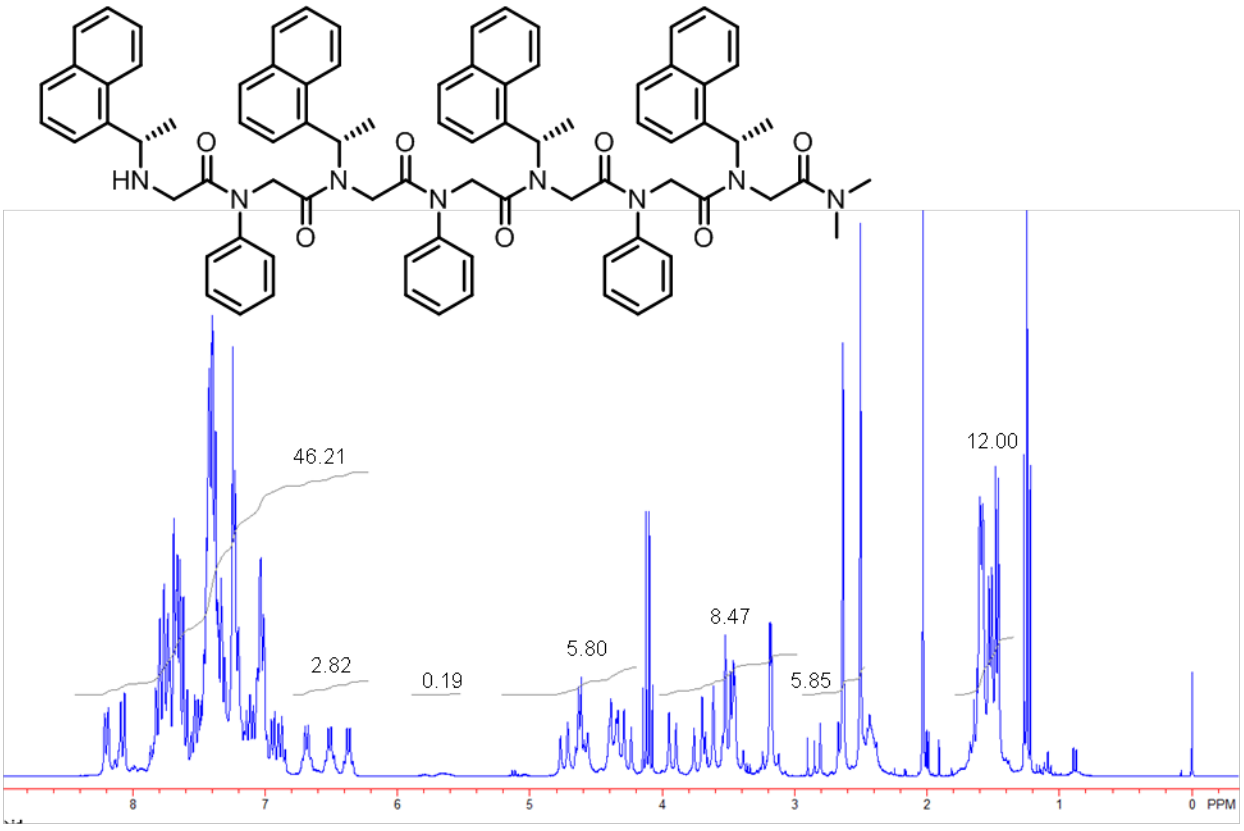

Br-*N*s1npe-*N*ph-*N*s1npe-*N*ph-*N*s1npe-*N*ph-*N*s1npe-dma. After a general acylation procedure from H-*N*s1npe-*N*ph-*N*s1npe-*N*ph-*N*s1npe-*N*ph-*N*s1npe-Dma and aqueous work-up, the crude brown oil was loaded onto a column of silica gel (equilibrated with 5% hexanes in EtOAc) and eluted by flash column chromatography using 5% hexanes in EtOAc to afford a white foam. Isolated yield = 90%; TLC: R_f = 0.30 (5% hexanes in EtOAc); HR-MS (ESI): $C_{84}H_{81}BrN_8NaO_8$, $[M+Na]^+$ calcd m/z = 1431.5253, observed m/z = 1431.5266.

HPLC (220 nm)

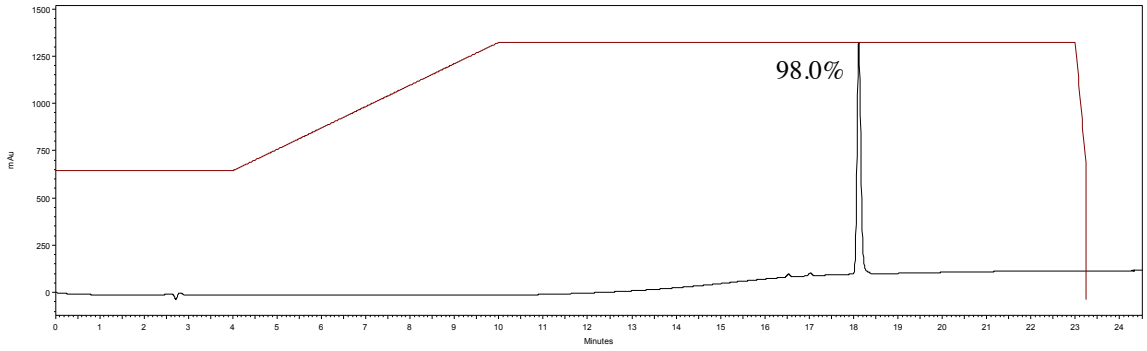

^{1}H NMR (300 MHz, $CDCl_3$) – "X" marks trace solvent peak (EtOAc).

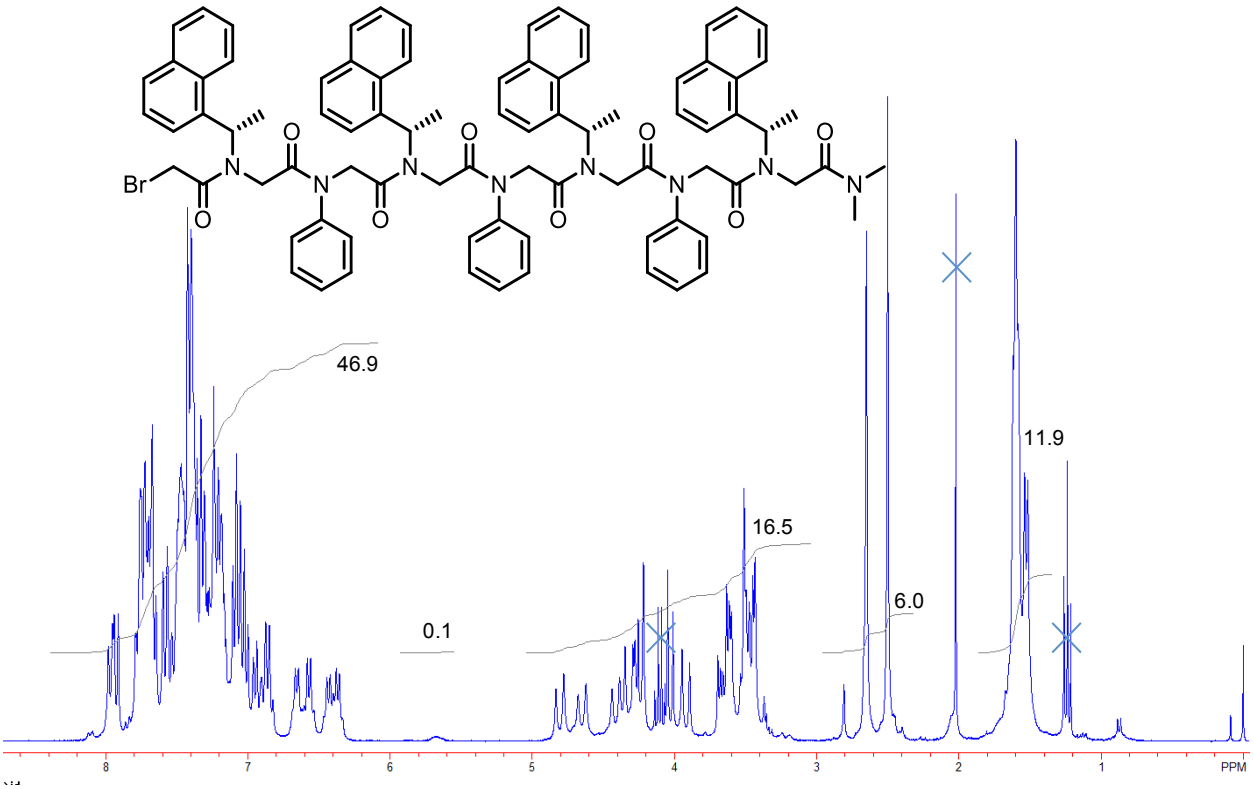

H-*N*ph-*N*s1npe-*N*ph-*N*s1npe-*N*ph-*N*s1npe-*N*ph-*N*s1npe-dma. After a general alkylation procedure from Br-*N*s1npe-*N*ph-*N*s1npe-*N*ph-*N*s1npe-*N*ph-*N*s1npe-Dma and aqueous work-up, the crude brown oil was loaded onto a column of silica gel (equilibrated with 9:1 EtOAc/hexanes) and eluted by flash column chromatography using 5% hexanes in EtOAc to afford an off-white powder. Isolated yield = 84 %; TLC: R_f = 0.33 (5% hexanes in EtOAc); HR-MS (ESI): $C_{90}H_{87}N_9NaO_8$, $[M+Na]^+$ calcd m/z = 1444.6570, observed m/z = 1444.6555.

HPLC (220 nm)

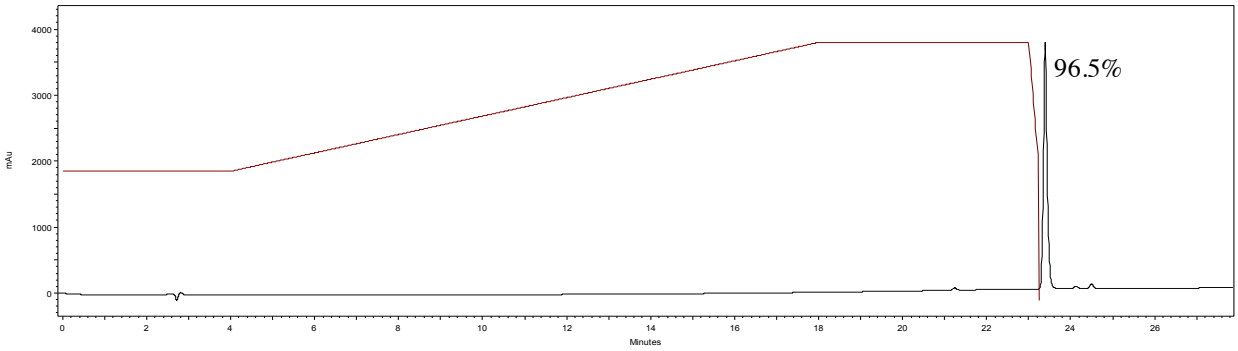

^{1}H NMR (300 MHz, $CDCl_3$) – "X" marks trace solvent peak (EtOAc).

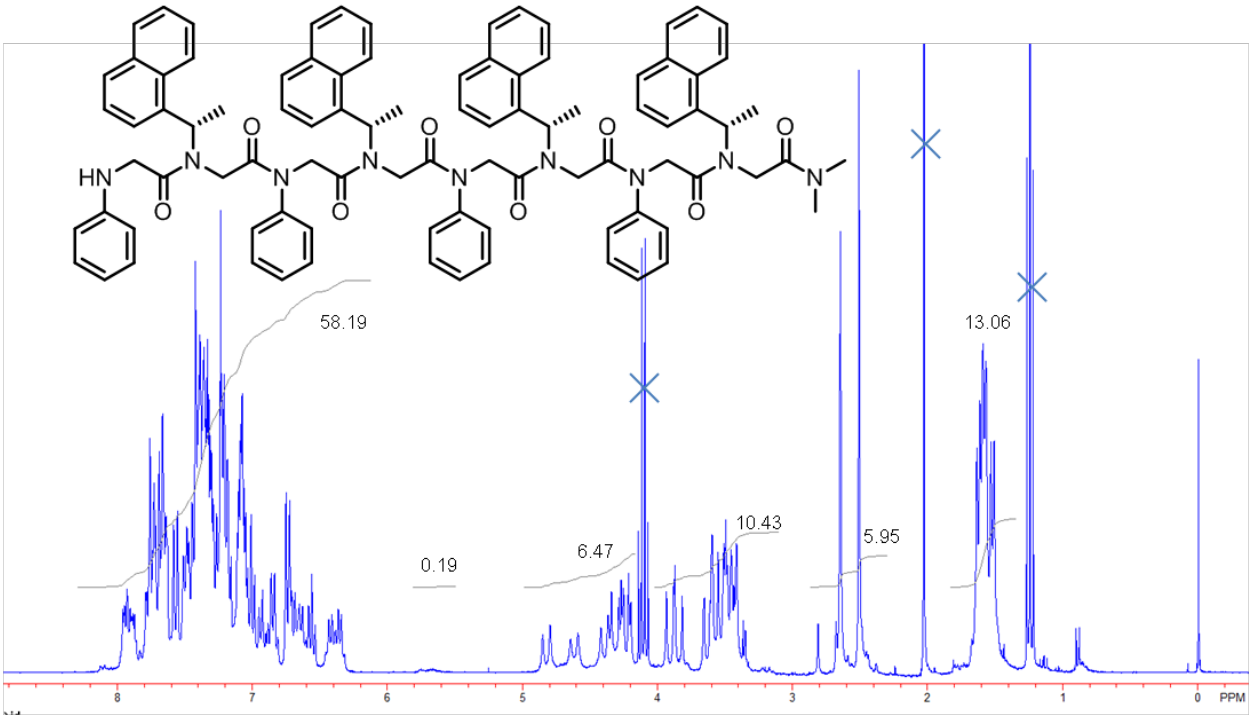

Characterization data for target peptoids 2, 2', and 3–8.

Peptoid 2. Ac-*N*ph-*N*s1npe-dma. After a general acetylation procedure from H-*N*ph-*N*s1npe-dma and aqueous work-up, the crude tan oil was loaded onto a column of silica gel (equilibrated with EtOAc) and eluted by flash column chromatography using EtOAc. Two rounds of chromatography resulted in a transparent oil that was lyophilized from 1:1 ACN/H_2O to afford a white fluffy powder. Isolated yield = 66%; TLC: R_f = 0.26 (EtOAc); HR-MS (ESI): $C_{26}H_{29}N_3NaO_3$ $[M+Na]^+$ calcd m/z = 454.2102, observed m/z = 454.2101.

HPLC (218 nm)

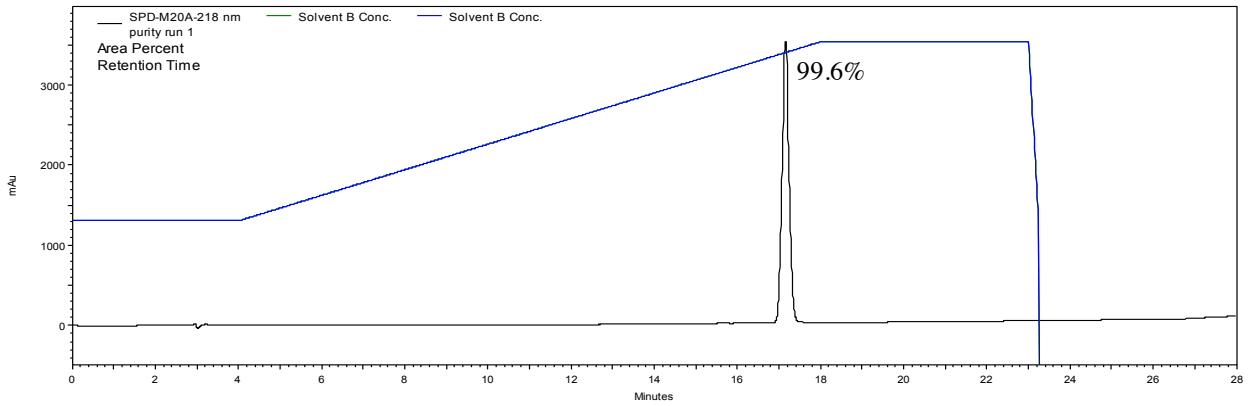

^{1}H NMR (600 MHz, $CDCl_3$, 10 mM)

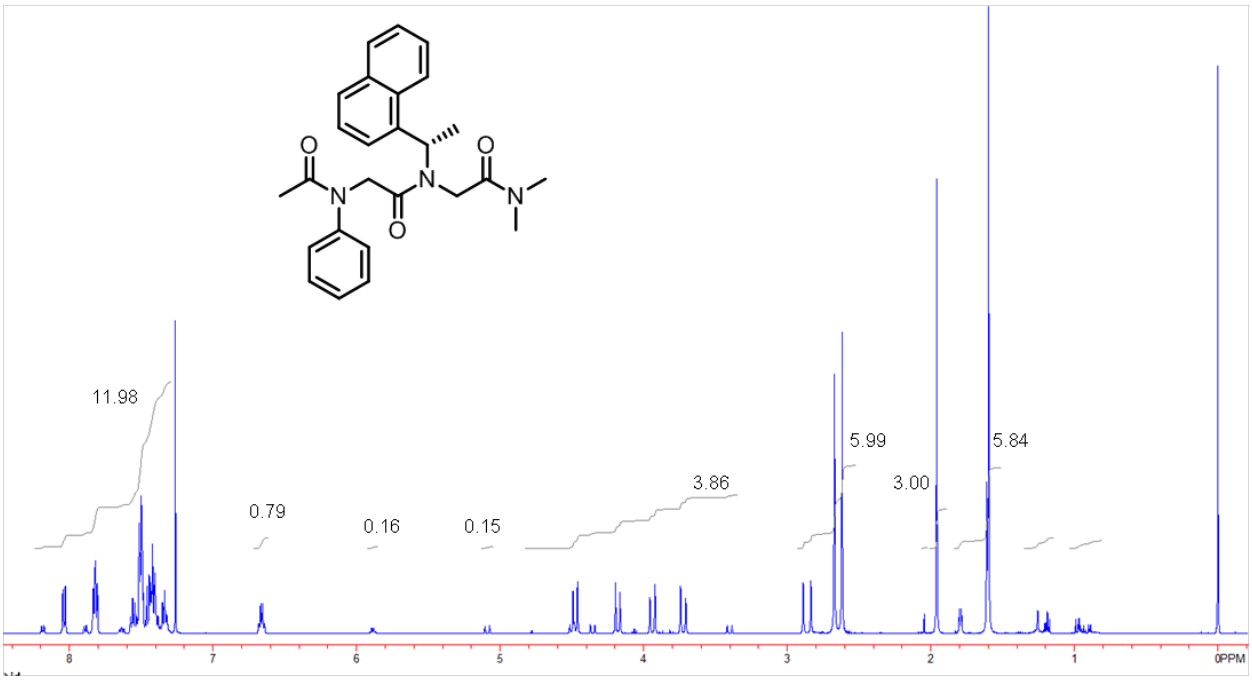

Peptoid 2′. Ac-*N*s1npe-*N*ph-dma. After a general acetylation procedure from H-*N*s1npe-*N*ph-dma and aqueous work-up, the crude tan oil was loaded onto a column of silica gel (equilibrated with 5% MeOH in EtOAc) and eluted by flash column chromatography using 5% MeOH in EtOAc. Two rounds of chromatography resulted in a transparent oil that was lyophilized from 1:1 ACN/H_2O to afford a white fluffy powder. Isolated yield = 85%; TLC: R_f = 0.14 (5% MeOH in EtOAc), 0.31 (1:1 acetone/hexanes); HR-MS (ESI): $C_{26}H_{29}N_3NaO_3$ $[M+Na]^+$, calcd m/z = 454.2102, observed m/z = 454.2097.

HPLC (220 nm)

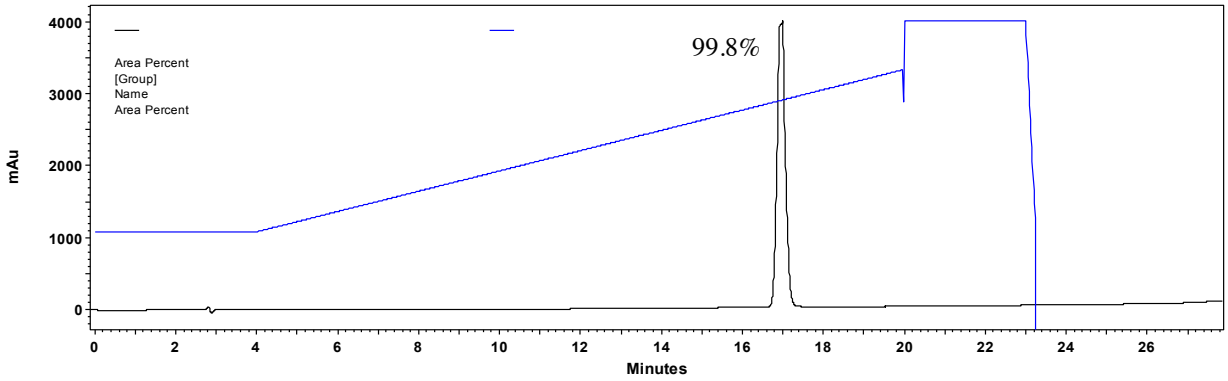

^{1}H NMR (600 MHz, $CDCl_3$, 10 mM)

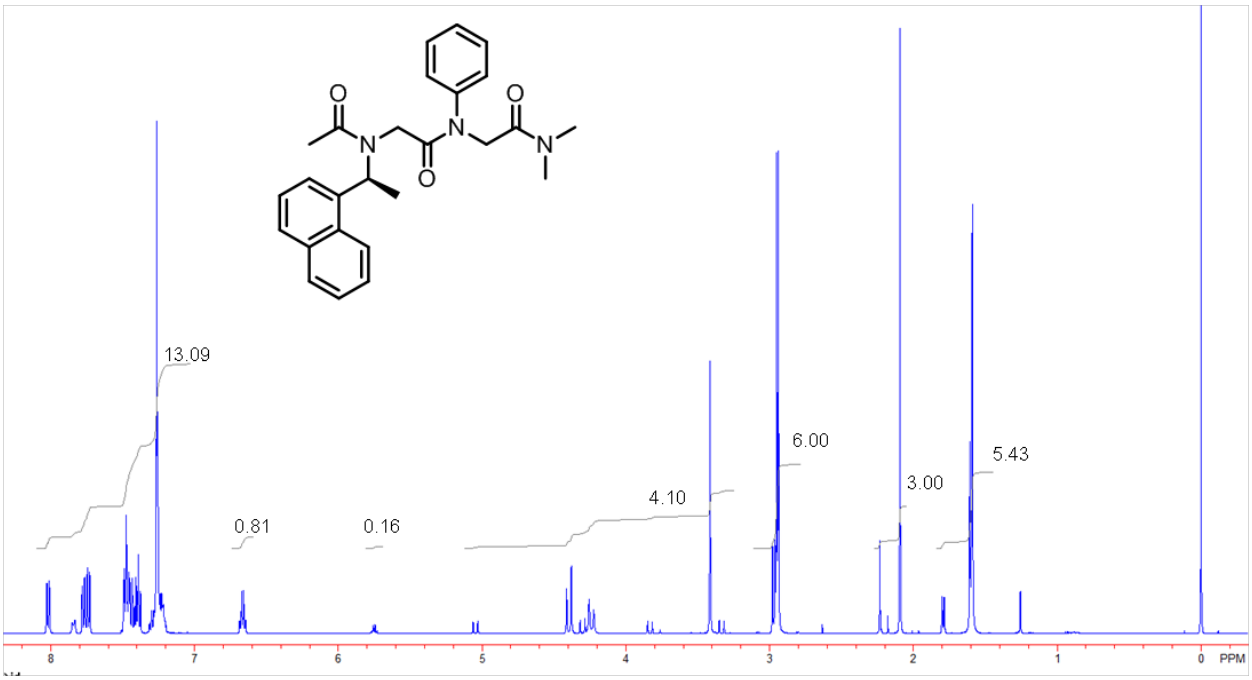

Peptoid 3. Ac-*N*s1npe-*N*ph-*N*s1npe-dma. After a general acetylation procedure from H-*N*s1npe-*N*ph-*N*s1npe-dma and aqueous work-up, the crude tan oil was loaded onto a column of silica gel (equilibrated with 5% MeOH in EtOAc) and eluted by flash column chromatography using 5% MeOH in EtOAc. Two rounds of chromatography resulted in a transparent oil that was lyophilized from 3:2 ACN/H_2O to afford a white fluffy powder. Isolated yield = 55%; TLC: R_f = 0.18 (5% MeOH/EtOAc); HR-MS (ESI): $C_{40}H_{42}N_4NaO_4$, $[M+Na]^+$ calcd m/z = 665.3099, observed m/z = 665.3087.

HPLC (220 nm)

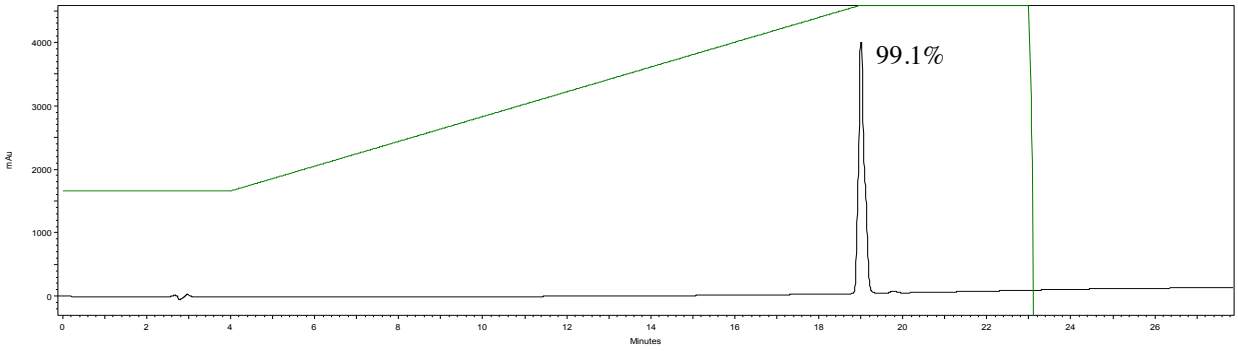

^{1}H NMR (300 MHz, $CDCl_3$)

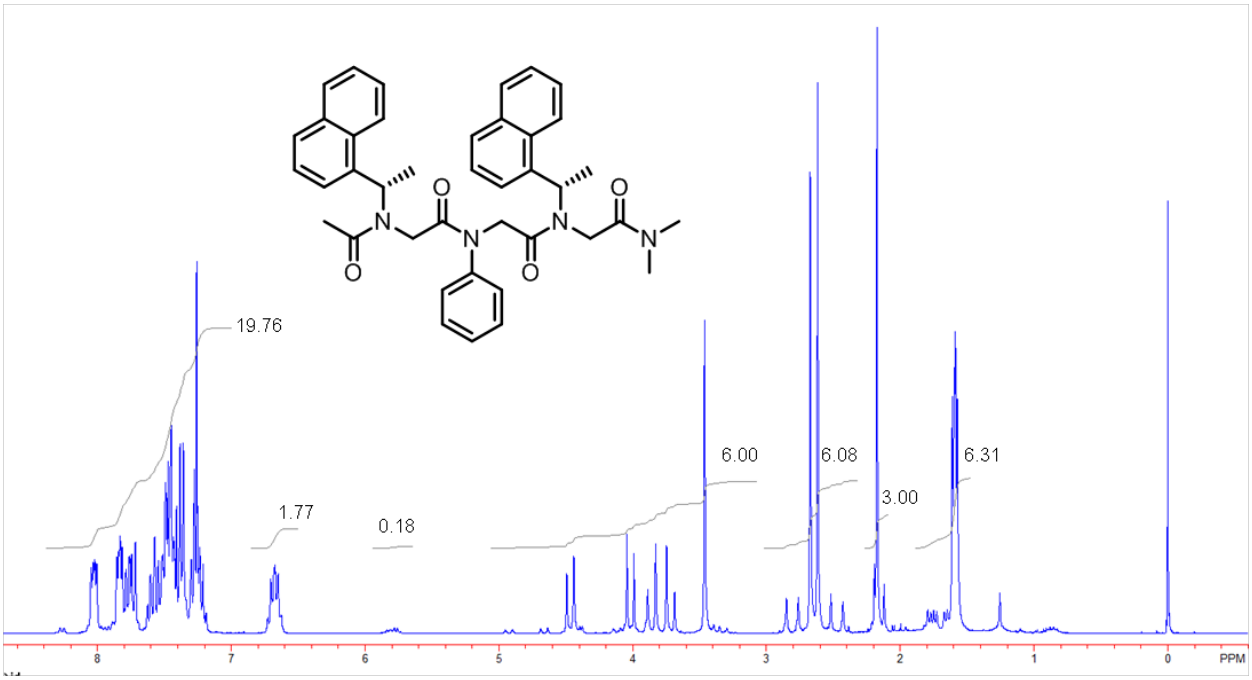

Peptoid 4a. Ac-*N*2,6mph-*N*s1npe-*N*ph-*N*s1npe-dma. After a general acetylation procedure from H-*N*2,6mph-*N*s1npe-*N*ph-*N*s1npe-dma and aqueous work-up, the crude tan oil was loaded onto a column of silica gel (equilibrated with 5% hexanes in EtOAc) and eluted by flash column chromatography using 5% hexanes in EtOAc. Two rounds of chromatography resulted in a transparent oil that was lyophilized from 3:2 ACN/H_2O to afford a white fluffy powder. Isolated yield = 50%; TLC: R_f = 0.33 (5% hexanes in EtOAc); HR-MS (ESI): $C_{50}H_{53}N_5NaO_5$, $[M+Na]^+$ calcd m/z = 826.3939, observed m/z = 826.3980.

HPLC (220 nm)

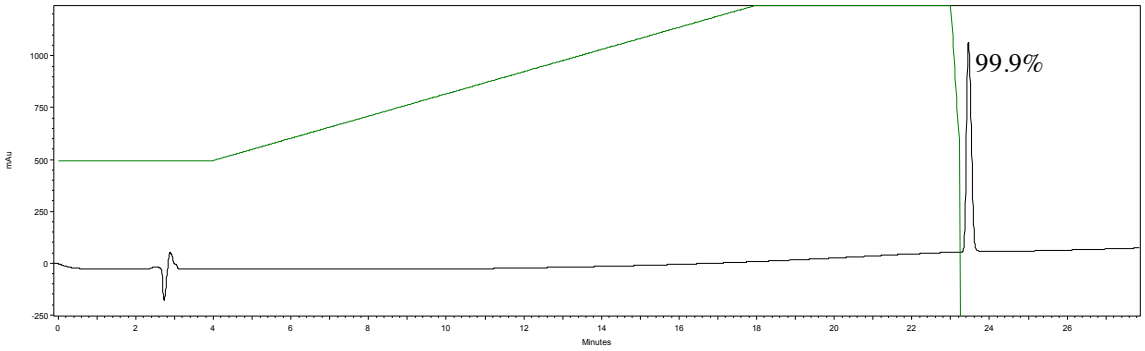

^{1}H NMR (600 MHz, $CDCl_3$, 10 mM) – "X" marks trace solvent peak (H_2O).

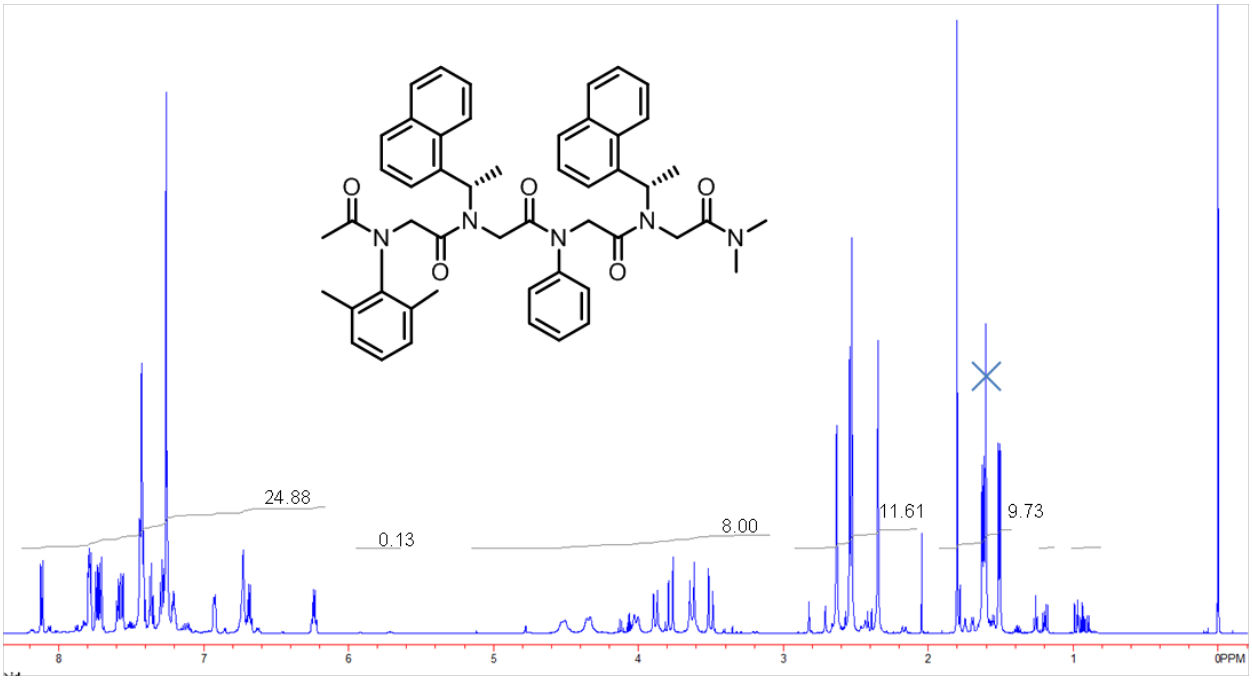

Peptoid 4b. Ac-*N*3,5mph-*N*s1npe-*N*ph-*N*s1npe-dma. After a general acetylation procedure from H-*N*3,5mph-*N*s1npe-*N*ph-*N*s1npe-dma and aqueous work-up, the crude tan oil was loaded onto a column of silica gel (equilibrated with 3:2 hexanes/acetone) and eluted by flash column chromatography using 3:2 hexanes/acetone to give a transparent oil. This oil was lyophilized from 3:2 ACN/H_2O to afford a white fluffy powder. Isolated yield = 94%; TLC: R_f = 0.26 (3:2 hexanes/acetone); HR-MS (ESI): $C_{50}H_{53}N_5NaO_5$, $[M+Na]^+$ calcd m/z = 826.3939, observed m/z = 826.3942.

HPLC (218 nm)

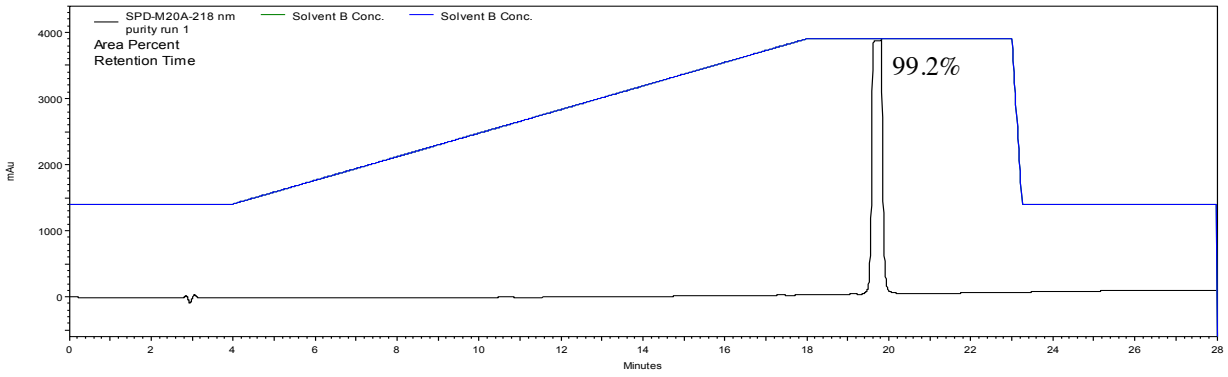

^{1}H NMR (600 MHz, $CDCl_3$, 10 mM) – "X" marks trace solvent peak (H_2O).

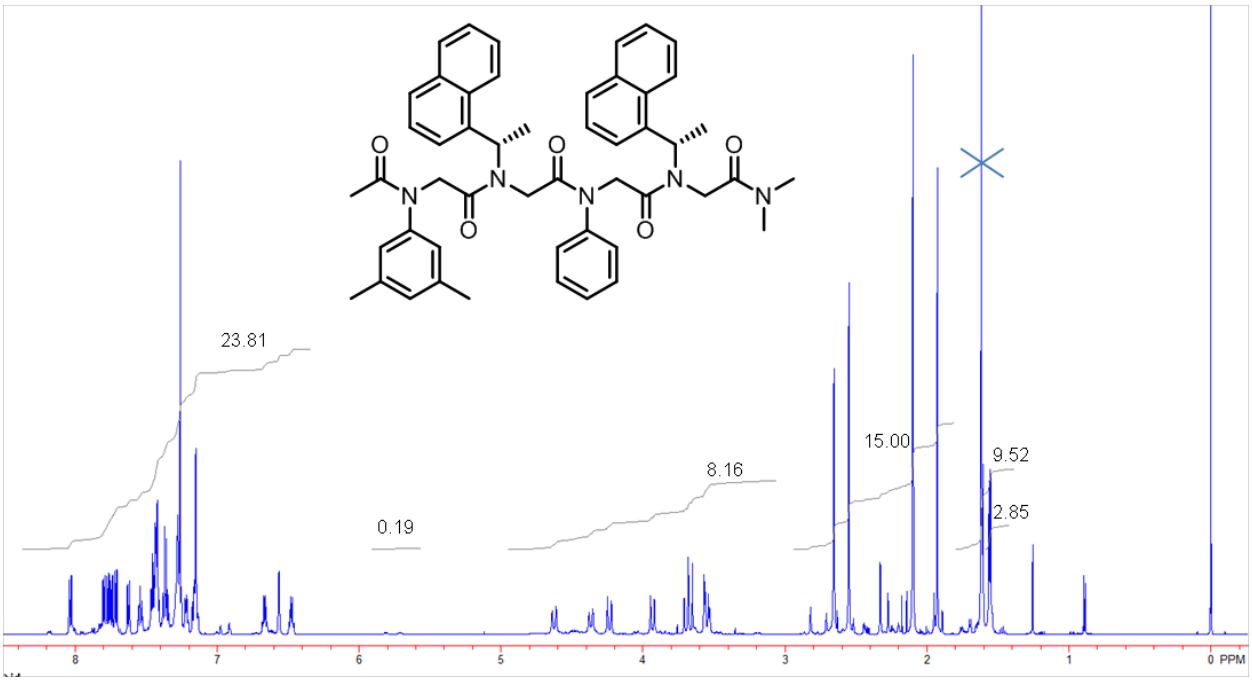

Peptoid 5. Ac-*N*s1npe-*N*ph-*N*s1npe-*N*ph-*N*s1npe-dma. After a general acetylation procedure from H-*N*s1npe-*N*ph-*N*s1npe-*N*ph-*N*s1npe-dma and aqueous work-up, the crude tan oil was loaded onto a column of silica gel (equilibrated with 5% MeOH in EtOAc) and eluted by flash column chromatography using 5% MeOH in EtOAc. Two rounds of chromatography resulted in a transparent oil that was lyophilized from 3:2 ACN/H_2O to afford a white fluffy powder. Isolated yield = 67%; TLC: R_f = 0.27 (5% MeOH in EtOAc); HR-MS (ESI): $C_{62}H_{62}N_6NaO_6$, $[M+Na]^+$ calcd m/z = 1009.4624, observed m/z = 1009.4654.

HPLC (220 nm)

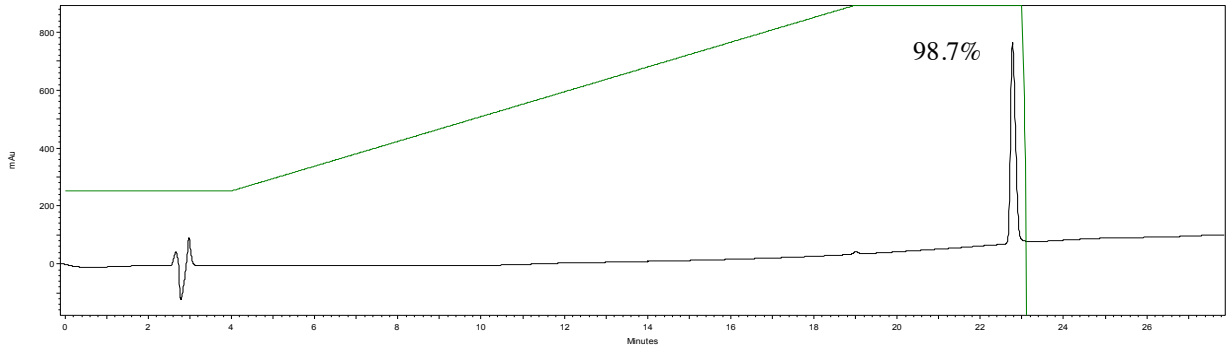

^{1}H NMR (300 MHz, $CDCl_3$)

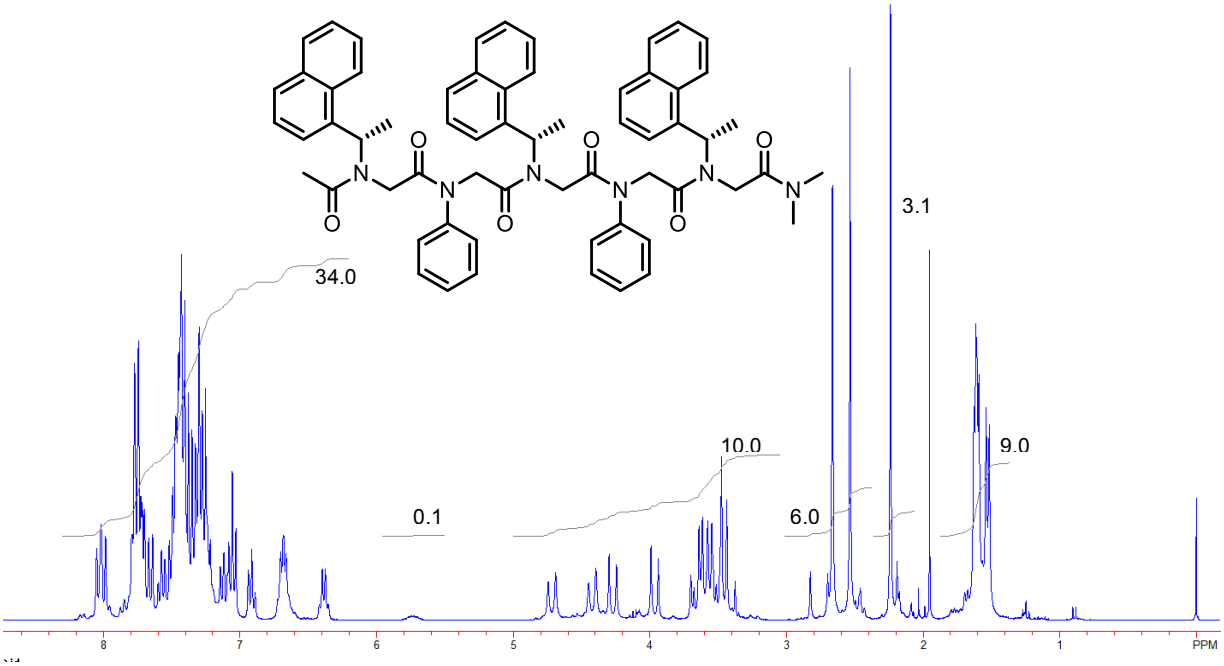

Peptoid 6. Ac-*N*ph-*N*s1npe-*N*ph-*N*s1npe-*N*ph-*N*s1npe-dma. After a general acetylation procedure from H-*N*ph-*N*s1npe-*N*ph-*N*s1npe-*N*ph-*N*s1npe-dma and aqueous work-up, the crude tan oil was loaded onto a column of silica gel (equilibrated with 9:1 EtOAc/MeOH) and eluted by flash column chromatography using 9:1 EtOAc/MeOH. Two rounds of chromatography resulted in a transparent oil that was lyophilized from 3:1 ACN/H_2O to afford a white fluffy powder. Isolated yield = 75%; TLC: R_f = 0.22 (9:1 EtOAc/MeOH); HR-MS (ESI): $C_{70}H_{69}N_7NaO_7$, $[M+H]^+$ calcd m/z = 1142.5151, observed m/z = 1142.5128.

HPLC (220 nm)

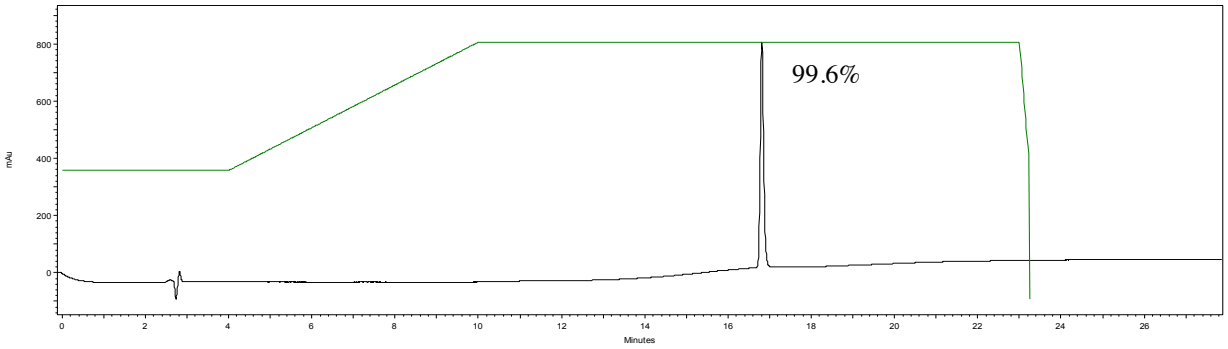

^{1}H NMR (300 MHz, $CDCl_3$)

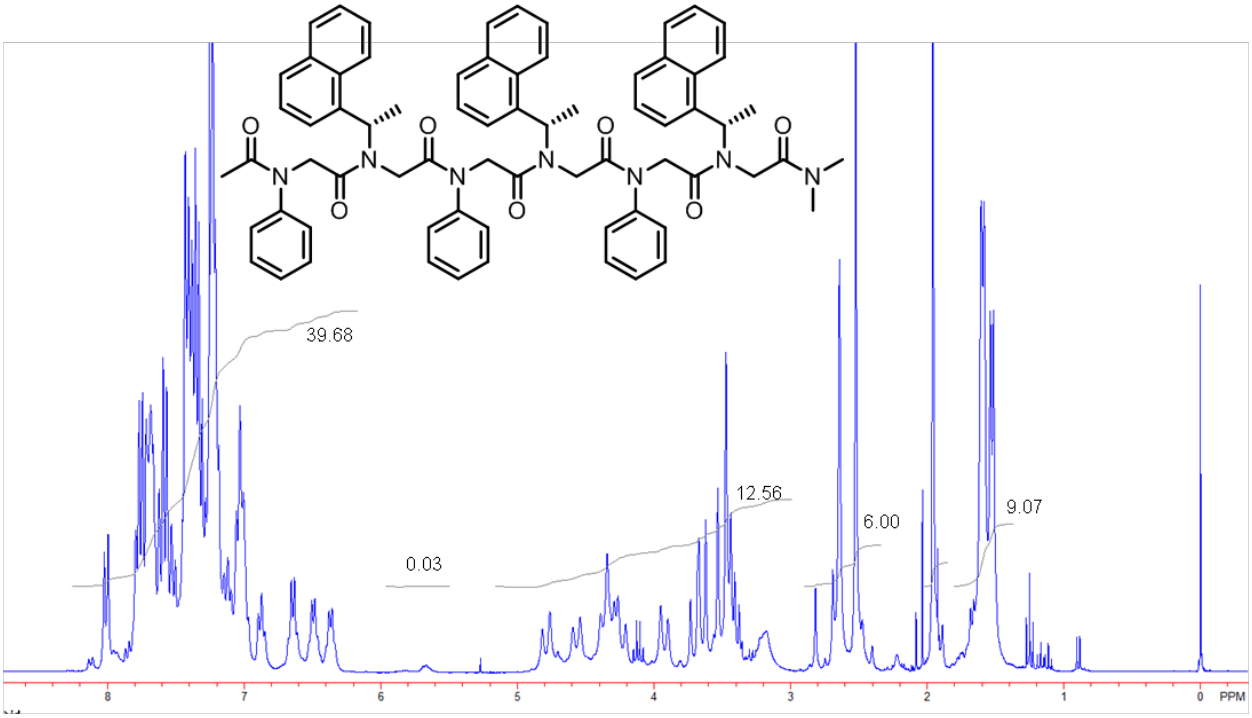

Peptoid *6i*. Ac-*N*3,5mph-*N*s1npe-*N*2,6mph-Ac*^{13}C-*N*s1npe-*N*4fph-*N*s1npe-dma. After a general acetylation procedure from H-*N*3,5mph-*N*s1npe-*N*2,6mph-Ac*^{13}C-*N*s1npe-*N*4fph-*N*s1npe-dma and aqueous work-up, the crude tan oil was loaded onto a column of silica gel (equilibrated with 5:1 EtOAc/hexane) and eluted by flash column chromatography using 5:1 EtOAc/hexane. Two rounds of chromatography resulted in a transparent oil that was lyophilized from 3:1 ACN/H_2O to afford a white fluffy powder. Isolated yield = 72%; TLC: R_f = 0.22 (5:1 EtOAc/hexane), HR-MS (ESI): $C_{72}C^{13}{}_2H_{76}FN_7NaO_7$, $[M+Na]^+$ calcd m/z = 1218.5750, observed m/z = 1218.5713.

HPLC (220 nm)

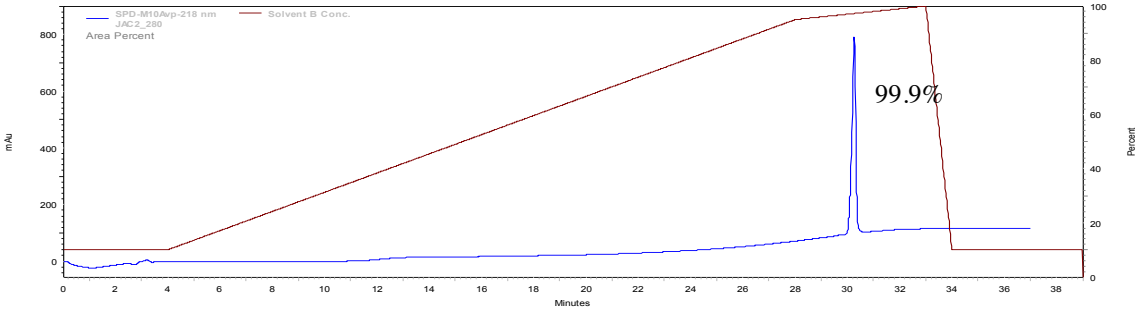

^{1}H NMR (600 MHz, $CDCl_3$) – "X" marks trace solvent peak (H_2O).

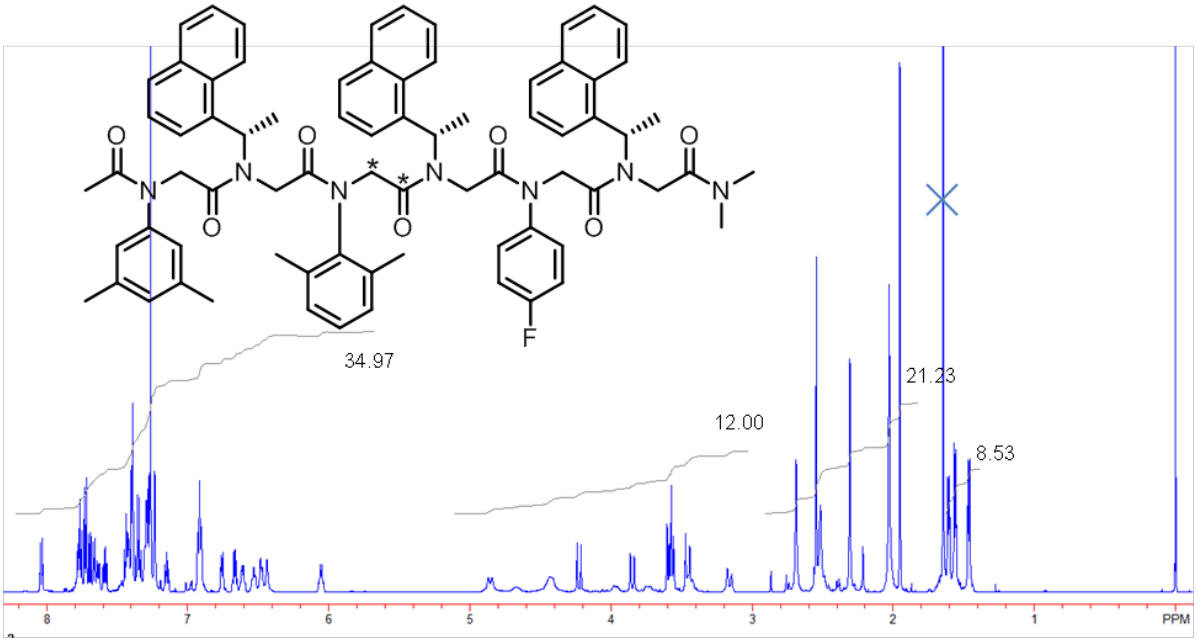

Peptoid 7. Ac-*N*s1npe-*N*ph-*N*s1npe-*N*ph-*N*s1npe-*N*ph-*N*s1npe-dma. After a general acetylation procedure from H-*N*s1npe-*N*ph-*N*s1npe-*N*ph-*N*s1npe-*N*ph-*N*s1npe-dma and aqueous work-up, the crude tan oil was loaded onto a column of silica gel (equilibrated with EtOAc) and eluted by flash column chromatography using EtOAc. Two rounds of chromatography resulted in a transparent oil that was lyophilized from 3:1 ACN/H_2O to afford a white fluffy powder. Isolated yield = 65%; TLC: R_f = 0.21 (EtOAc); HR-MS (ESI): $C_{84}H_{82}N_8NaO_8$, $[M+Na]^+$ calcd m/z = 1353.6148, observed m/z = 1353.6115.

HPLC (220 nm)

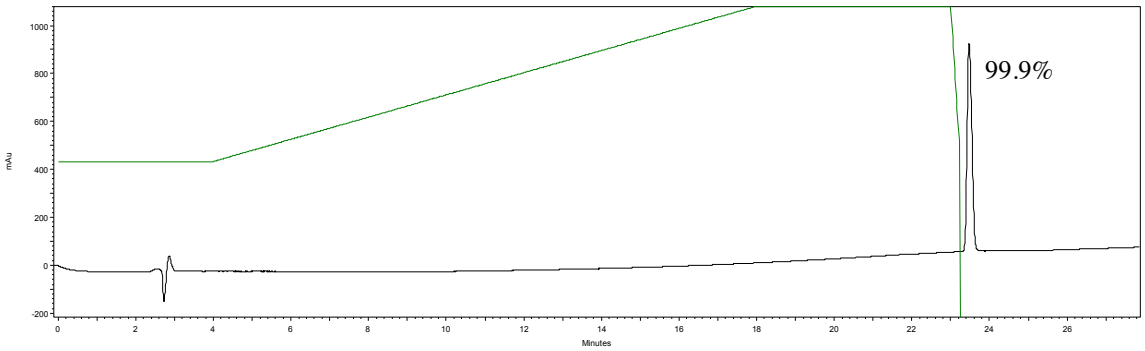

^{1}H NMR (300 MHz, $CDCl_3$)

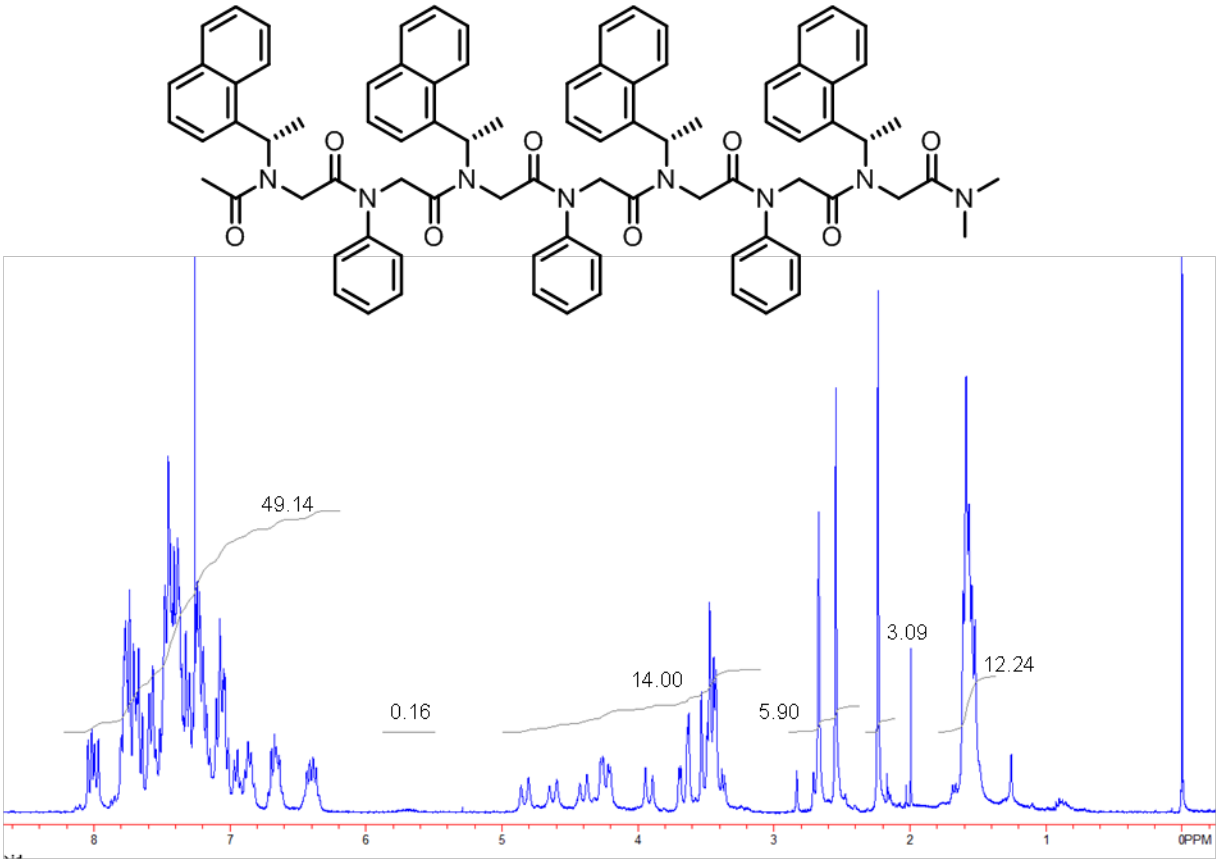

Peptoid 8. Ac-*N*ph-*N*s1npe-*N*ph-*N*s1npe-*N*ph-*N*s1npe-*N*ph-*N*s1npe-dma. After a general acetylation procedure from H-*N*ph-*N*s1npe-*N*ph-*N*s1npe-*N*ph-*N*s1npe-*N*ph-*N*s1npe-dma and aqueous work-up, the crude tan oil was loaded onto a column of silica gel (equilibrated with EtOAc) and eluted by flash column chromatography using EtOAc. Two rounds of chromatography resulted in a transparent oil that was lyophilized from 4:1 ACN/H_2O to afford a white fluffy powder. Isolated yield = 70%; TLC: R_f = 0.20 (EtOAc); HR-MS (ESI): $C_{92}H_{89}N_9NaO_9$, $[M+Na]^+$ calcd m/z = 1486.6676, observed m/z = 1486.6639.

HPLC (220 nm)

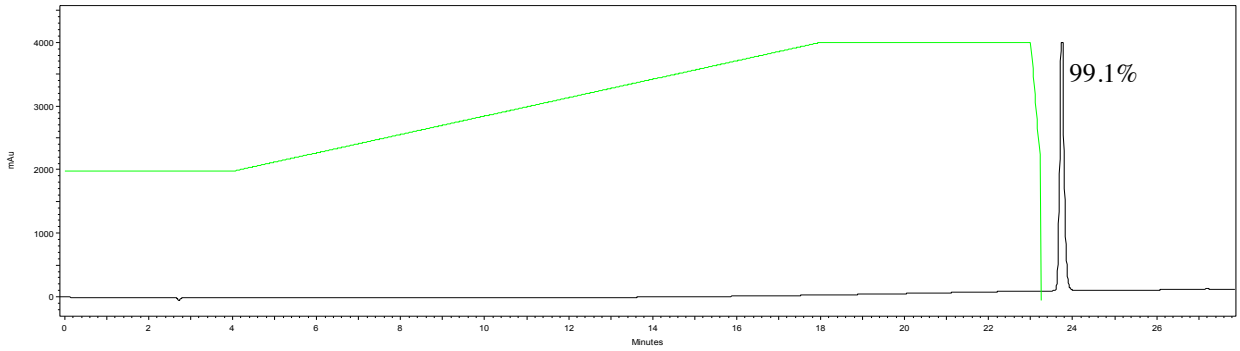

^{1}H NMR (300 MHz, $CDCl_3$)

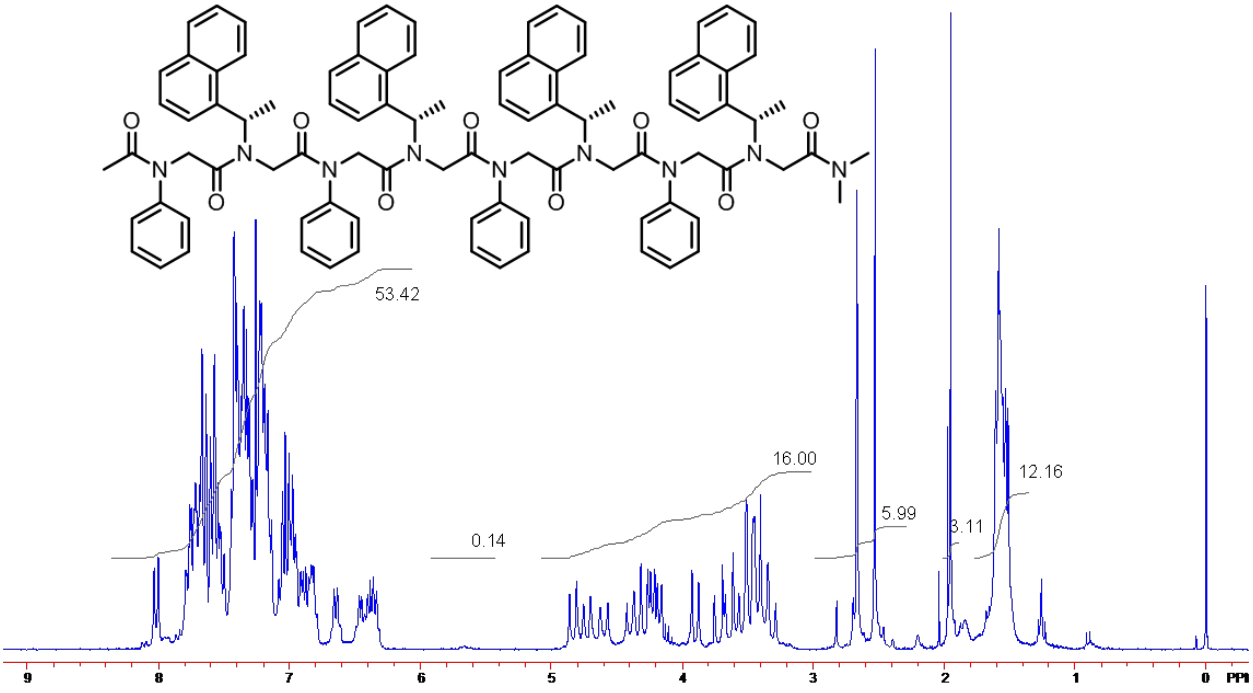

References for Supporting Information.

(1) Still, W. C.; Kahn, M.; Mitra, A. *J. Org. Chem.* **1978**, *43*, 2923-2925.

(2) Palmer, A. G.; Cavanagh, J.; Wright, P. E.; Rance, M. *J. Magn. Reson.* **1991**, *93*, 151-170.

(3) Kay, L. E.; Keifer, P.; Saarinen, T. *J. Am. Chem. Soc.* **1992**, *114*, 10663-10665.

(4) Schleucher, J.; Schwendinger, M.; Sattler, M.; Schmidt, P.; Schedletzky, O.; Glaser, S. J.; Sorensen, O. W.; Griesinger, C. *J. Biomol. NMR* **1994**, *4*, 301-306.

(5) Goddard, T. D.; Kneller, D. G. *Sparky, v.3.114*, University of California, San Francisco, 2007.

(6) Bradley, E.; Kerr, J.; Richter, L.; Figliozzi, G.; Goff, D.; Zuckermann, R.; Spellmeyer, D.; Blaney, J. *Mol. Diversity* **1997**, *3*, 1-15.

(7) Huang, K.; Wu, C. W.; Sanborn, T. J.; Patch, J. A.; Kirshenbaum, K.; Zuckermann, R. N.; Barron, A. E.; Radhakrishnan, I. *J. Am. Chem. Soc.* **2006**, *128*, 1733-1738.

(8) Armand, P.; Kirshenbaum, K.; Goldsmith, R. A.; Farr-Jones, S.; Barron, A. E.; Truong, K. T. V.; Dill, K. A.; Mierke, D. F.; Cohen, F. E.; Zuckermann, R. N.; Bradley, E. K. *Proc. Natl. Acad. Sci. U. S. A.* **1998**, *95*, 4309-4314.

(9) Stringer, J. R.; Crapster, J. A.; Guzei, I. A.; Blackwell, H. E. *J. Am. Chem. Soc.* **2011**, *133*, 15559-15567.

(10) Gorske, B. C.; Bastian, B. L.; Geske, G. D.; Blackwell, H. E. *J. Am. Chem. Soc.* **2007**, *129*, 8928-8929.

(11) Hjelmgaard, T.; Faure, S.; Caumes, C.; De Santis, E.; Edwards, A. A.; Taillefumier, C. *Org. Lett.* **2009**, *11*, 4100-4103.

(12) Gorske, B. C.; Stringer, J. R.; Bastian, B. L.; Fowler, S. A.; Blackwell, H. E. *J. Am. Chem. Soc.* **2009**, *131*, 16555-16567.

(13) Bruker-AXS. (2007) APEX2, SADABS, and SAINT Software Reference Manuals. Bruker-AXS, Madison, Wisconsin, USA.

(14) Sheldrick, G. M. SHELXL. *Acta Cryst.* **2008**, *A64*, 112-122.

(15) Dolomanov, O. V.; Bourhis, L. J.; Gildea, R. J.; Howard, J. A. K.; Puschmann, H. *J. Appl. Cryst.* **2009**, *42*, 339-341.

(16) Guzei, I.A. (2006-2008). Internal laboratory computer programs “Inserter”, “FCF_filter”, and “Modicifer”.

Full citations for references [2] and [13] in text.

(2) Simon, R. J., Kania, R. S., Zuckermann, R. N., Huebner, V. D., Jewell, D. A., Banville, S., Ng, S.; Wang, L.; Rosenberg, S., Marlowe, C. K., Spellmeyer, D. C., Tan, R.; Frankel, A. D., Santi, D. V., Cohen, F. E., Bartlett, P. A. *Proc. Natl. Acad. Sci. U.S.A.* **1992**, *89*, 9367-9371.

(13) Case, D. A.; Darden, T. A.; Cheatham, T. E. III; Simmerling, C. L.; Wang, J.; Duke, R. E.; Luo, R.; Walker, R. C.; Zhang, W.; Merz, K. M.; Roberts, B.; Wang, B.; Hayik, S.; Roitberg, A.; Seabra, G.; Kolossváry, I.; Wong, K. F.; Paesani, F.; Vanicek, J.; Liu, J.; Wu, X.; Brozell, S. R.; Steinbrecher, T.; Gohlke, H.; Cai, Q.; Ye, X.; Wang, J.; Hsieh, M.-J.; Cui, G.; Roe, D. R.; Mathews, D. H.; Seetin, M. G.; Sagui, C.; Babin, V.; Luchko, T.; Gusarov, S.; Kovalenko, A.; Kollman, P. A. *AMBER 11*, **2010**, University of California, San Francisco.